AD NUMBER
AD921330
LIMITATION CHANGES

TO:

Approved for public release; distribution is unlimited.

FROM:

Distribution authorized to U.S. Gov't. agencies only; Test and Evaluation; JUL 1974. Other requests shall be referred to Armament Development Test Center, Eglin AFB, FL 32542.

AUTHORITY

AFATL ltr 13 Jan 1977

AERODYNAMIC AND PERFORMANCE CHARACTERISTICS OF THE AFATL TRAJECTORY CONTROL TEST VEHICLE

H. Kaupp and L. E. Rittenhouse
ARO, Inc.

PROPULSION WIND TUNNEL FACILITY
ARNOLD ENGINEERING DEVELOPMENT CENTER
AIR FORCE SYSTEMS COMMAND
ARNOLD AIR FORCE STATION, TENNESSEE 37389

July 1974

Final Report for Period July 16 — September 18, 1973

Prepared for

AIR FORCE ARMAMENT LABORATORY (DLMS)
EGLIN AIR FORCE BASE, FLORIDA 32542

NOTICES

When U. S. Government drawings specifications, or other data are used for any purpose other than a definitely related Government procurement operation, the Government thereby incurs no responsibility nor any obligation whatsoever, and the fact that the Government may have formulated, furnished, or in any way supplied the said drawings, specifications, or other data, is not to be regarded by implication or otherwise, or in any manner licensing the holder or any other person or corporation, or conveying any rights or permission to manufacture, use, or sell any patented invention that may in any way be related thereto.

Qualified users may obtain copies of this report from the Defense Documentation Center.

References to named commercial products in this report are not to be considered in any sense as an endorsement of the product by the United States Air Force or the Government.

APPROVAL STATEMENT

This technical report has been reviewed and is approved.

LAMAR R. KISSLING
Lt Colonel, USAF
Chief Air Force Test Director, PWT
Directorate of Test

FRANK J. PASSARELLO
Colonel, USAF
Director of Test

REPORT DOCUMENTATION PAGE		READ INSTRUCTIONS BEFORE COMPLETING FORM
1. REPORT NUMBER AEDC-TR-74-69 AFATL-TR-74-109	2 GOVT ACCESSION NO.	3. RECIPIENT'S CATALOG NUMBER
4. TITLE *(and Subtitle)* AERODYNAMIC AND PERFORMANCE CHARACTERISTICS OF THE AFATL TRAJECTORY CONTROL TEST VEHICLE		5. TYPE OF REPORT & PERIOD COVERED Final Report – July 26 – September 18, 1973
		6 PERFORMING ORG. REPORT NUMBER
7. AUTHOR(s) H. Kaupp and L. E. Rittenhouse – ARO, Inc.		8. CONTRACT OR GRANT NUMBER(s)
9. PERFORMING ORGANIZATION NAME AND ADDRESS Arnold Engineering Development Center(DYFS) Arnold Air Force Station Tennessee 37389		10. PROGRAM ELEMENT. PROJECT. TASK AREA & WORK UNIT NUMBERS Program Element 63741F Project 5977
11. CONTROLLING OFFICE NAME AND ADDRESS Air Force Armament Laboratory (DLMS) Eglin Air Force Base Florida, 32542		12. REPORT DATE July 1974
		13. NUMBER OF PAGES 83
14 MONITORING AGENCY NAME & ADDRESS*(if different from Controlling Office)*		15. SECURITY CLASS. *(of this report)* UNCLASSIFIED
		15a. DECLASSIFICATION/DOWNGRADING SCHEDULE

16. DISTRIBUTION STATEMENT *(of this Report)*

Distribution limited to U. S. Government agencies only; this report contains information on test and evaluation of military hardware; July 1974; other requests for this document must be referred to Air Force Armament Laboratory (DLMS), Eglin Air Force Base, Florida 32542.

17. DISTRIBUTION STATEMENT *(of the abstract entered in Block 20, if different from Report)*

18. SUPPLEMENTARY NOTES

Available in DDC

19. KEY WORDS *(Continue on reverse side if necessary and identify by block number)*

aerodynamic characteristics
performance
trajectories
scale model

transonic flow
control surfaces

20 ABSTRACT *(Continue on reverse side if necessary and identify by block number)*

The Air Force Armament Laboratory (AFATL) and the Arnold Engineering Development Center (AEDC) are participating in a joint effort to develop a trajectory control test vehicle (TCTV). The vehicle is to be used as a test bed for various seeker, autopilot, and flap actuator systems now in development. The aerodynamic characteristics of the vehicle were obtained from wind tunnel tests using a 0.25-scale model and are presented for Mach numbers 0.5 to 1.05 at angles of attack to 20 deg. The control effectiveness

DD FORM
1 JAN 73 1473   EDITION OF 1 NOV 65 IS OBSOLETE

20. ABSTRACT (Continued)

parameters presented were obtained using a single flap test technique in the wind tunnel. Also the computer-generated flight performance is presented for a nominal launch condition.

AFSC
Arnold AFS Tenn

PREFACE

The test program reported herein was conducted by the Arnold Engineering Development Center (AEDC), Air Force Systems Command (AFSC), at the request of the Air Force Armament Laboratory (AFATL/DLMS), AFSC, under Program Element 63741F, Project 5977. The results were obtained by ARO, Inc. (a subsidiary of Sverdrup & Parcel and Associates, Inc.), contract operator of the AEDC, AFSC, Arnold Air Force Station, Tennessee. The wind tunnel tests were conducted in two phases during the time periods from July 26 through August 2 and September 14 through 18, 1973, under ARO Project No. PA302. Test analysis was conducted under ARO Project No. PA419. Data reduction was completed on March 13, 1974, and the manuscript (ARO Control No. ARO-PWT-TR-74-46) was submitted for publication on June 11, 1974.

CONTENTS

ILLUSTRATIONS

TABLES

1.0 INTRODUCTION

The Air Force Armament Laboratory (AFATL) is currently developing a 2400-lb-class glide vehicle to be used as a test bed for evaluation of new components designed for extended-range air-to-ground munitions. The vehicle will be launched from a high altitude and guided during a glide phase to a general target area. A seeker will then be locked onto a particular target, and the vehicle will operate in the normal lock-on-before-launch mode for the remainder of the flight. The vehicle is called the trajectory control test vehicle (TCTV).

The Arnold Engineering Development Center (AEDC) was asked by the AFATL to participate in an "in house" effort to develop the TCTV. The AEDC effort included the following tasks:

1. Provide an aerodynamic design to accomplish the mission requirements.

2. Design and fabricate an 0.25-scale and a 0.05-scale model of the TCTV. Moreover, to develop the test plans and conduct the wind tunnel tests.

3. Set up a computer simulation program and perform flight simulations using the wind tunnel results.

4. Develop an autopilot for midcourse guidance. Also specify and procure the gyros and dynamic pressure sensors for the flight test vehicle.

5. Provide some assistance during the flight test phase.

The work reported herein covers tasks 1, 2, and 3 assigned to AEDC. The autopilot design is not included and the flight tests have not yet been conducted. The approach used to develop the vehicle was to utilize the MK-84 warhead and the KMU-353A/B guidance and control system. The first task was to define the physical envelope for carriage of the vehicle on the inboard MAU-12 pylon of the F-4 aircraft. The space envelope involves the wing leading-edge flap, the landing gear door, and a 3-in. ground clearance (compressed strut, flat tire, and static loading) required for the aircraft. By using these geometric constraints, the vehicle was designed, and a digital computer program was used to determine the general aerodynamic characteristics of the vehicle. Configuration studies were made to determine the fin geometry that would provide a large lift-curve slope and maintain a static margin sufficient to fulfill the maneuvering requirements. A wind tunnel program was then conducted to determine the final geometry of the vehicle and obtain all the aerodynamic coefficients. These data were then used in a 6 deg of freedom flight simulation computer program to study the vehicle flight characteristics. Launch conditions were chosen as Mach number 0.95 at an altitude of 40,000 ft.

A second phase of the wind tunnel tests involved determining the separation characteristics of the vehicle from the inboard pylon of the F-4 aircraft. This test was necessary to qualify the vehicle for flight tests at the Eglin test range.

Presented are the aerodynamic characteristics of the vehicle, the separation characteristics of the vehicle from the F-4 aircraft, and the flight simulation results. The control effectiveness parameters were obtained using a single flap test technique that is described in the text.

2.0 FULL-SCALE VEHICLE

The full-scale vehicle is a combination of the MK-84 (2000-lb) munition and a modified KMU-353A/B guidance and control kit. A photograph of the 0.25-scale wind tunnel model is shown in Fig. 1. Full-scale mass properties are given in Table 1. The MK-84 and the KMU-353A/B kit are components of the Rockwell International Corporation (RIC) HOBOS guided munition. Original control section hardware included four cruciform fins (rectangular planform), strakes, and trailing-edge flaps having a tip-to-tip span of 44 in. These were replaced by the four large fins and blunt trailing edge flaps shown in Fig. 1. Total span of the vehicle is 61.32 in. (including counter weights). Three circumferential bands located forward, center, and aft on the MK-84 body are used for fin attachment. Another external change in the guidance and control hardware was the addition of a dynamic pressure sensor on the vehicle. Internal modifications included the integration of attitude control circuitry which was coupled to the dynamic pressure sensor, a gyro for azimuth control, a data link, and a demand supply nitrogen system to extend the usable gas time of the flap actuator system. Design changes in the guidance system were made at the AEDC, and physical modifications to the system were made at the AFATL.

The dynamic pressure sensor and associated circuitry mentioned above are components of the vehicle attitude control system which is used during the midcourse phase of flight. Several other schemes such as an angle-of-attack sensor, a gyro, or accelerometers were considered for determining vehicle attitude. The dynamic pressure device, however, lends itself to simplicity and minimal flight path excursions during the glide phase. The operation of the control system may be explained as follows: The dynamic pressure sensor is intergrated into the control network such that the vehicle attitude is adjusted during flight to maintain a near constant dynamic pressure at the sensor. If the measured pressure is above a selected value, the control system will decrease the vehicle glide path angle, thus reducing velocity and dynamic pressure. If the measured pressure is below the selected value, the control system will cause the vehicle to dive (increase glide path angle), thus increasing the velocity and dynamic pressure. The desired flight dynamic pressure is that value corresponding to $(L/D)_{max}$ (minimum flight path angle), thus producing a condition

for maximum range. Because the angle of attack at $(L/D)_{max}$ varies with Mach number, the value of the dynamic pressure chosen for an anticipated flight will not be an optimum for all flight conditions. By using the digital computer flight simulation, a value was found that provided a maximum range over a fairly wide band of launch conditions. For the TCTV, a dynamic pressure of 320 psf was found to provide the maximum range when launched at Mach number 0.95 at an altitude of 40,000 ft.

A full-scale calibration of the dynamic pressure sensor can be found in Ref. 1.

3.0 WIND TUNNEL TEST PROGRAM

3.1 GENERAL

The wind tunnel tests were conducted in the Aerodynamic Wind Tunnel (4T) in two phases. The tests provided the required information for the trajectory analysis (simulator program) and to qualify the vehicle for flight carriage and separation on the F-4 aircraft. The vehicle mass properties and dimensions used in the store separation phase of the wind tunnel tests, as well as the simulator work, are tabulated in Table 1. In each phase of the wind tunnel tests, the model aerodynamic forces and moments were measured using a six-component internal strain-gage balance. The particular test conditions and the precision of the reduced data for each phase of testing are given in Table 2.

3.1.1 Phase 1

The 0.25-scale model of the TCTV (Figs. 2a and b) was designed and fabricated at AEDC to obtain static stability and control effectiveness data. Vehicle surface protuberances such as launch lugs, cable harness, and body bands were included on the model. Tests were made with fin sweep angles (midchord) of 55 and 73 deg (see Fig. 2a). The 73-deg sweep angle was found to produce the desired value for the static margin; thus, the data presentation has been limited to that configuration. The 55-deg sweep angle configuration resulted in an unstable configuration at the lower Mach numbers.

Pins located in the model base were used to set the individual flaps to angles of 0, ±5, ±10, ±15, or ±20 deg. The faces of the pins were ground to an angle corresponding to the desired flap angle settings. The face of the pin was forced against a flat on the flap shaft by a retaining screw, thus rotating the flap to the desired angle. The uncertainty in setting the flap angles was found to be ±0.25 deg. A limited amount of hinge moment data was obtained on flaps 3 and 4 with strain-gage balances located at the flap hinge line.

A "single flap" test technique (see Section 3.2) was used to obtain the data at Mach numbers 0.5, 0.65, and 0.85 at angles of attack up to 20 deg and at Mach numbers 0.95 and 1.05 at angles of attack up to 12 deg. Data were obtained at roll angles from 0 to 360 deg in increments of 22.5 deg. For comparison purposes, a limited amount of data was taken using the conventional multiple flap test technique. The aerodynamic coefficients for the phase 1 test are presented in an aeroballistic (nonrolling) body axis system. The zero roll reference plane passes through the longitudinal axis of the vehicle and the attachment lugs. The vehicle fin orientation during flight is in the X configuration with the attachment lugs up.

3.1.2 Phase 2

The separation characteristics of the TCTV from the right inboard pylon on a 0.05-scale F-4 aircraft were determined during phase 2 testing (Fig. 3). A captive trajectory support (CTS) system was used to obtain the data. Separation trajectories were obtained with the airplane in a trimmed condition at simulated altitudes of 5,000 and 10,000 ft with Mach number 0.65 and altitudes of 5,000 to 40,000 ft with Mach number 0.95. Tests were conducted with the TCTV flaps fixed at zero ($\delta q = 0$) and plus and minus fifteen deg ($\delta q = \pm 15$).

It should be noted that the control surface settings ($\delta q = \pm 15$) on the model are contrary to the way the actual flight hardware operates. During the first 2 sec of flight after the vehicle has been released from the pylon, the guidance system commands the control surfaces in such a manner as to maintain the vehicle in the release attitude. Therefore, no pitch, yaw, or roll maneuvers should occur and only translational movements result. In this context, the wind tunnel results for $\delta q = 0$ are pessimistic in that pitch and yaw angles for the vehicle are allowed. This condition ($\delta q = 0$) represents the jettison mode of release. The results for $\delta q = \pm 15$ deg does represent a possible failure mode of the control system in which the control surfaces are driven to their electrical limits.

3.2 TEST FACILITY

The Aerodynamic Wind Tunnel (4T) is a closed-loop, continuous-flow, variable density tunnel in which the Mach number can be varied from 0.1 to 1.3. At all Mach numbers, the stagnation pressure can be varied from 300 to 3700 psfa. The test section is 4 ft square and 12.5 ft long with perforated, variable porosity (0.5- to 10-percent open) walls. It is completely enclosed in a plenum chamber from which the air can be evacuated, allowing part of the tunnel airflow to be removed through the perforated walls of the test section.

For store separation testing (phase 2), two separate and independent support systems are used to support the models. The parent-aircraft model is inverted in the test section and supported in the test section by a sting attached to the main pitch sector. The store model is supported by the CTS which extends down from the tunnel top wall and provides store movement (six degrees of freedom) independent of the parent-aircraft model. An isometric drawing of a typical store separation installation is shown in Fig. 4.

Also shown in Fig. 4 is a block diagram of the computer control loop used during captive trajectory testing. The analog system and the digital computer work as an integrated unit which, by utilizing required input information, control the store movement during a trajectory.

A complete description of the test facility can be found in Ref. 2.

3.3 SINGLE FLAP TEST TECHNIQUE

The multiple flap deflection testing method is the conventional method in which all four flaps (control surfaces) are positioned to produce a specified δp, δq, δr or combination thereof. To obtain aerodynamic data at all possible combinations of settings (5 deg increments) would require an unreasonable amount of wind tunnel time. However, to fully examine the aerodynamic characteristics of a vehicle as well as provide sufficient data for a six-degree-of-freedom flight simulation program, all of these data are needed. To obtain these data in this test program a technique termed "single flap" test technique was used. Using this technique requires significantly less tunnel time and is especially applicable to symmetric bodies with a cruciform tail arrangement. To use the technique, it must be assumed that any protuberances existing on the body will not create flow disturbances which influence the control effectiveness of the flaps, or if flow disturbances do occur, each flap is affected in a like manner. Also the technique assumes no mutual aerodynamic interference exists between flaps when they are deflected.

The single flap testing technique relies on the determination of the incremental change in the six aerodynamic coefficients (three forces and three moments) resulting from the deflection of a single flap. These incremental values are obtained for a series of model roll positions at each angle of attack and Mach number. Because the model has aerodynamic symmetry in the pitch and yaw planes, it is possible to determine the incremental coefficients of any of the remaining three flaps, assuming they were deflected in a like manner. The incremental coefficients determined for the four flaps can then be summed to obtain the total control effectiveness of the vehicle or they can be added to the aerodynamic coefficients obtained with the vehicle with flaps set to zero, thus providing the total model aerodynamic coefficients for any δp, δq, or δr or combination thereof.

9

During this test, flap No. 1 was used for single flap testing. Deflection angles of 0, -5, -10, -15, and -20 deg were used.

Figure 5 is presented to explain the procedure of applying incremental coefficients obtained with flap No. 1 to the remaining three flaps. The figure shows that the data obtained for a negative deflection of fin No. 2 at any aeroballistic roll angle (ϕ_a) can be obtained by using a negative deflection on flap No. 1 and rolling the model an additional 90 deg or $\phi_m = \phi_a + 90$. The data that would be obtained for positive deflections on flaps No. 3 and 4 at any aeroballistic roll angle can be obtained using a negative flap deflection on flap No. 1 and model roll angles of $\phi_m = \phi_a + 180$ deg and $\phi_m = \phi_a - 90$ deg, respectively. For positive deflections of flaps No. 1 and 2 and negative deflections of flaps No. 3 and 4, the data are used for the negatively deflected No. 1 flap oriented in a position which is the mirror image of the desired flap deflection. A positive deflection of fin No. 1 at any aeroballistic roll angle, (ϕ_a) can be obtained as the mirror image of a negative deflection of fin No. 1 at a model roll angle of $\phi_m = -\phi_a - 90$, etc. The magnitude of the incremental data is the same; however, the signs on the incremental aeroballistic side-force, yawing-moment, and rolling-moment coefficients must be changed.

A more thorough discussion of the single flap test technique is given in Ref. 3.

4.0 WIND TUNNEL RESULTS

4.1 PHASE 1

The longitudinal aerodynamics characteristics of the vehicle at pitch control settings from -15 to 15 deg are presented in Figs. 6a through e. These data were obtained using the single flap testing technique and the data reduction procedure described in Section 3.3. Smooth variations of the normal-force and pitching-moment coefficient with angle of attack are exhibited throughout the Mach number range. The trim normal-force coefficient $(C_{N,a})_{trim}$ and trim angle of attack $(a_a)_{trim}$ both decrease with Mach number as shown in Fig. 7.

The primary control effectiveness parameters are presented in Figs. 8a through 11e as functions of a_a. The axial-force parameter $(C_{A\delta q})$ is also presented. In general, the parameters do not exhibit a uniform variation with flap settings. Typical values of the pitch, yaw, and roll control parameters for flap settings of $\delta q = -10$, $\delta r = 10$, and $\delta p = 10$ deg and for zero-degree angle of attack are as follow:

M_∞	0.5	0.65	0.85	0.95	1.05
$C_{m,a_{\delta q}}$	-0.320	-0.300	-0.320	-0.290	-0.290
$C_{n,a_{\delta r}}$	-0.308	-0.301	-0.313	-0.272	-0.288
$C_{\ell_{\delta p}}$	0.094	0.099	0.091	0.090	0.095

With few exceptions, the values presented above remain constant or increase with angle of attack. It should be noted that generally the $C_{m,a_{\delta q}}$ and $C_{n,a_{\delta r}}$ values should be in agreement at each Mach number. The differences shown are possibly a result of the influence of the lugs and conduit on the flow field at the No. 1 flap. This influence, of course, would vary as the model is rolled. The differences also could be an indication of the accuracy of the data. To resolve the differences, data are required for the model without lugs and conduit.

The effect of cross coupling of the control surfaces on the control effectiveness parameters ($C_{m,a_{\delta q}}$, $C_{n,a_{\delta r}}$, and $C_{\ell_{\delta p}}$) are presented in Figs. 12a through 15c. The general trend of the data is a decrease in the magnitude of the control effectiveness parameters when combined controls are applied. This decrease is a result of the deflection angle of one or more of the individual flaps being increased above its original in-plane setting when combined settings are made. For example, combining a $\delta r = 10$ with a $\delta = -5$ requires the flaps be repositioned from a setting of $\delta 1 = \delta 2 = \delta 3 = \delta 4 = -5$ to $\delta 1 = \delta 3 = -15$ and $\delta 2 = \delta 4 = 5$. As the flap deflection angle is increased, the effectiveness of the control surface generally decreases as reflected in the data for in-plane δq deflections shown in Fig. 9. The effect of a positive deflection of rudder control or roll control on pitch control effectiveness ($C_{m,a_{\delta q}}$) is the same as a negative deflection (Figs. 12a through d). This, of course, is because the combined deflections of pitch with negative deflections of yaw or roll are a mirror image of the combined deflections of pitch with positive deflections of yaw and roll. This is not true, however, when pitch control or roll control is applied with yaw control or when pitch control or yaw control is applied with roll control. Nonsymmetric variations of the $C_{n,a_{\delta r}}$ and $C_{\ell_{\delta p}}$ occur in these cases as shown in Figs. 13 through 15c. The effect is most evident in Fig. 15a, which shows the magnitude of $C_{\ell_{\delta p}}$ to be larger for negative than positive deflections of δq.

The vehicle maximum lift-drag ratio ($\delta q = 0$) and minimum drag or axial-force coefficient variation with Mach number is shown in Fig. 16. The maximum lift-to-drag ratio is 4.1 at Mach number 0.65, decreasing to 3.1 at Mach number 1.05. The minimum axial-force coefficient ($C_{A_0} = 0.445$) occurs at Mach number 0.65. The drag coefficient rises sharply to a value of 0.895 at Mach number 1.05.

The variation of the static margin $(X/d)_{trim}$ with Mach number for various trim conditions is shown in Fig. 17. The vehicle is stable with a minimum static margin of -0.175 body diameters which occurs at Mach number 0.5 for a $\delta q = 0$.

An indication of the vehicle maneuverability is also illustrated in Fig. 17. At Mach number 0.6, a pitch deflection of -10 deg will produce a load factor of 3.75 at sea level. This value is reduced approximately 30 to 26 percent at an altitude of 10,000 ft.

To evaluate the validity of the single flap technique $C_{N,a_{\delta q}}$, $C_{m,a_{\delta q}}$, $C_{Y,a_{\delta r}}$, $C_{n,a_{\delta r}}$, and $C_{\ell_{\delta p}}$ values obtained using the single flap technique are compared with values obtained using the multiple flap technique. These comparisons are shown in Figs. 18a through 22b. Comparisons are made for both pure (δp, δq, or δr) and combined control surface deflections. In most of the figures, the single flap technique exhibits lower values of the effectiveness parameters than the multiple flap test. The differences could be a result of the errors in setting the flaps. However, errors of at least 1 deg and in many cases more than 10 deg would be required to account for the differences in the data. These values are much larger than the uncertainty of ±0.25 deg that was found during the calibration of the flaps. A more probable cause for the differences is flap-to-flap interference. For example, flap No. 1 at a negative deflection produces a certain value for the flap-to-body interference factor. The same is true with flap No. 4 at a negative deflection. However, with flaps No. 1 and 4 both deflected, the flap-to-body interference factor may be much larger (which is the direction the data indicate) than when only one of the flaps is deflected. This reasoning would lead to the conclusion that the pure roll control data should agree, since all flaps are deflected away from each other. In general, the comparisons are better for roll than pitch or yaw control as shown in Fig. 22. The effect of these differences should not be significant in the trajectory analysis phase of this project. However, the calculated values for δp, δq, and δr would be high by 1 or 2 deg as compared with the multiple flap results.

In Fig. 23, flap hinge-moment coefficients obtained for flaps No. 3 and 4 are presented as a function of model angle of attack for Mach numbers 0.65 and 0.95. The maximum value of the hinge-moment coefficient obtained for each flap was approximately 0.008 at Mach number 0.95. This corresponds to 350 in.-lb of moment at sea-level conditions and is within the actuator torque limit of 540 in.-lb available with the KMU-353A/B kit. At angles of attack less than 12 deg at Mach number 0.65, a negative hinge-moment coefficient is obtained for the two flaps. The negative coefficient is an aiding aerodynamic moment, that is acting in the same direction as the flap actuator. The reverse is true at Mach number 0.95 where the flap center of pressure has moved behind the hinge line and produces opposing moments.

4.2 PHASE 2

The second series of test consisted of captive trajectory tests using an 0.05-scale model of the F-4 aircraft. Data were obtained with the TCTV located on the right inboard pylon (MAU-12) of the aircraft. Tests were conducted with and without the two outboard 370-gal fuel tanks. The data presented in Fig. 24 are for the aircraft with tanks at Mach number 0.95. Trajectories were obtained with the TCTV flap settings (δq) fixed at 0, 15, and -15 deg. The attitude of the parent aircraft was set to correspond to a trim condition

when flying at an altitude of 40,000 ft. Simulated ejector forces used to drive the vehicle away from the aircraft were 3,000 lb/ejector and were terminated after a stroke length of 3.8 in. The data are presented in terms of full-scale distances and real time.

The data in Fig. 24 show a clean separation from the aircraft when the flap settings were zero deg. When the flap settings were either δq = -15 deg (Fig. 24a) or δq = 15 deg (Fig. 24b) the vehicle experienced a high pitch rate and in both cases struck the parent aircraft. The 15-deg settings were tested to simulate a control system malfunction which would drive the flaps to the electrical limits of travel. The test results indicate that stringent preflight checks must be performed to prevent a failure in the vehicle control system resulting in hard-over commands.

5.0 DIGITAL SIMULATION

5.1 SIMULATOR PROGRAM

The computer program used to simulate the flight characteristics of the vehicle was originally written by Litton Systems (Ref. 4). The program was adapted to the MK-84 HOBOS munition by Rockwell International Corporation during the munition development. The program was again modified at the AEDC to support development of the Stubby HOBO munition; a description of that program can be found in Ref. 5. For use in flight simulation studies of the TCTV, further modifications were made to the program. The modifications included (1) the inclusion of the equations required for modeling the autopilot used for midcourse control and (2) the inclusion of the tables and table look-up routines required for determining the vehicle aerodynamic coefficients from the data obtained using the single flap test technique. The latter required assembling a four-dimensional table for each of the six aerodynamic coefficients. The coefficients in the tables were functions of M_∞, α_a, ϕ_m, and $\delta 1$. The tabulated values were the sum of one-fourth the coefficient obtained for the model with flaps set to zero and the incremental coefficient obtained from flap No. 1 deflections. Thus, the table look-up was rather unique. By using relations as discussed in Section 3.3 to establish the orientation of each fin (δ_m) and the computer program inputs of M_∞, α_a, ϕ_a, and δx; one-fourth of the total value of a aerodynamic coefficient, $C_{N,a}$ for example, could be obtained by one pass through a table. Four passes through the table (one each for $\delta 1$, $\delta 2$, $\delta 3$, and $\delta 4$) yielded four increments of data which were summed to obtain the total aerodynamic coefficient at a given M_∞, α_a, ϕ_a, and control setting. Interpolation procedures for each of the six tables were identical with respect to M_∞, α_a, and ϕ_a, thus only four interpolations corresponding to the flap settings were required. Using this technique no modeling of the data using trigonometric functions is required, since all the variables f(M_∞, α_a, ϕ_a, and $\delta 1$) are in the tables.

13

The characteristics of the flap actuator system (frequency, response, etc.) used in the simulation were the same as those used in Ref. 5.

5.2 PRESENTATION OF SIMULATOR PREDICTIONS

Trajectory and flight characteristics of the vehicle were examined using a digital computer flight simulation program. For a given altitude, a series of simulated flights were made to optimize the control system gain and the dynamic pressure setting. Figure 25 presents the trajectory and flight characteristics for the vehicle when launched from an altitude of 40,000 ft, a Mach number of 0.95, and a dynamic pressure setting of 320 psf. The vehicle maintains a near constant glide slope over a range of 175,000 ft or approximately 29.5 nautical miles (Fig. 25a). The trim angle of attack stabilizes at approximately 8.8 deg (Fig. 25c), whereas the Mach number decreases throughout the flight. The Mach number at impact is 0.46. Pitch flap requirements vary from -11.4 deg at 20 sec into the flight to -3.3 deg at impact. The results of the extended range flight simulations indicated the sensing of the dynamic pressure provided a satisfactory means of trimming and controlling the vehicle during extended range flight.

To investigate the lock-on-after-launch capability of the vehicle, the simulation program was reconfigured to accept the television-type seeker inputs. The initial program inputs describing the vehicle attitude and velocity were chosen as those existing at 10,000-ft altitude during the constant dynamic pressure flight. At this point, Mach number was 0.574 and the angle of attack was 8.8 deg. A sufficient number of simulated flights were made to obtain the footprint shown in Fig. 26. The minimum range corresponds to the maximum depression angle of the gimbal supporting the seeker which was -20 deg. The cross range on the footprint corresponds to the maximum seeker angle that could be obtained in yaw or ±15 deg. The downrange limit on the footprint represents the point at which the vehicle would impact at Mach number 0.5. The resultant footprint encompasses a downrange displacement varying from a minimum of 22,800 to a maximum of 42,400 ft. The cross range varied from 6,700 to 11,000 ft.

6.0 CONCLUDING REMARKS

Based on the wind tunnel test and the computer simulation results, the following conclusions can be made regarding the 2400-lb trajectory control test vehicle (TCTV).

1. The TCTV is a statically stable vehicle having a maximum lift-to-drag ratio of 4.1 and a minimum static margin of -0.175 body diameters for zero deg of flap deflection.

2. The KMU-353A/B guidance and control system can be modified to provide a controllable vehicle in both the midcourse and terminal phases of a

14

trajectory. By using the technique of flying at a constant dynamic pressure, the vehicle has a range of 29.5 nautical miles when launched at an altitude of 40,000 ft and Mach number 0.95.

3. The separation of the vehicle from the F-4 aircraft is clean in the jettison mode with controls locked. Simulation of a failure model with the control flaps deflected indicates that the vehicle would strike the aircraft.

4. The magnitude of the TCTV control effectiveness parameters obtained using the single flap test technique was generally found to be less than that obtained using the multiple flap test technique. In terms of wind tunnel test time, however, the single flap method is very efficient for obtaining large quantities of control effectiveness data. Because large quantities of data are required for computer flight simulation programs, the technique is valuable, and therefore, further investigation of the differences mentioned above is warranted.

REFERENCES

1. MacLanahan, D. A., Jr. "Calibration of Angle-of-Attack and Dynamic Pressure Sensors on the Modular-Guided Glide Bomb at Transonic Mach Numbers." AEDC-TR-72-124 (AFATL-TR-72-171) (AD902886L), September 1972.

2. Test Facilities Handbook (Tenth Edition). "The Propulsion Wind Tunnel Facility, Vol. 4." Arnold Engineering Development Center, May 1974.

3. Webb, J. A., Whoric, J. M., and Rittenhouse, L. E. "Aerodynamic Coefficients for the Pavestorm II Weapon Configuration Using Multiple and Single Fin Deflection Techniques." AEDC-TR-74-000.

4. "Modularized Six-Degree-of-Freedom (MODGDF) Computer Program." Volume I+II, Litton Systems, Inc., Guidance and Control Systems Division, Woodland Hills, California.

5. Rittenhouse, L. E. and Cunningham, J. W. "Wind Tunnel, Simulator, and Flight Test Correlation Results on the Stubby HOBO Munition and the BGM-234 Carrier Vehicle." AEDC-TR-72-140 (AFATL-TR-72-187) (AD753074), September 1972.
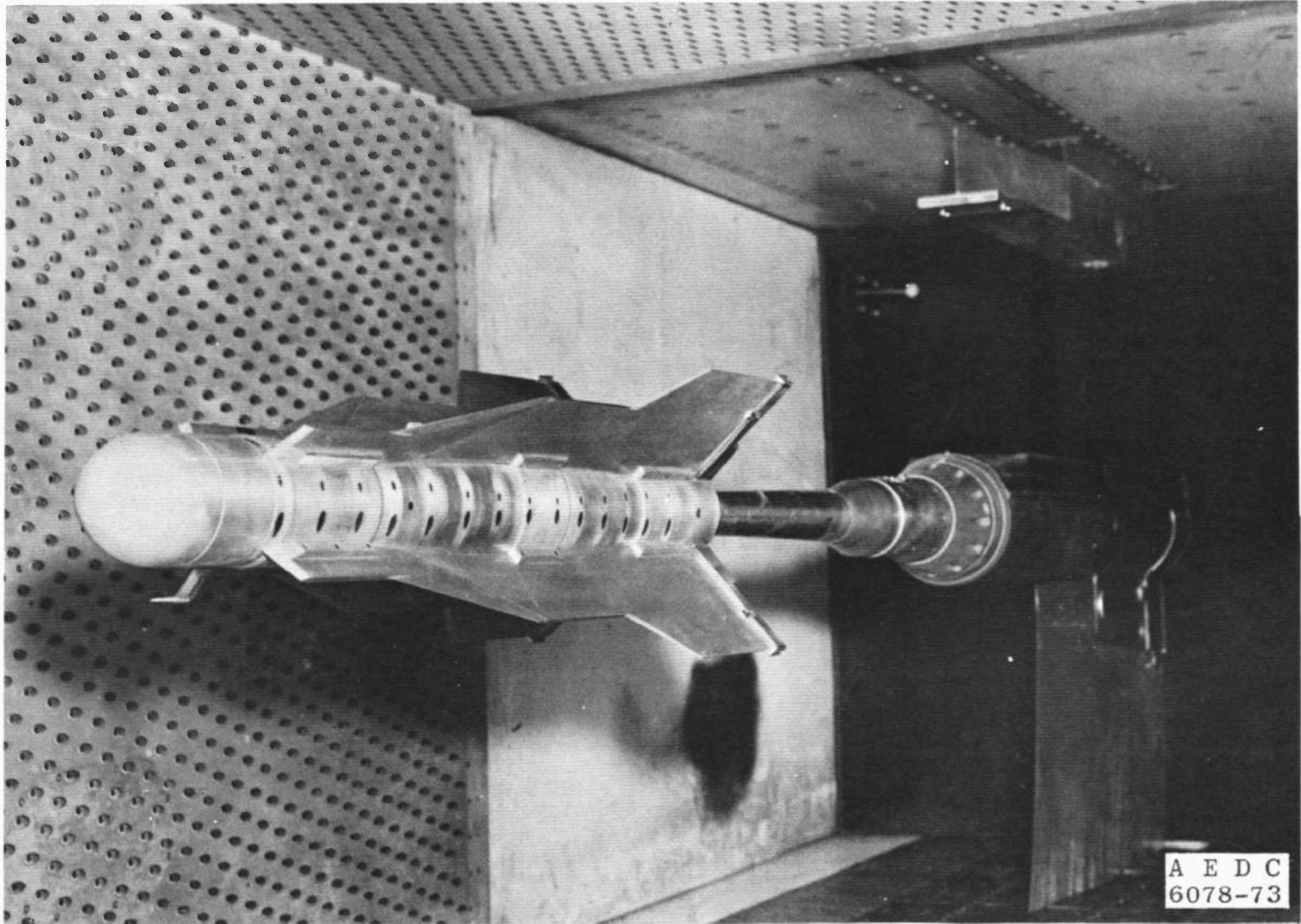
Figure 1. Installation photograph of the 0.25-scale TCTV wind tunnel model.
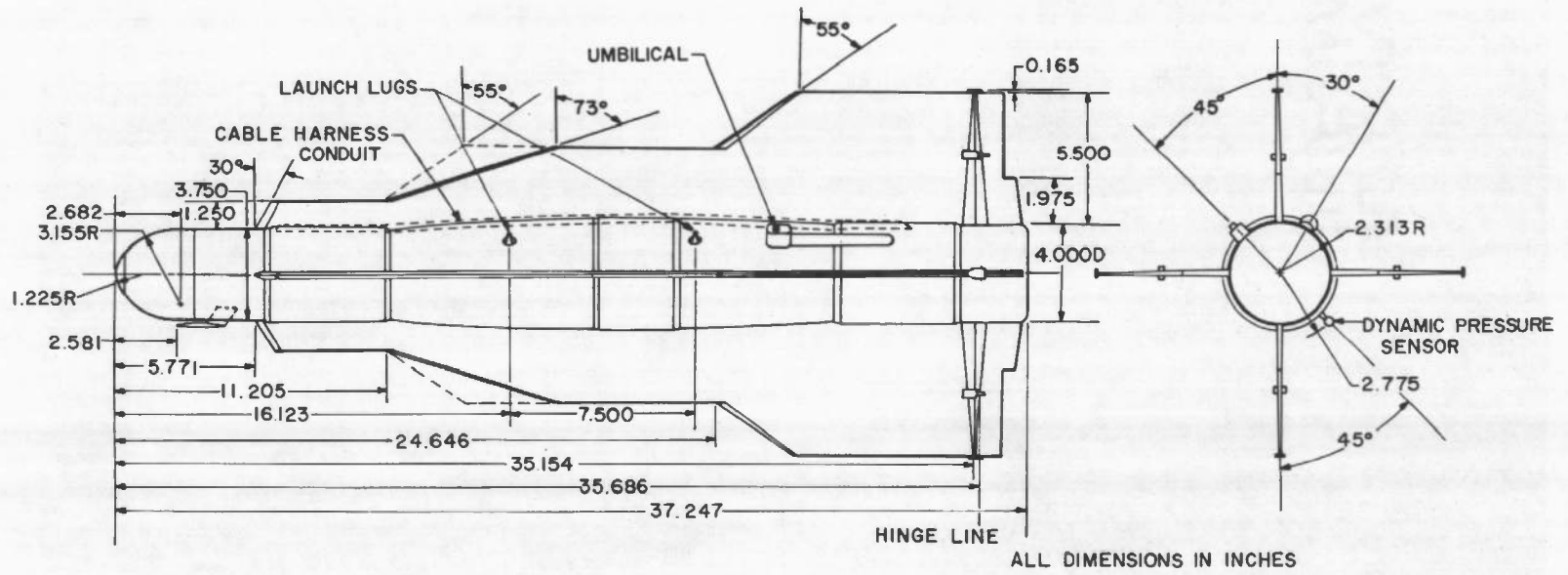
MOMENT REFERENCE = 19.879 AFT OF NOSE
S = 0.11045 ft²
c̄ = 4.5 in.

a. Model details
Figure 2. Model description.

COUNTER WEIGHT

HINGE
BRACKET

0.913 STRAIGHT
LENGTH

4.562
TAPERED
LENGTH
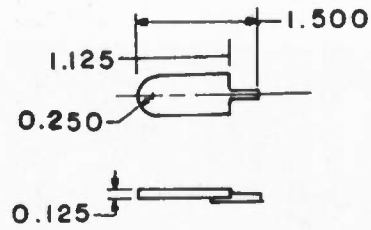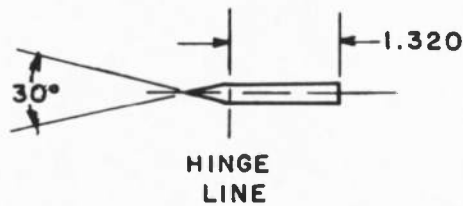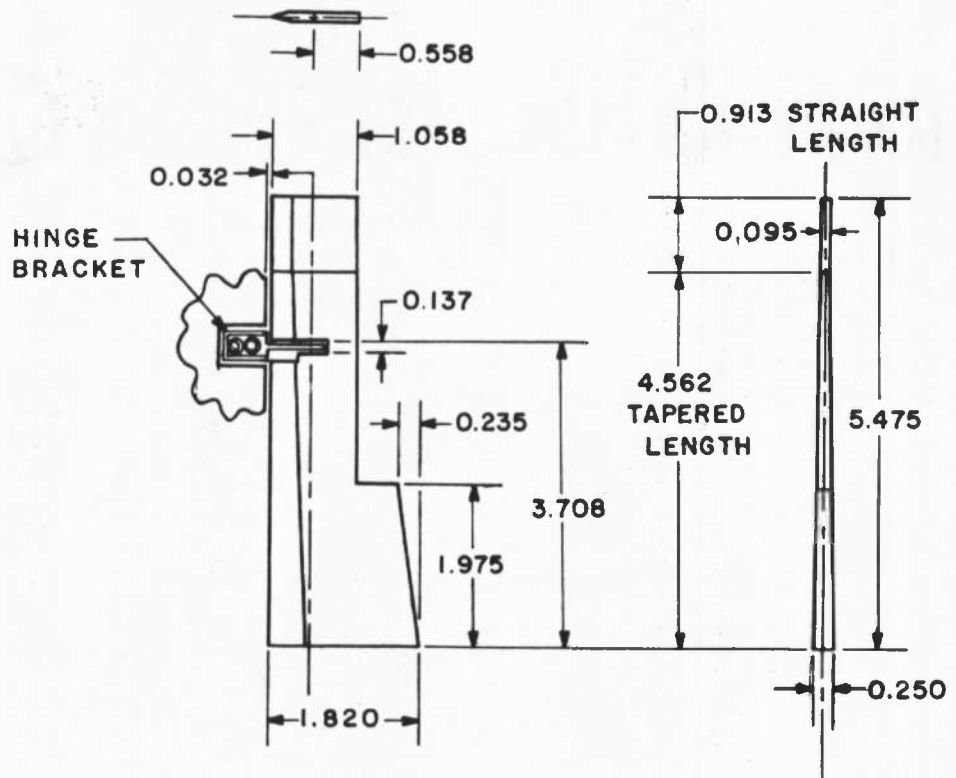
ALL DIMENSIONS IN INCHES

HINGE
LINE

b. Flap details
Figure 2. Concluded.

19
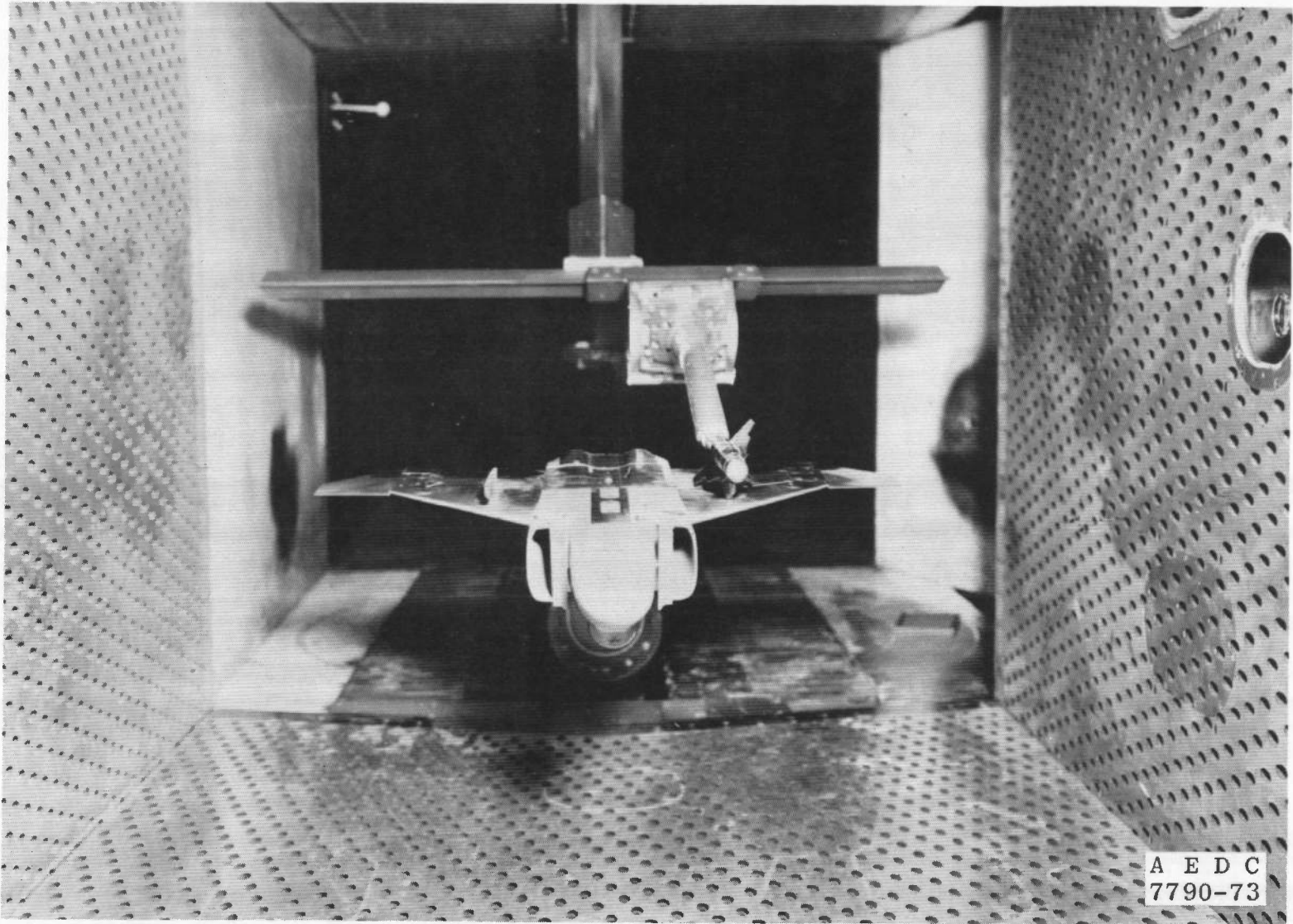
Figure 3. Installation photograph of the apparatus used for the F-4 aircraft separation tests (phase 2).
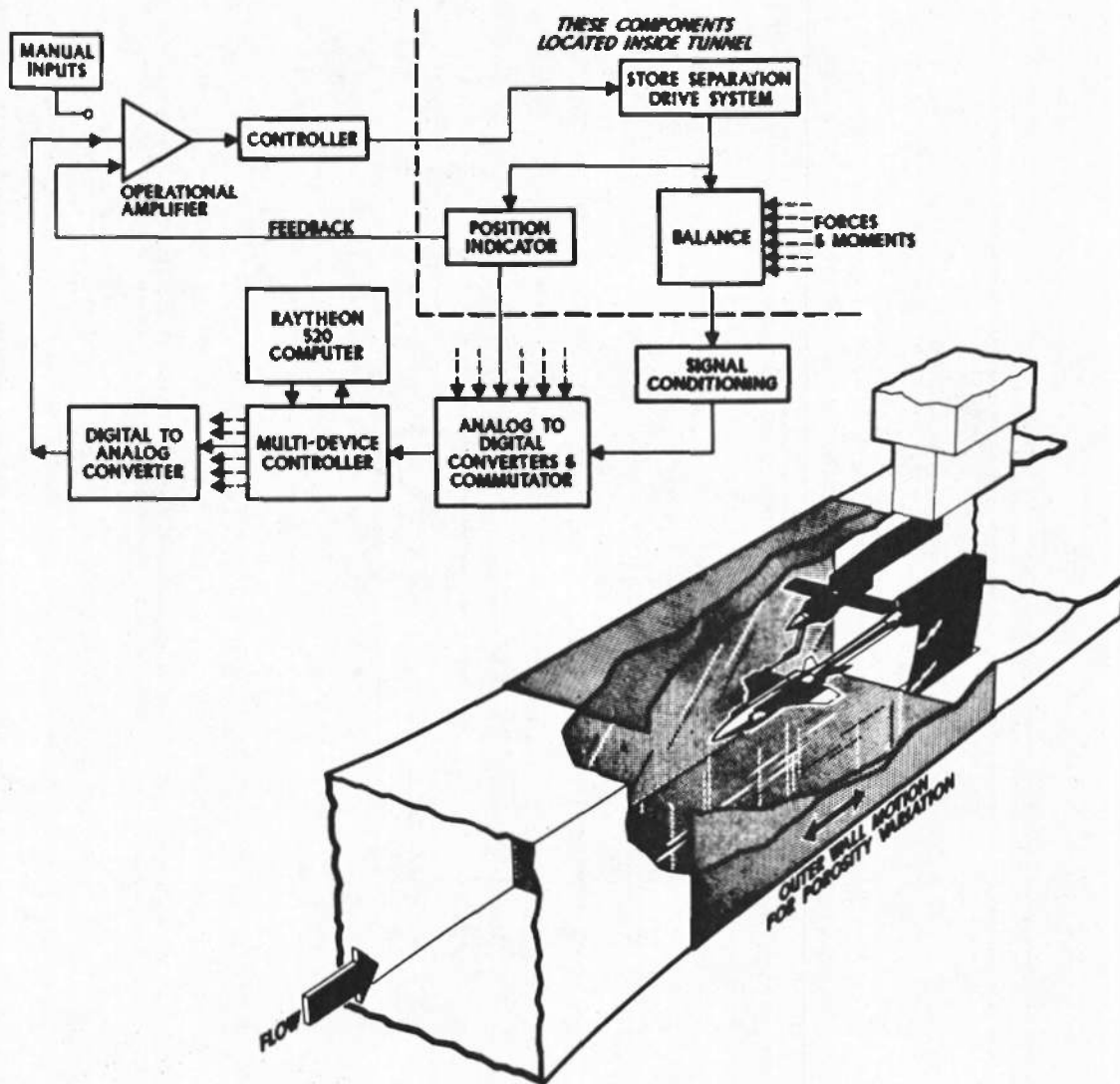
Figure 4. Isometric drawing of a typical store separation installation and a block diagram of the computer control loop.

(LOOKING UPSTREAM)
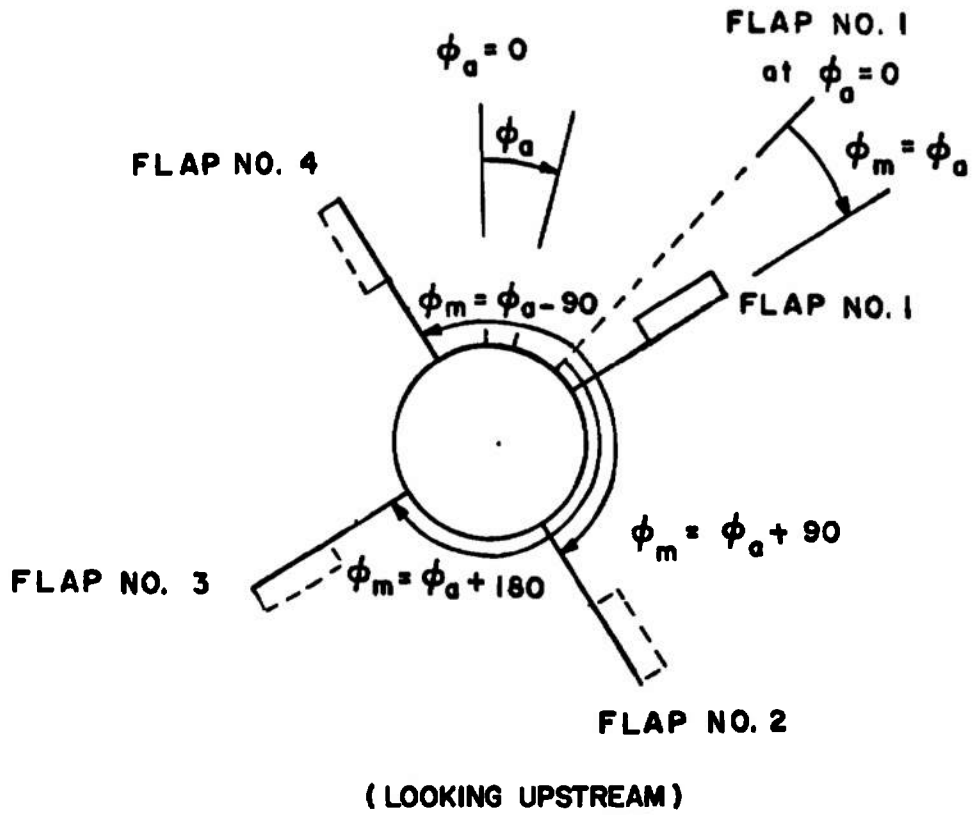
Figure 5. Model roll orientation for single flap test.

a. M∞ = 0.50
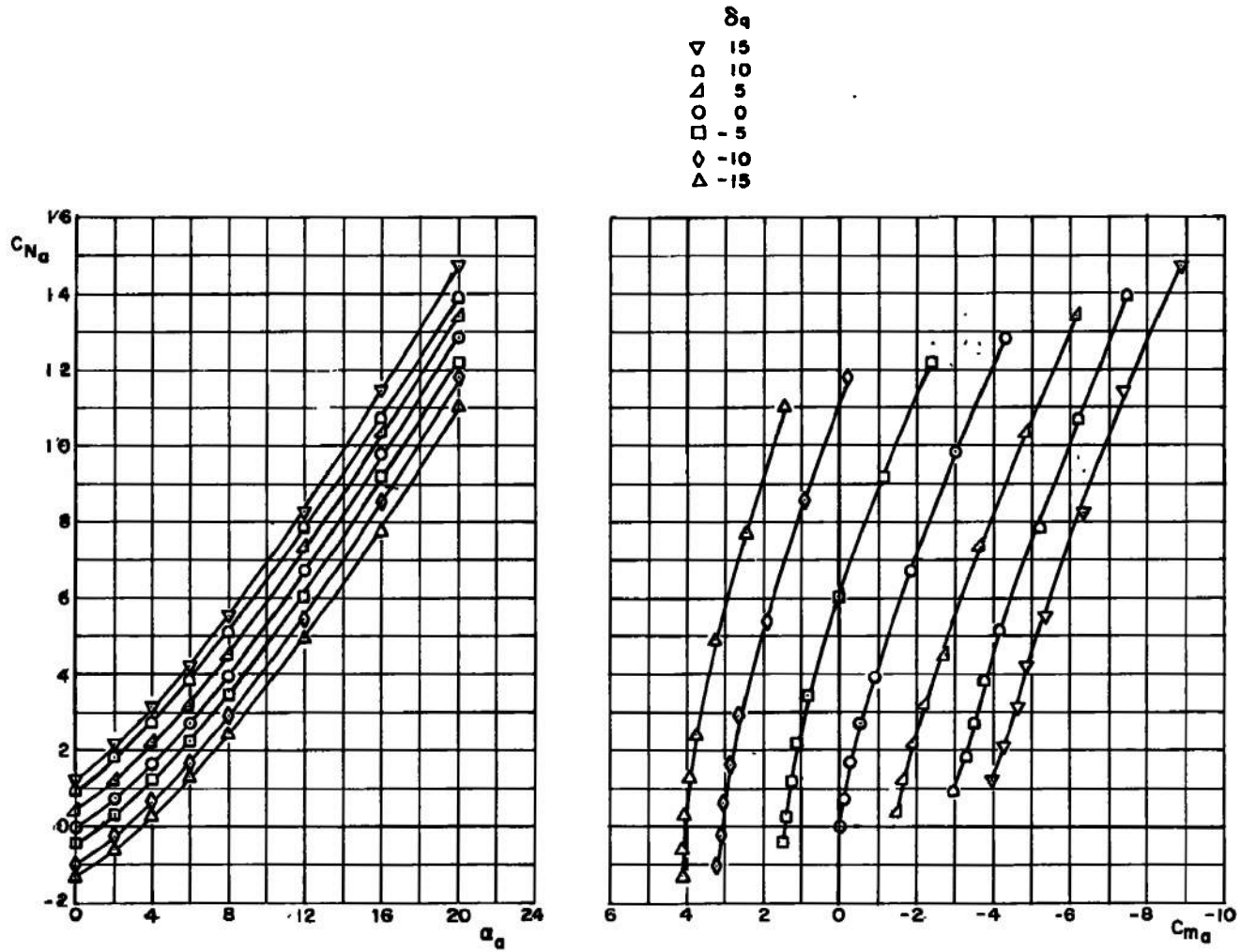
Figure 6. Variation of the normal-force coefficient and pitching-
moment coefficient with angle of attack.
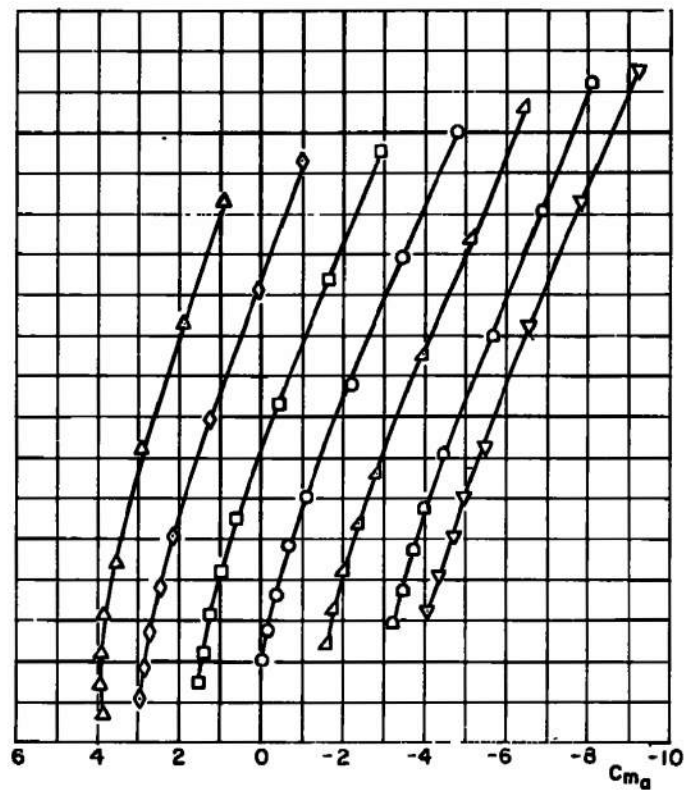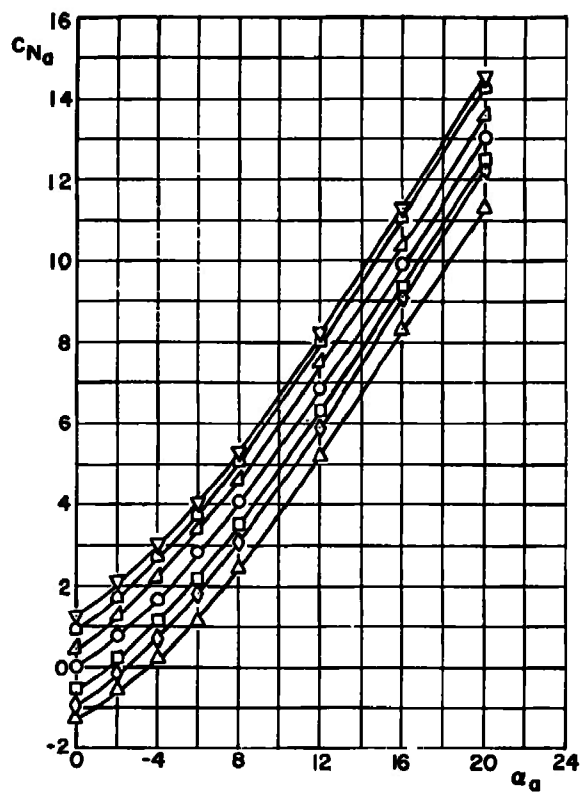
b. $M_\infty = 0.65$
Figure 6. Continued.
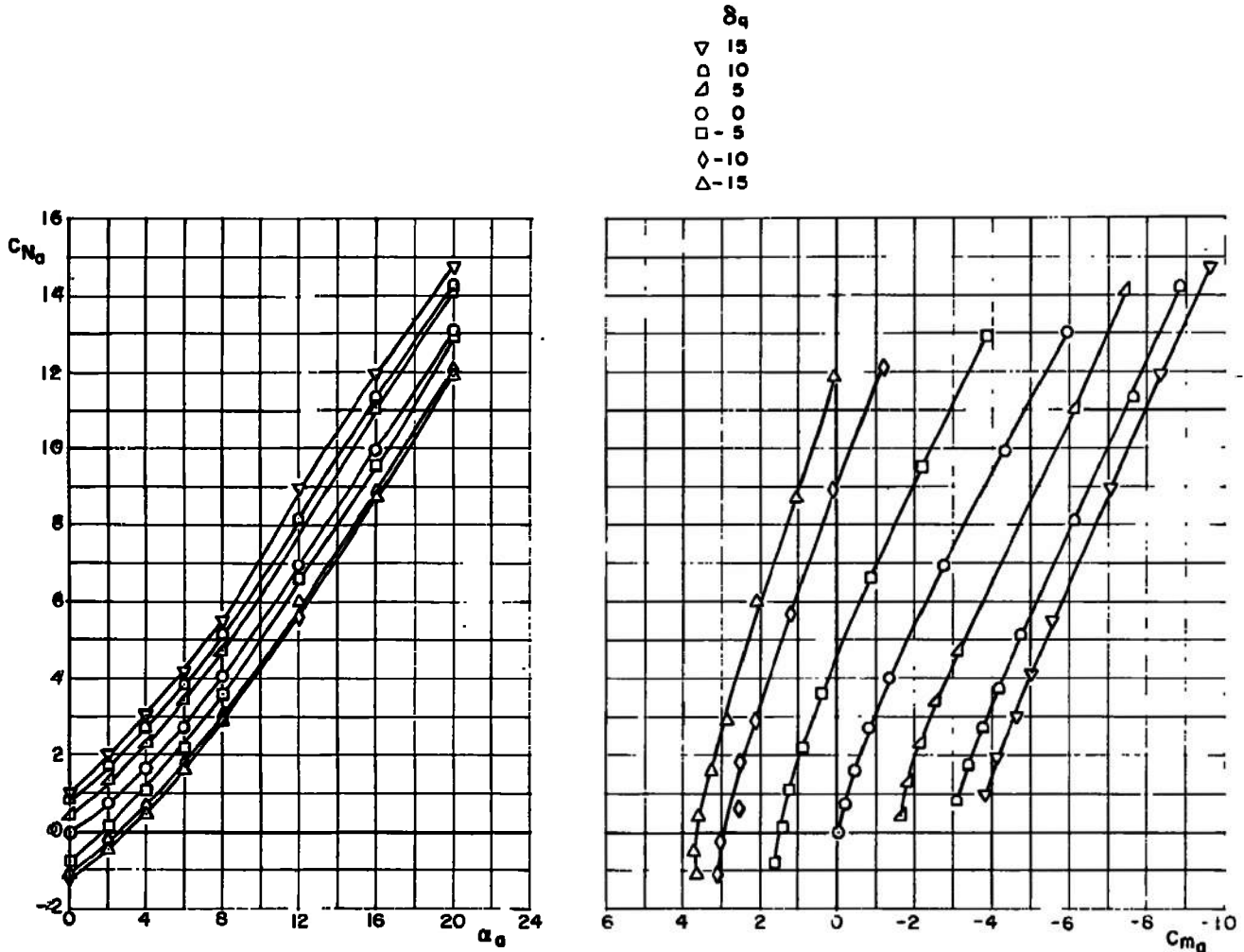
c. M∞ = 0.85
Figure 6. Continued.
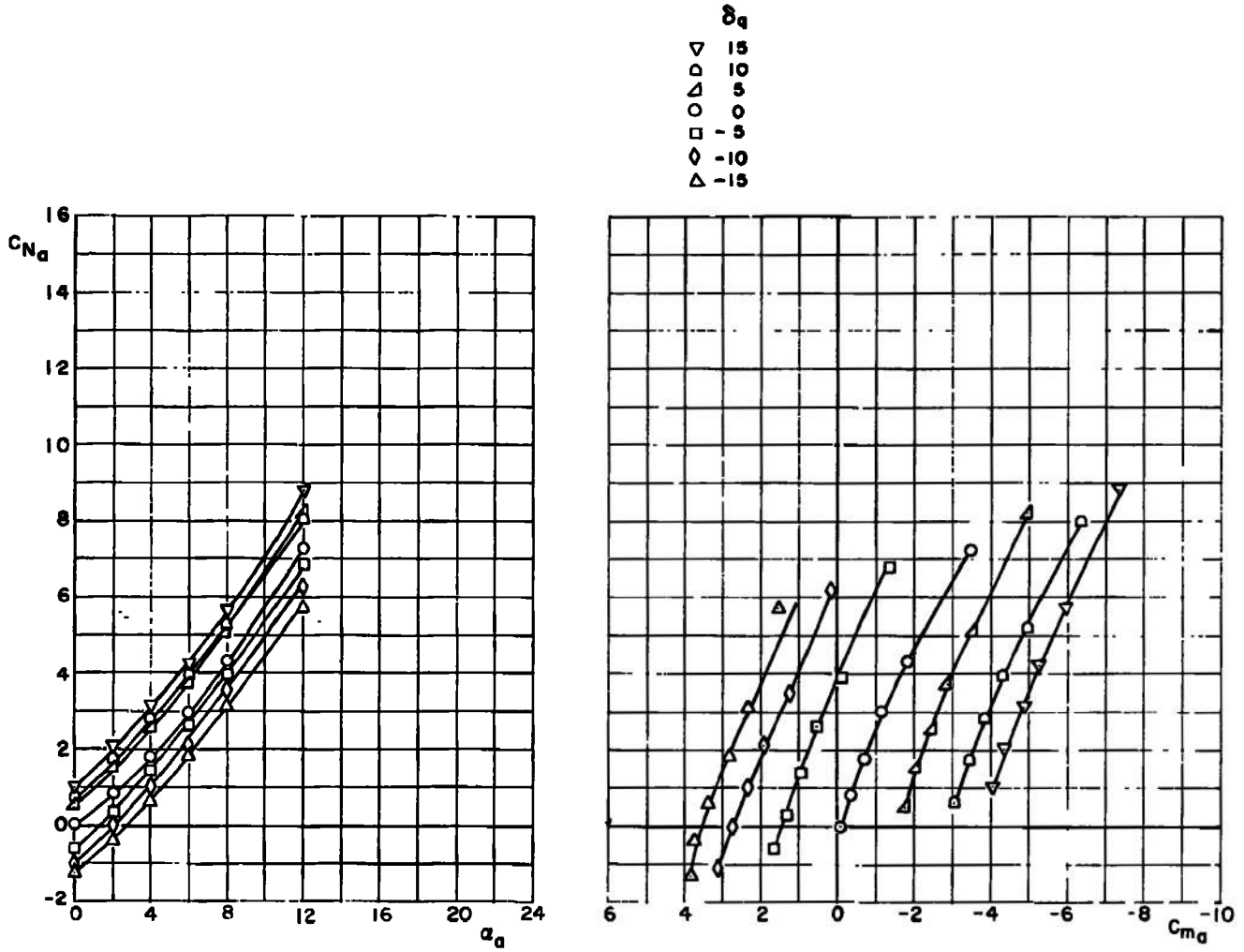
d. $M_\infty = 0.95$
Figure 6. Continued.
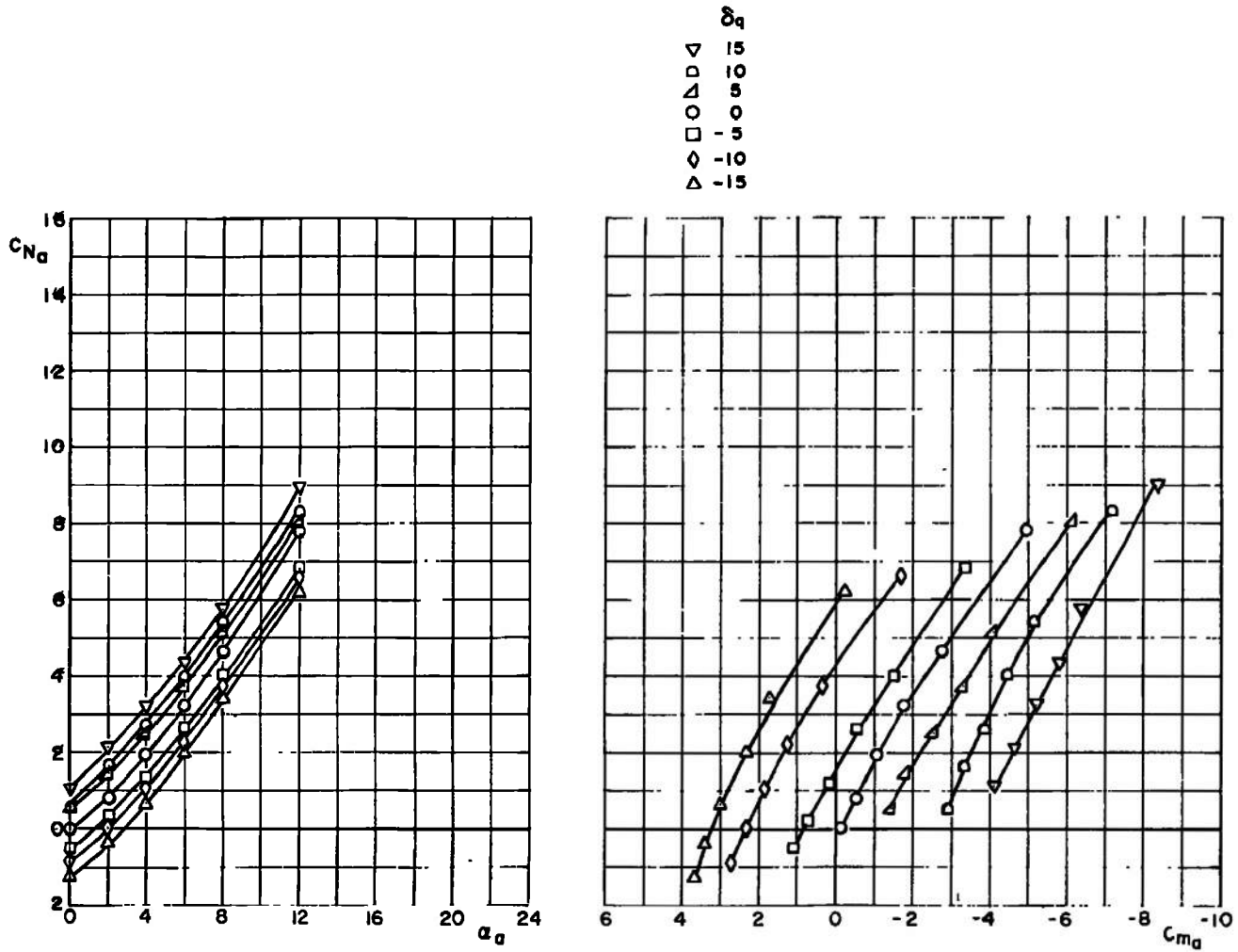
e. $M_\infty = 1.05$
Figure 6. Concluded.
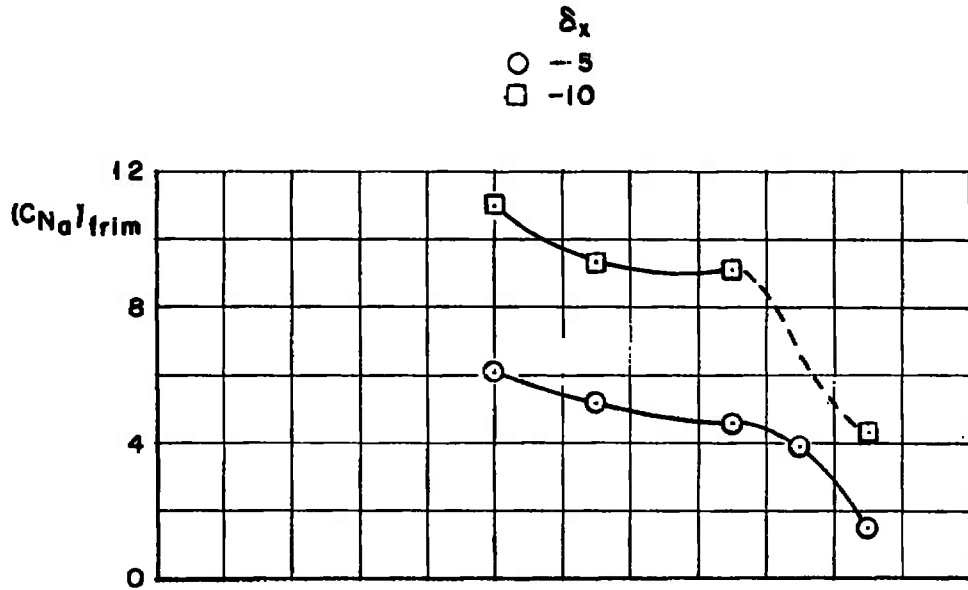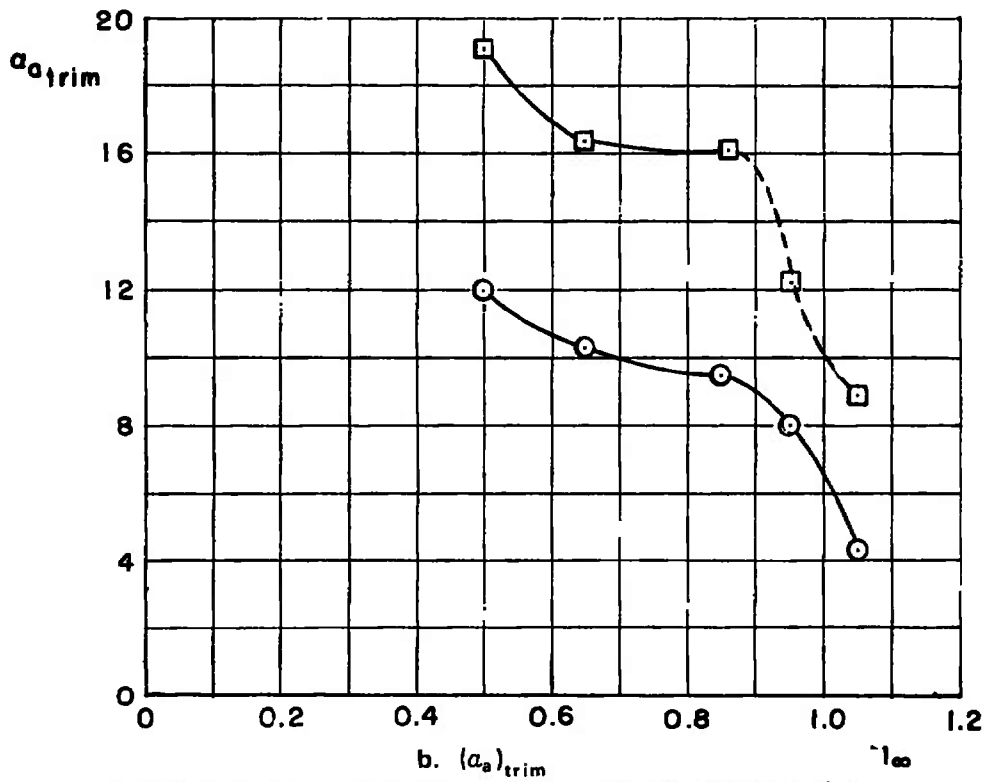
Figure 7. Varation of the trim normal-force coefficient and the trim angle of attack with Mach number.
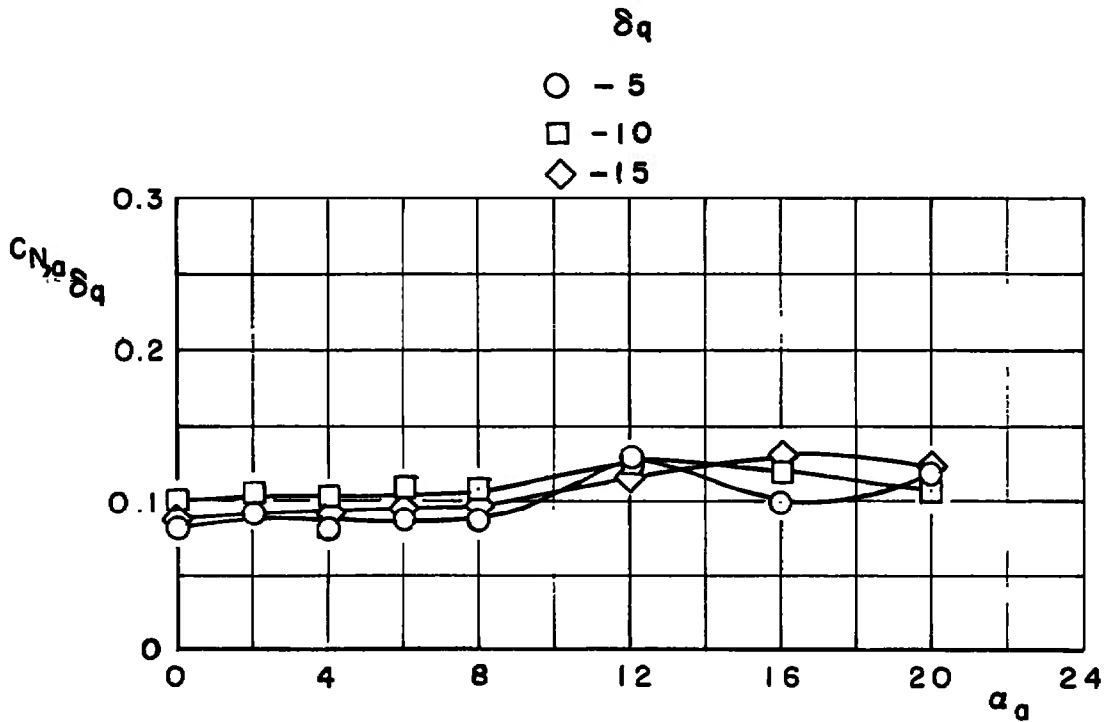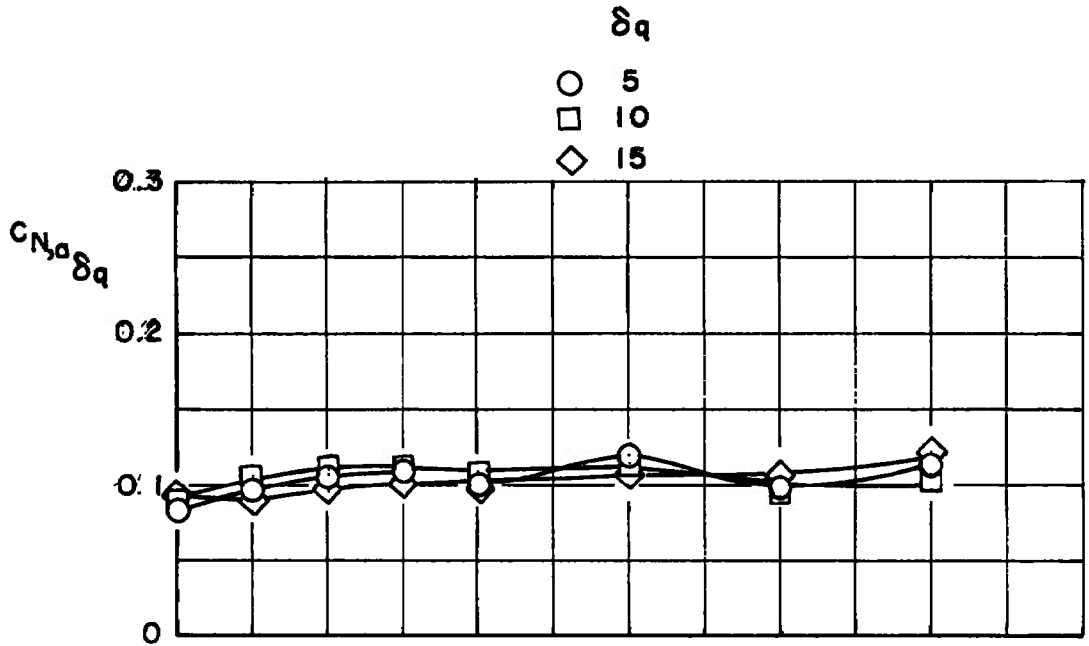
a. $M_\infty = 0.50$

Figure 8. Variation of the normal-force increment with angle of attack.
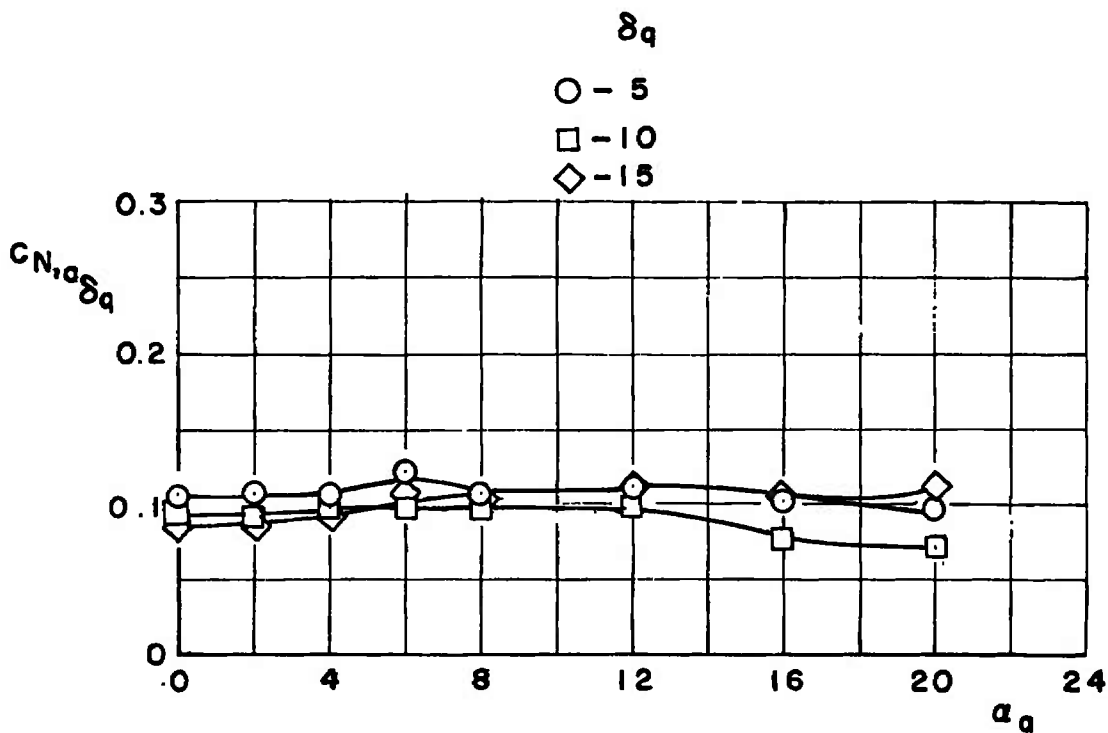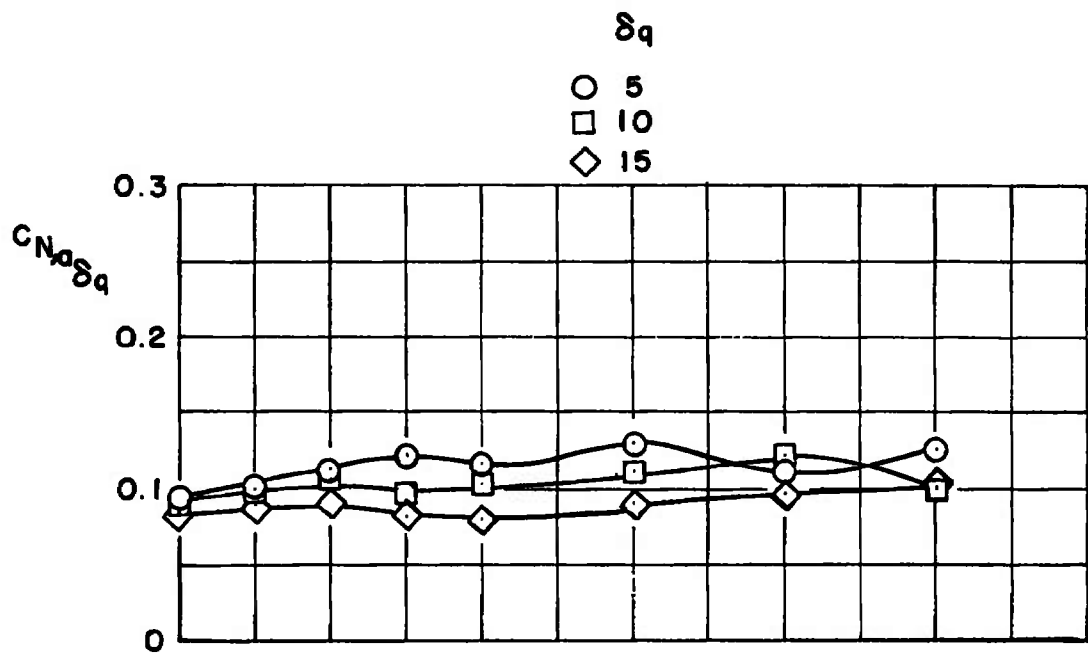
b. $M_\infty = 0.65$
Figure 8. Continued.
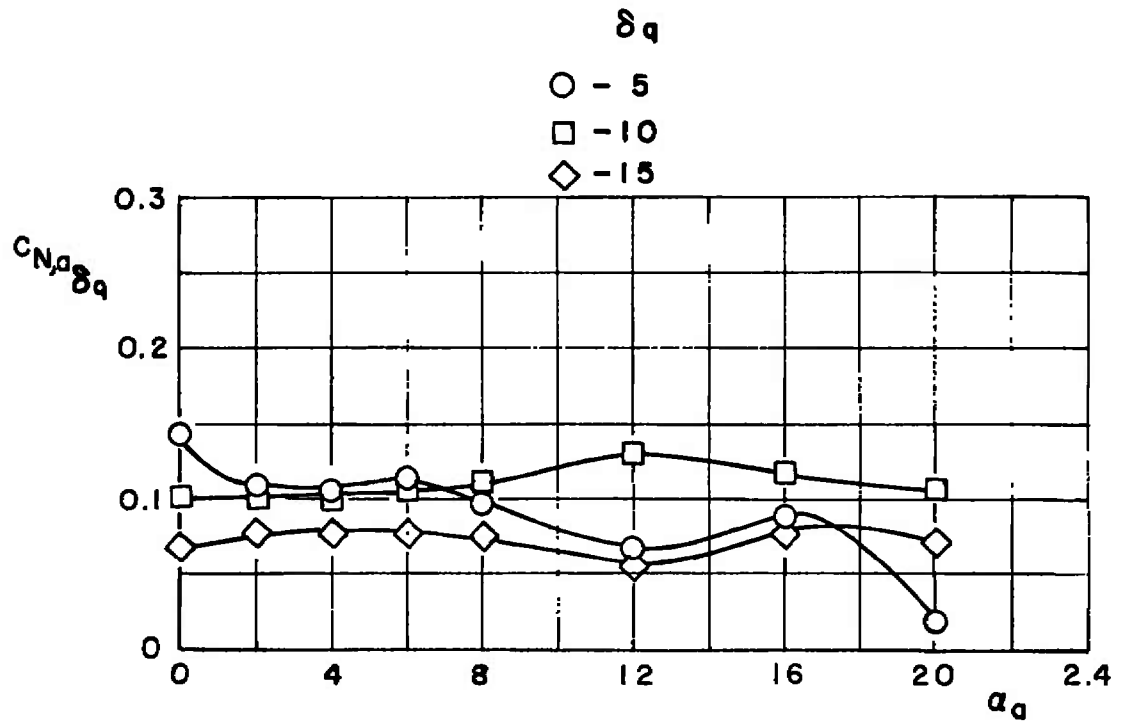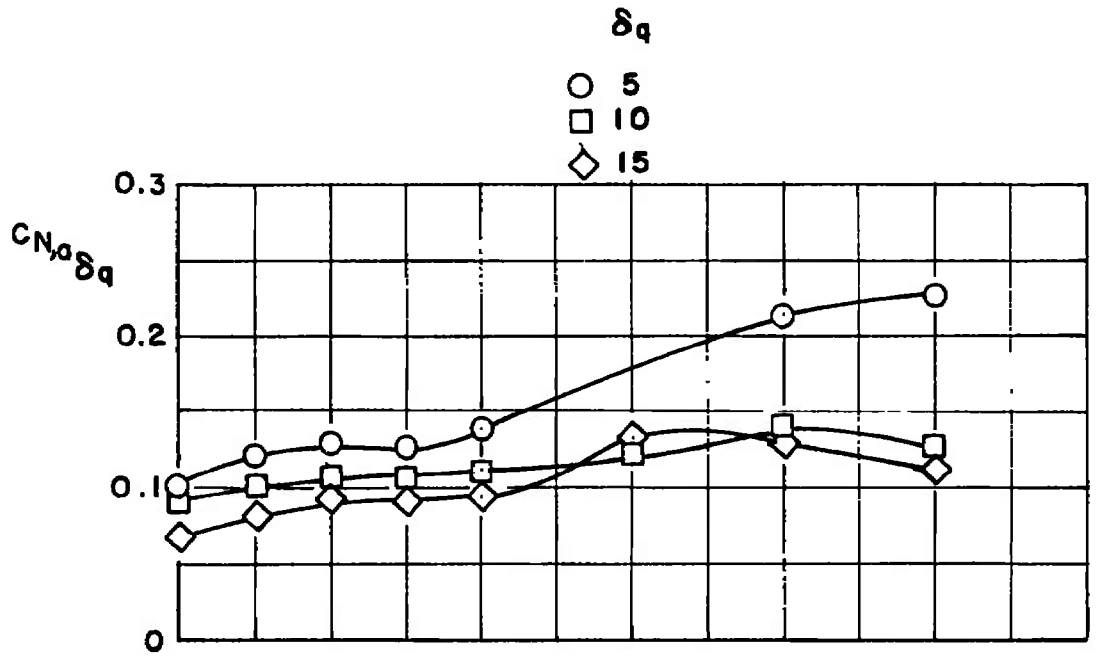
c. $M_\infty = 0.85$
Figure 8. Continued.
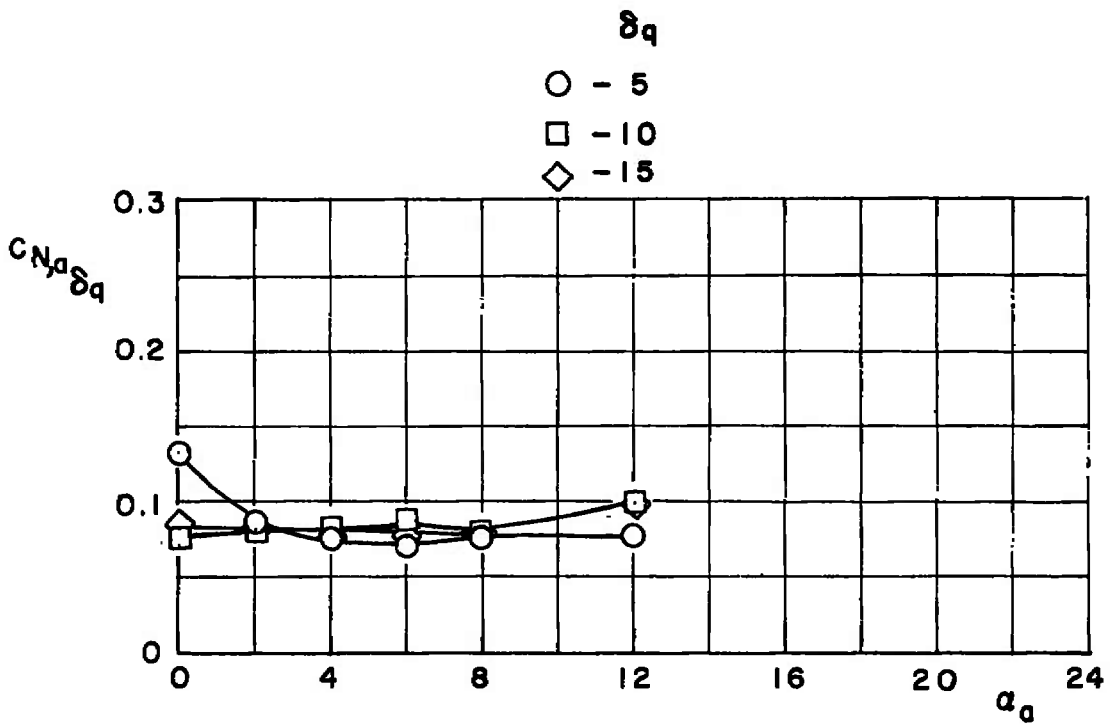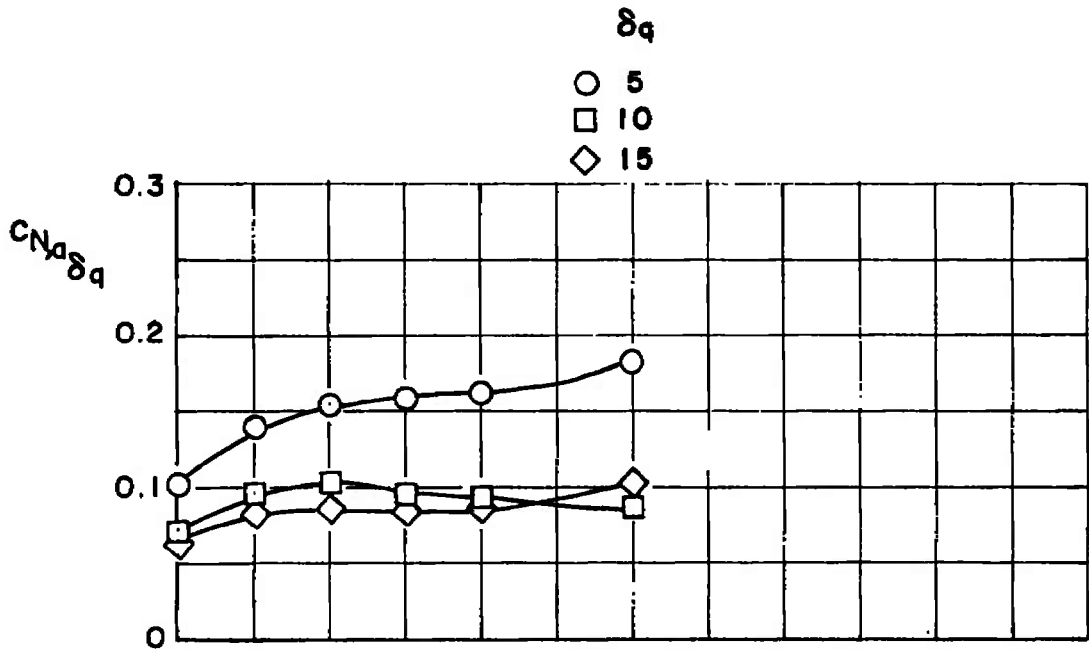
d. $M_\infty = 0.95$
Figure 8. Continued.
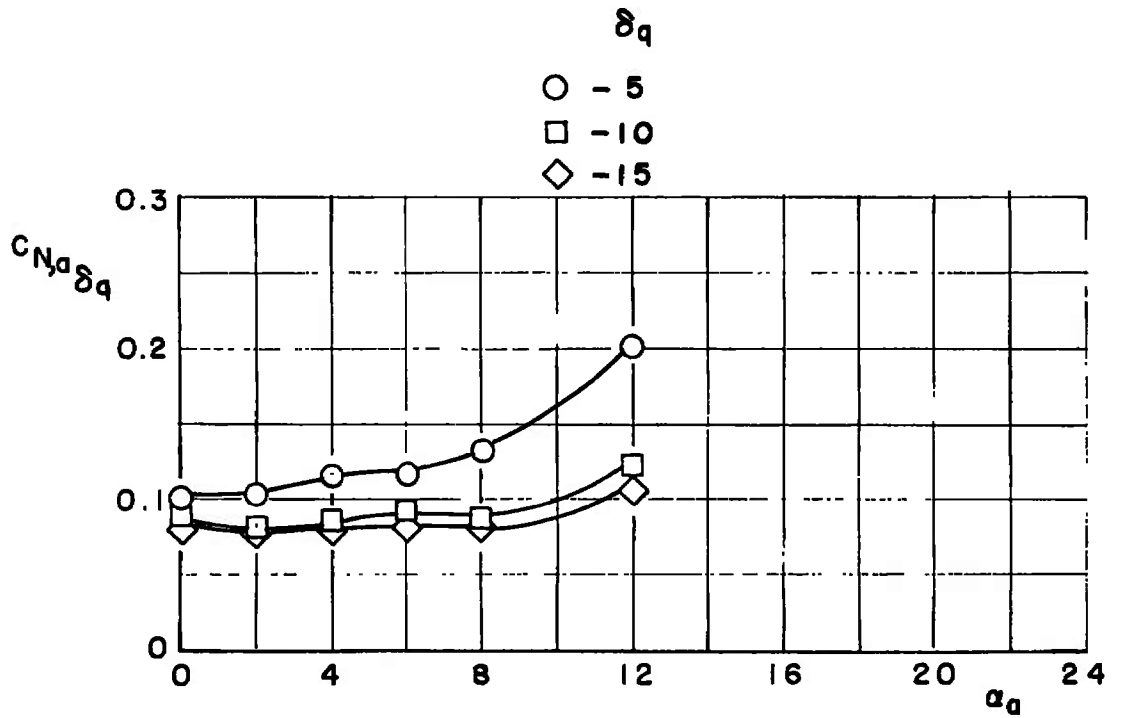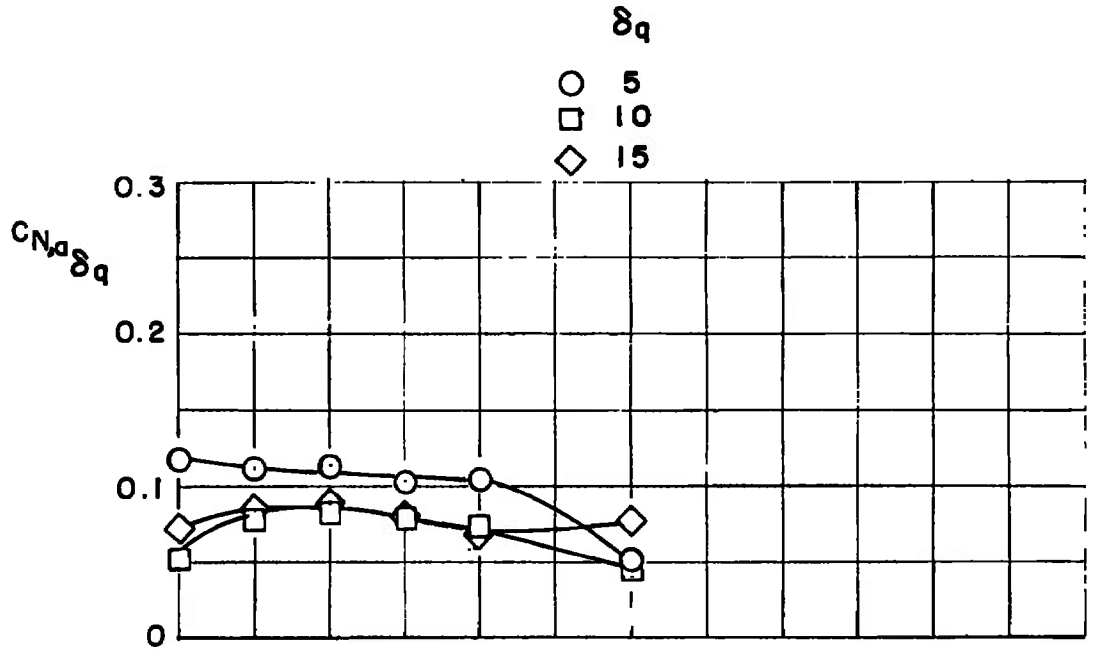
e. $M_\infty = 1.05$

Figure 8. Concluded.
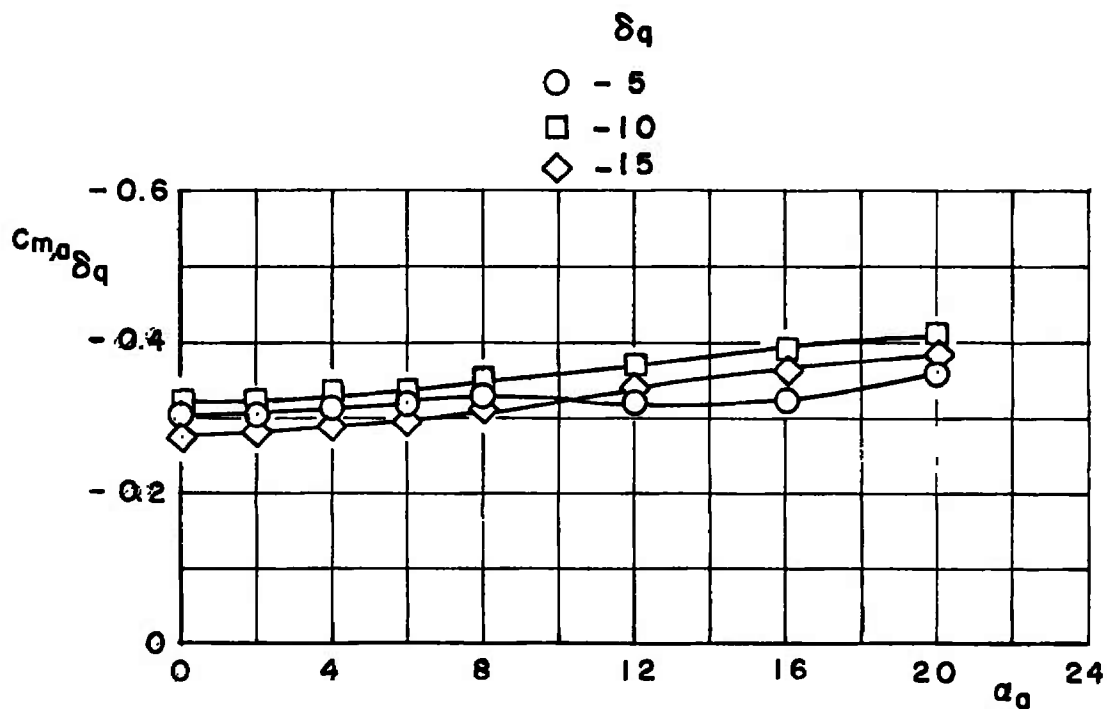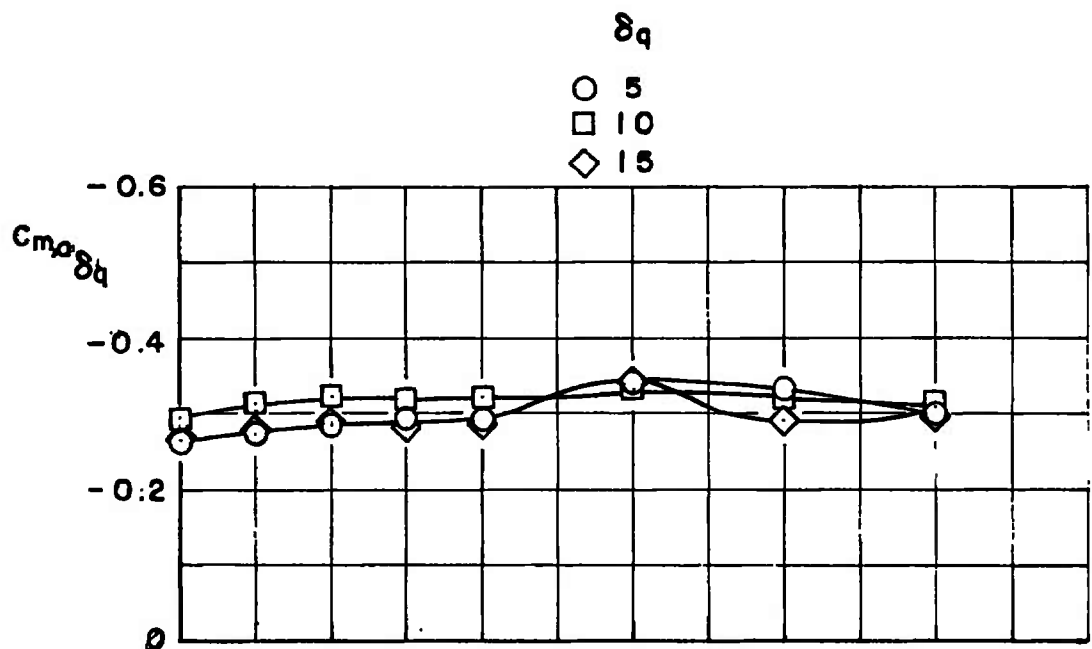
a. $M_\infty = 0.50$

Figure 9. Variation of the pitch control effectiveness with angle of attack.
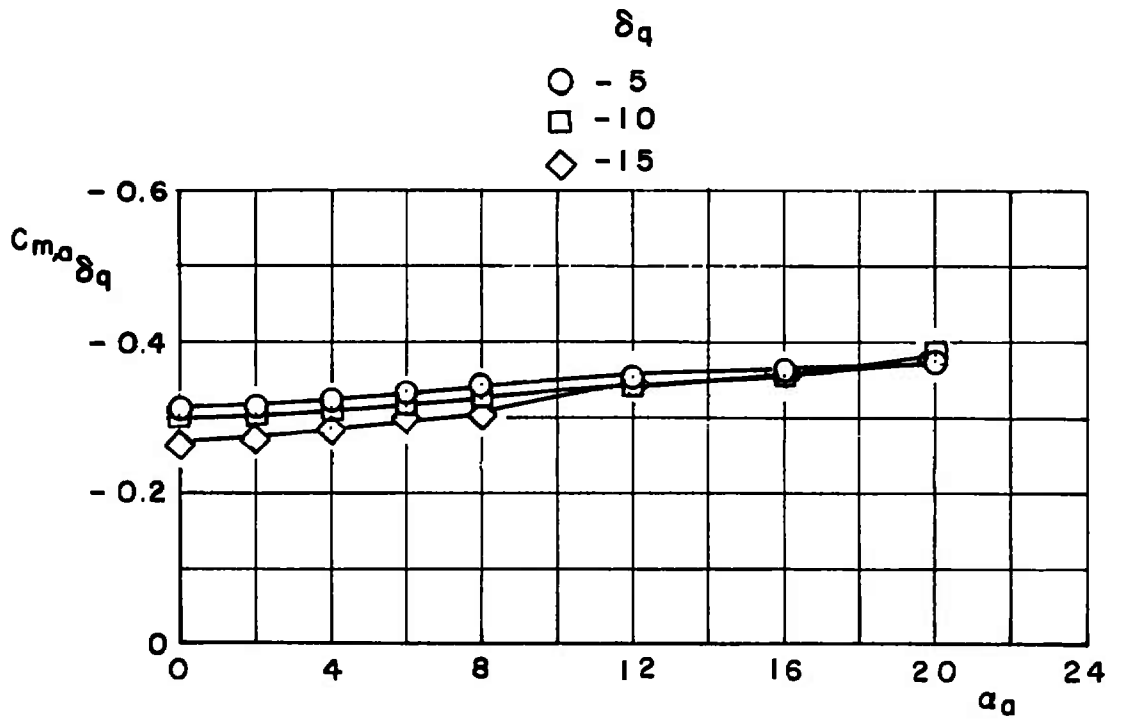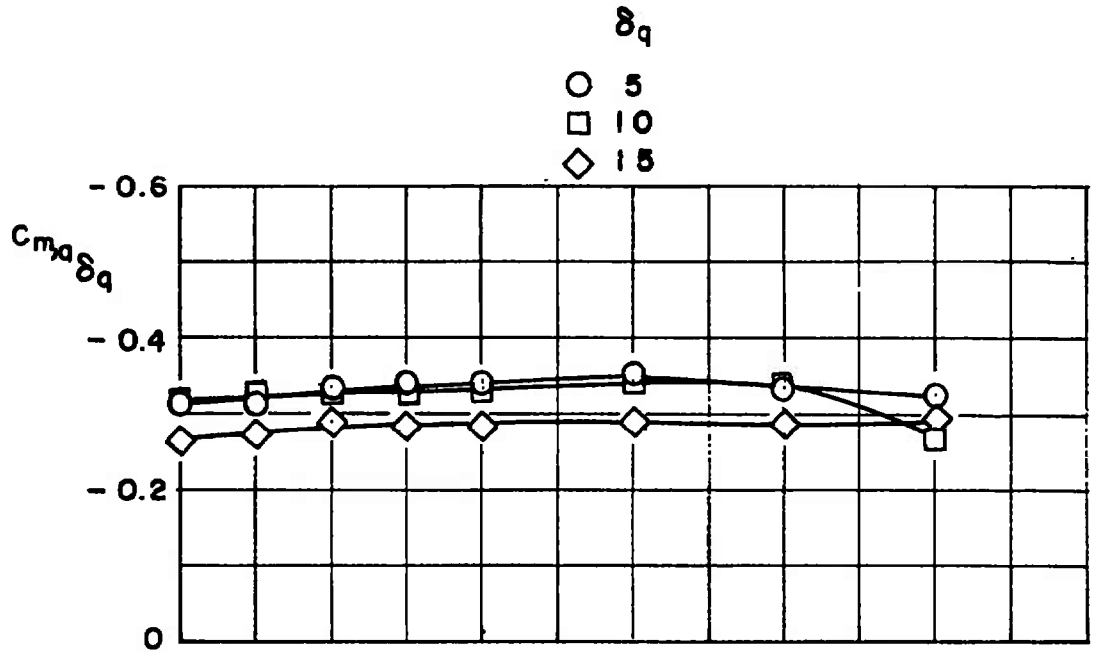
b. $M_\infty = 0.65$
Figure 9. Continued.
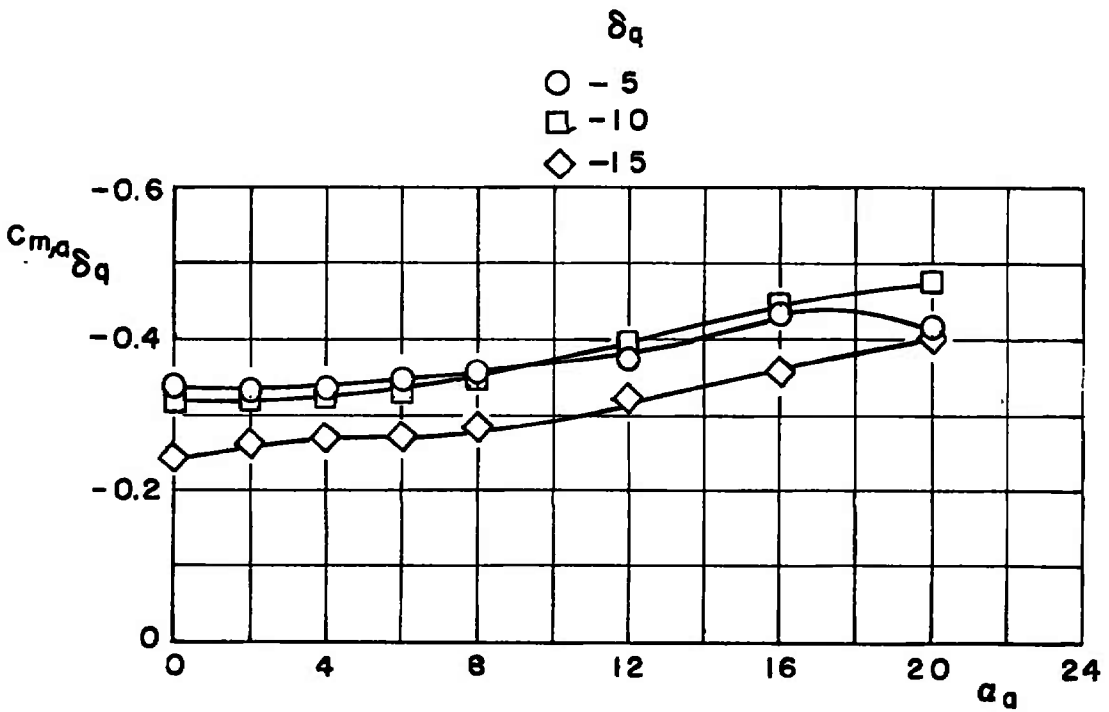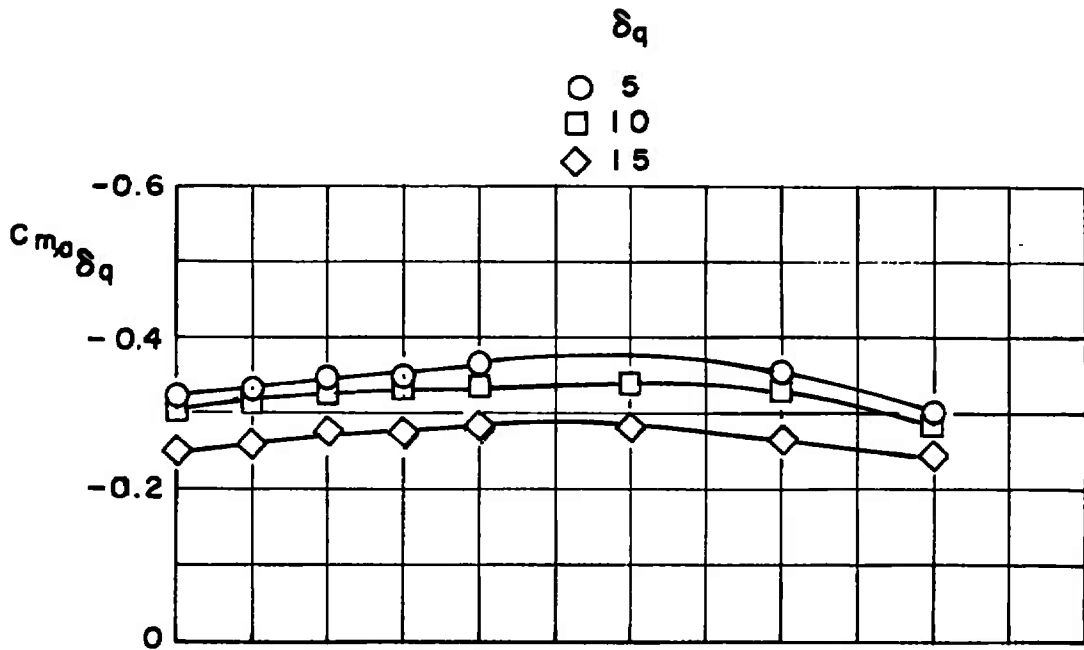
c. $M_\infty = 0.85$
Figure 9. Continued.
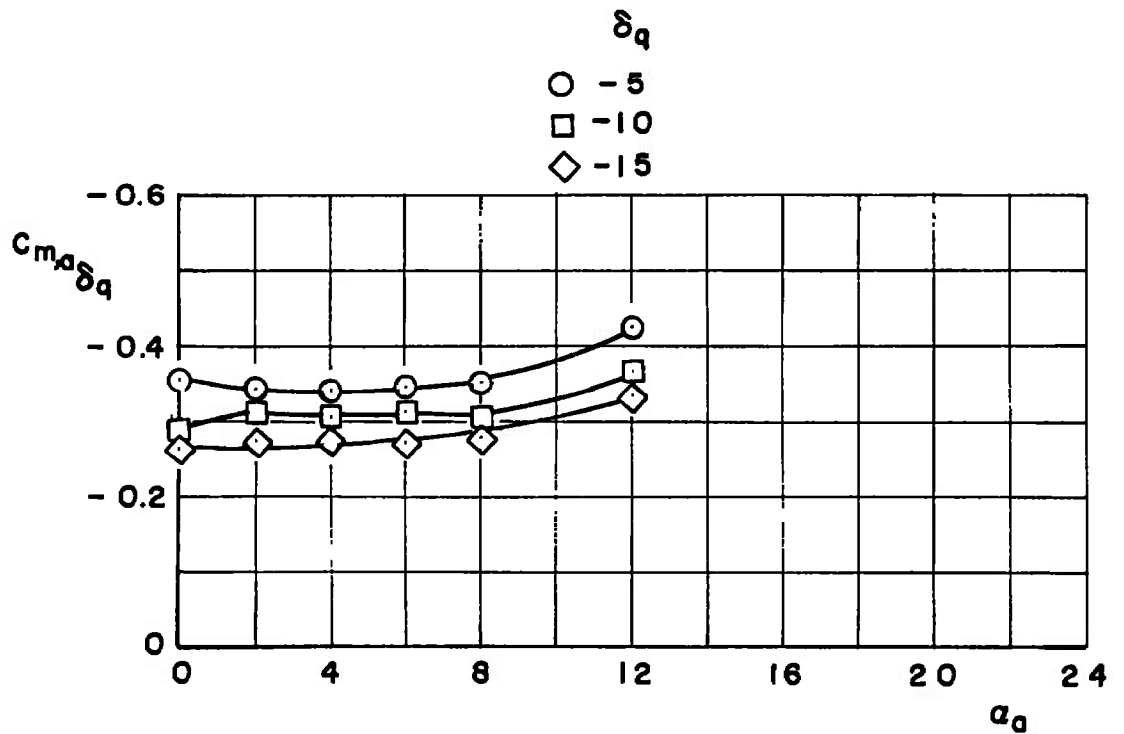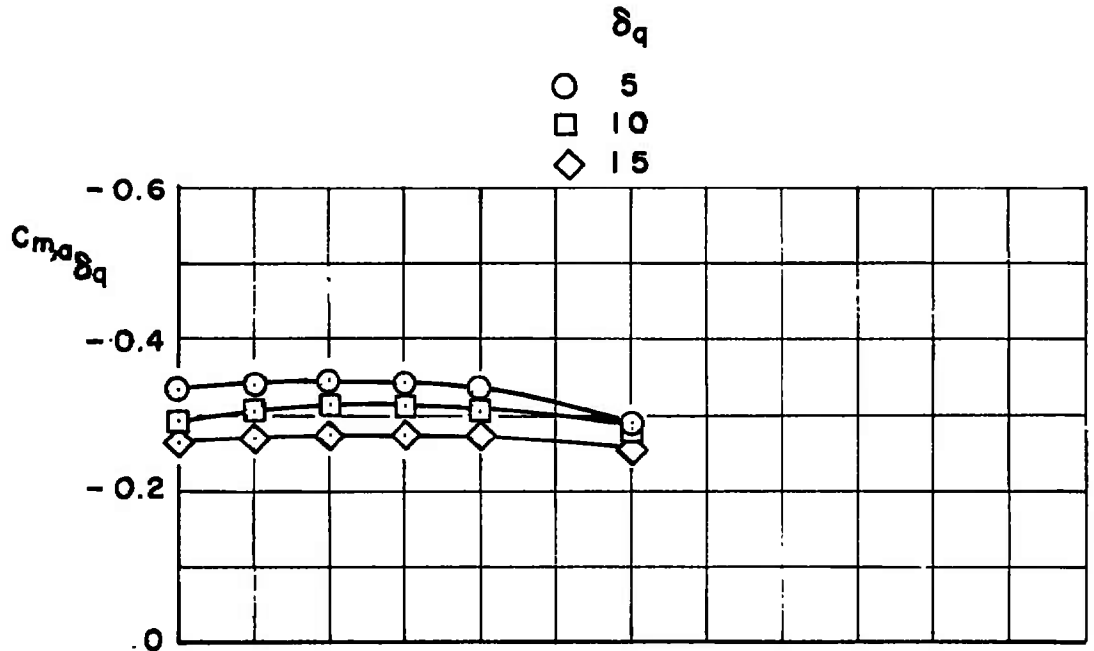
d. $M_\infty = 0.95$
Figure 9. Continued.
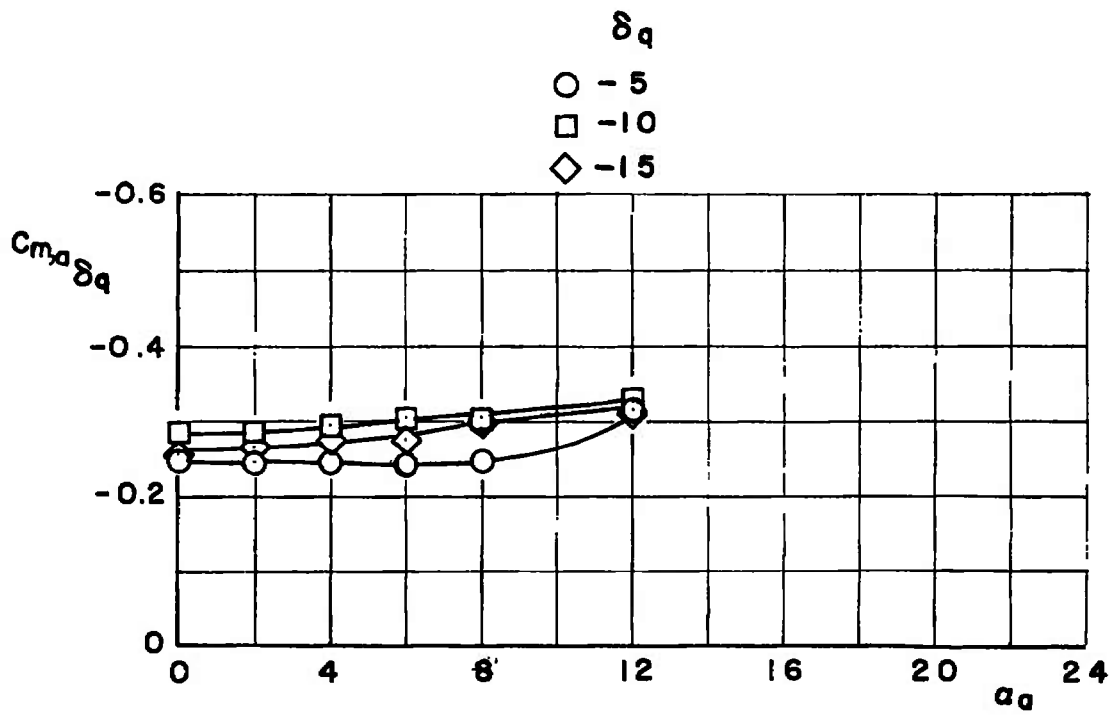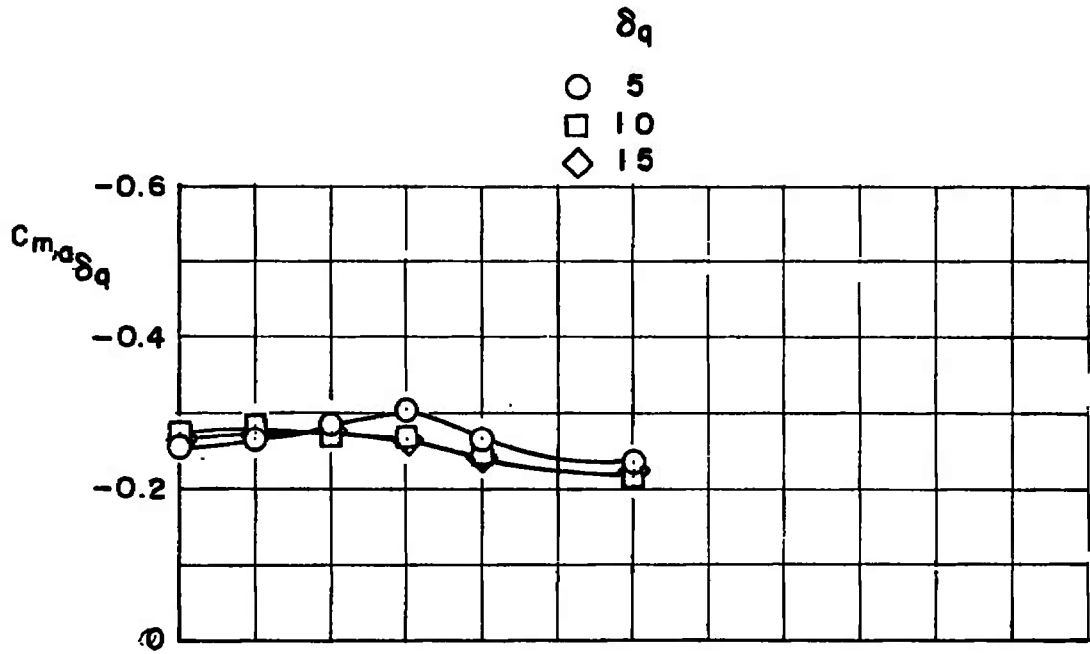
e. $M_\infty = 1.05$
Figure 9. Concluded.
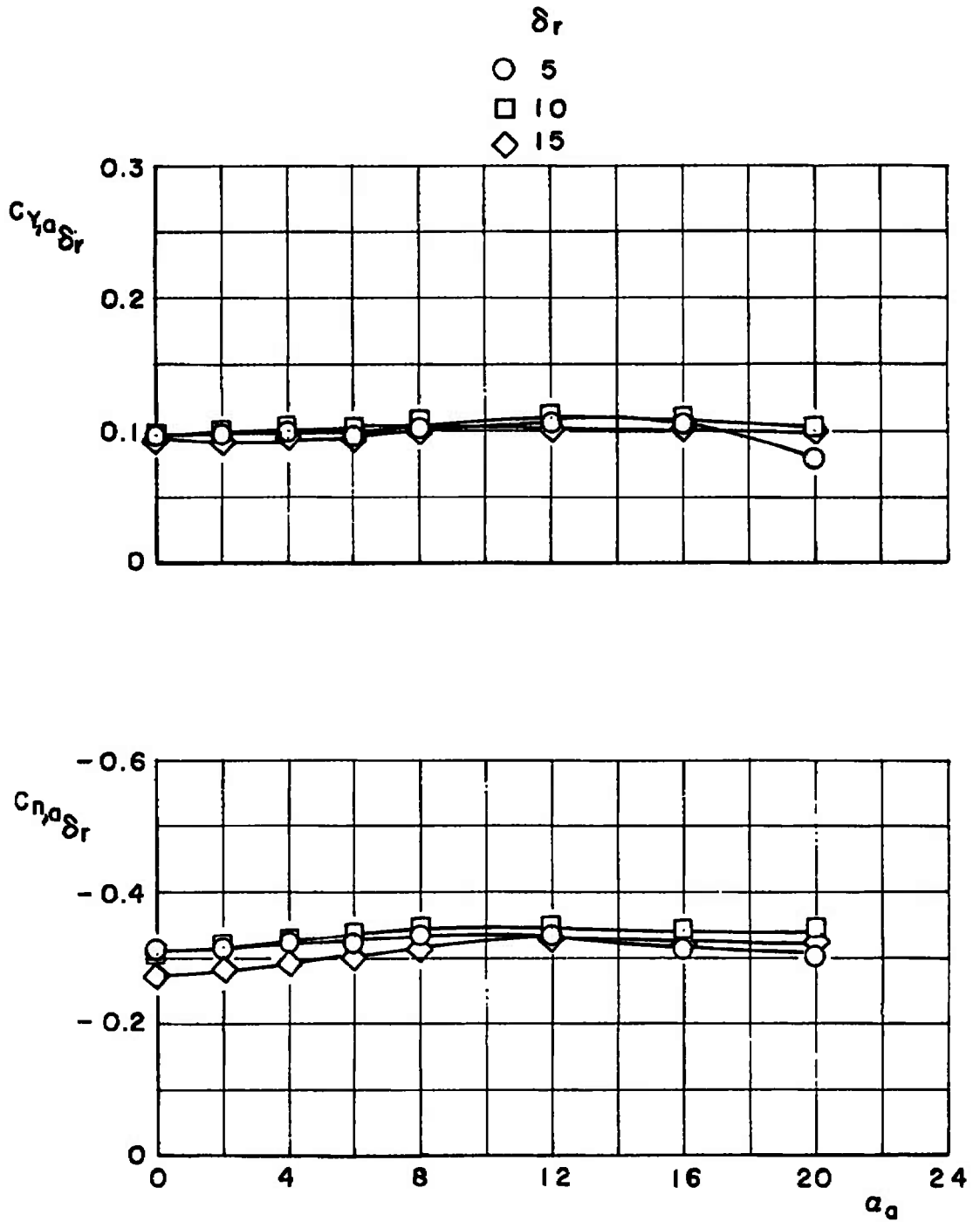
a. $M_\infty = 0.50$

Figure 10. Variation of the side-force increment and the yaw control effectiveness with angle of attack.
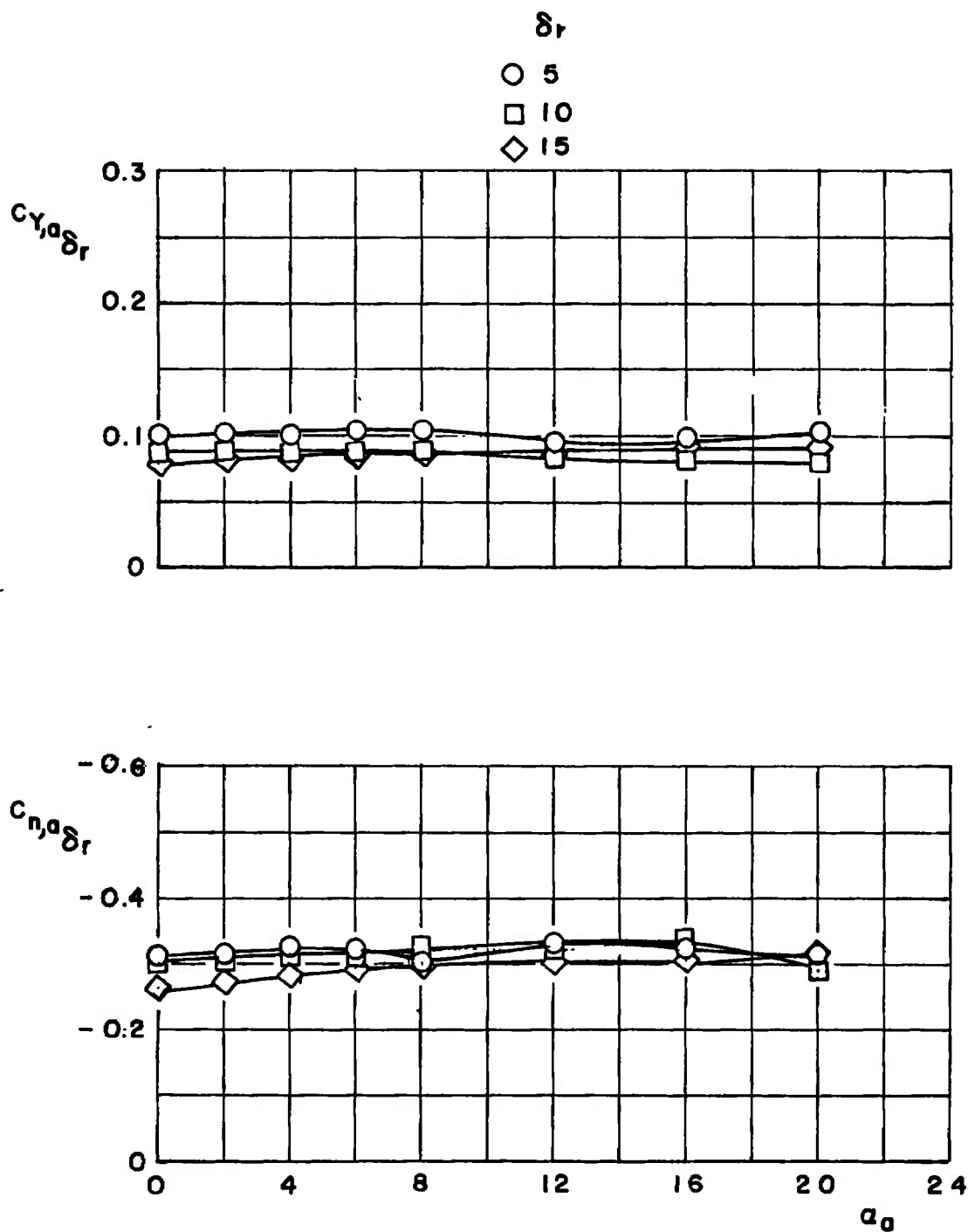
b. $M_\infty = 0.65$
Figure 10. Continued.

40
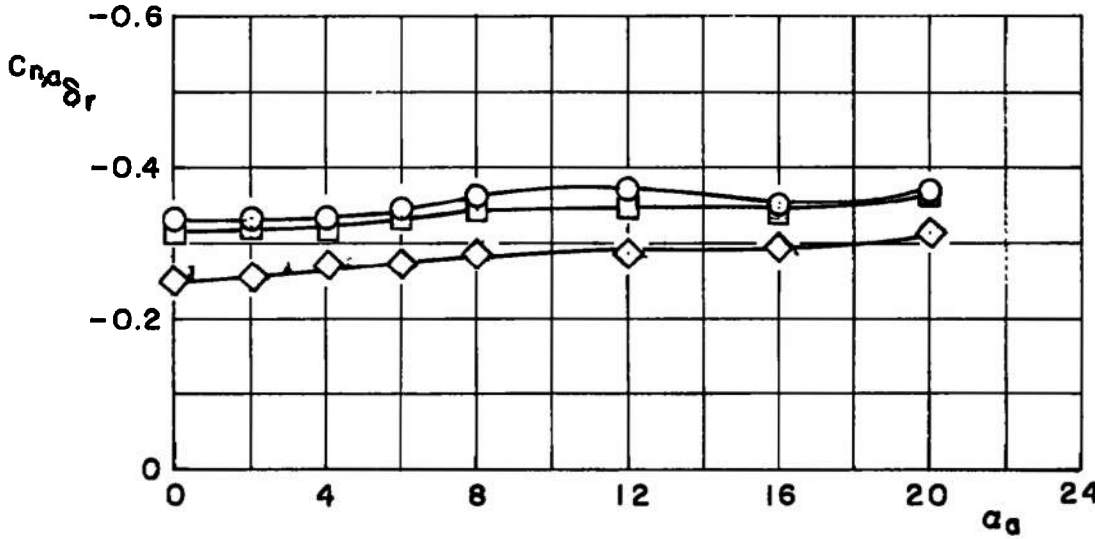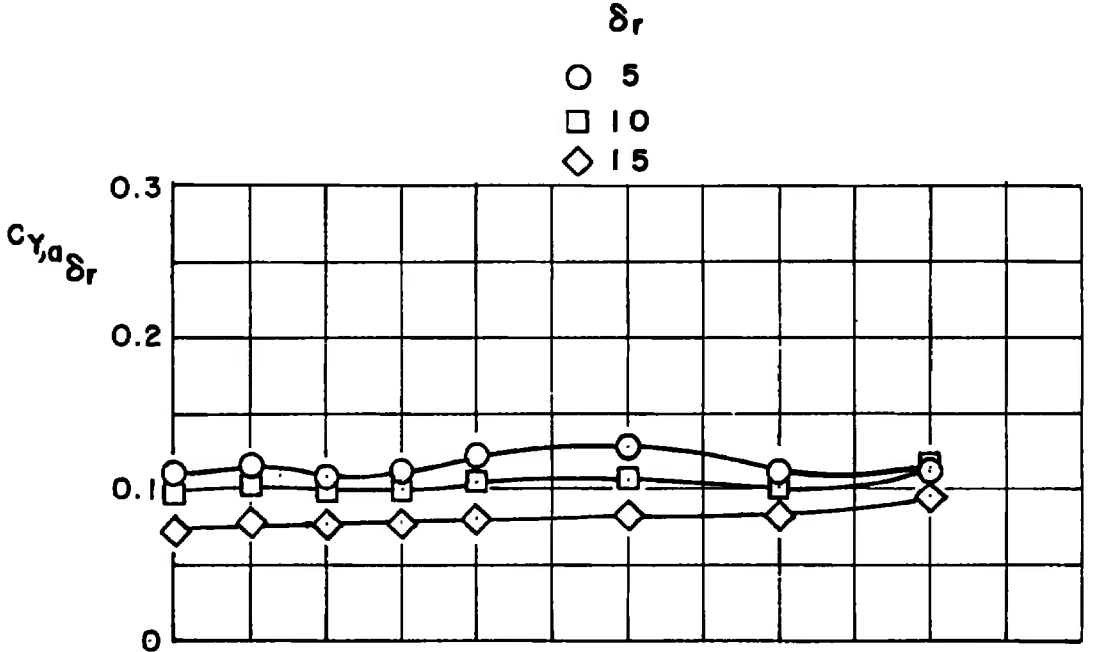
c. $M_\infty = 0.85$
Figure 10. Continued.
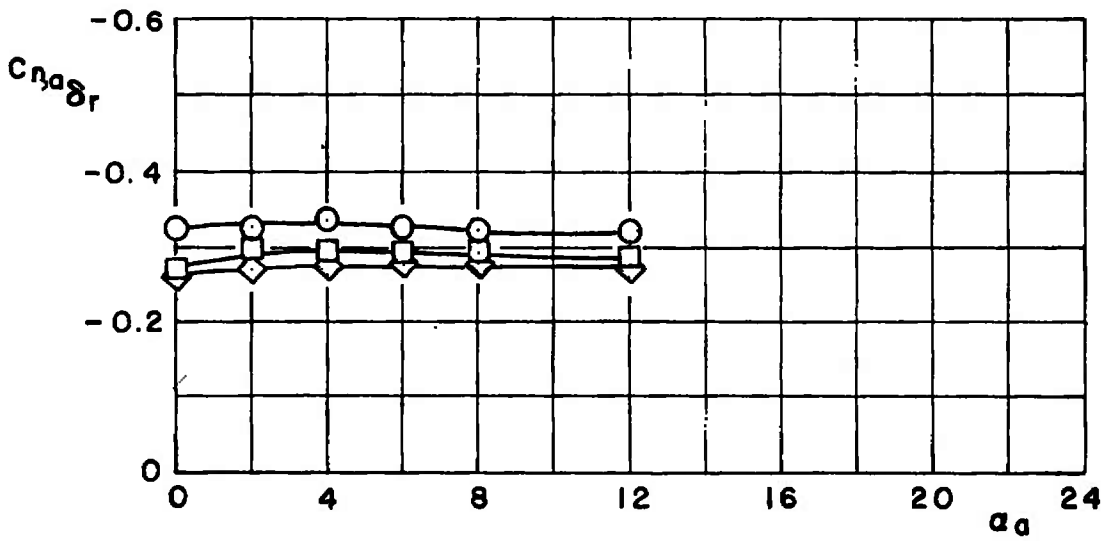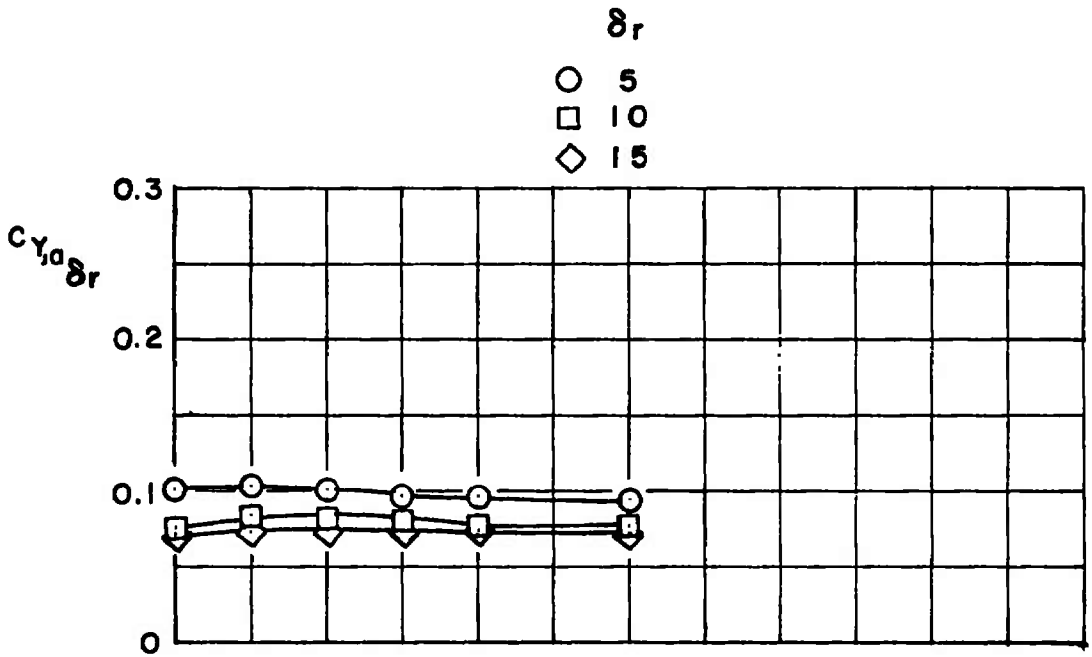
d. $M_\infty = 0.95$
Figure 10. Continued.
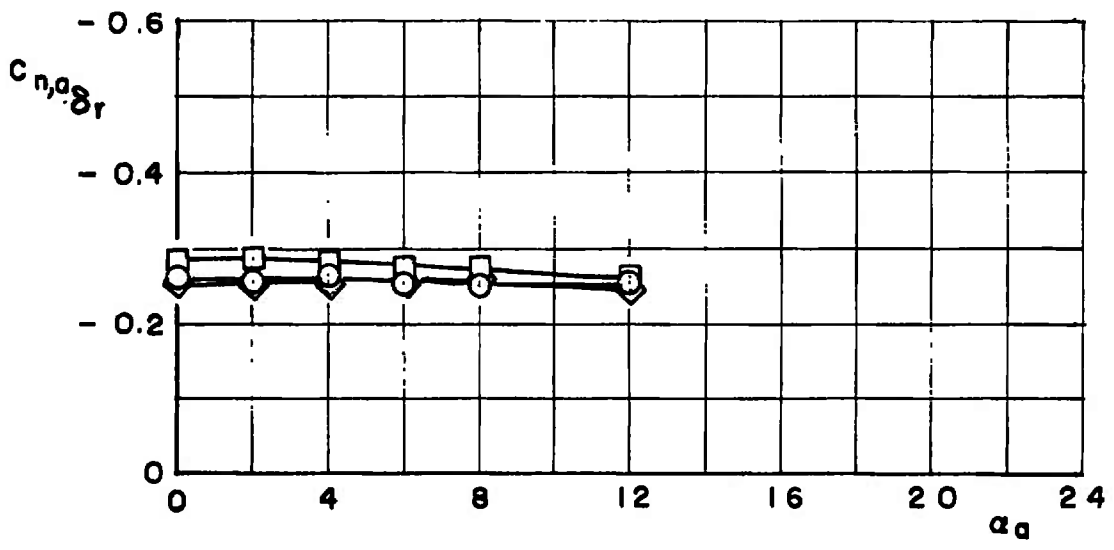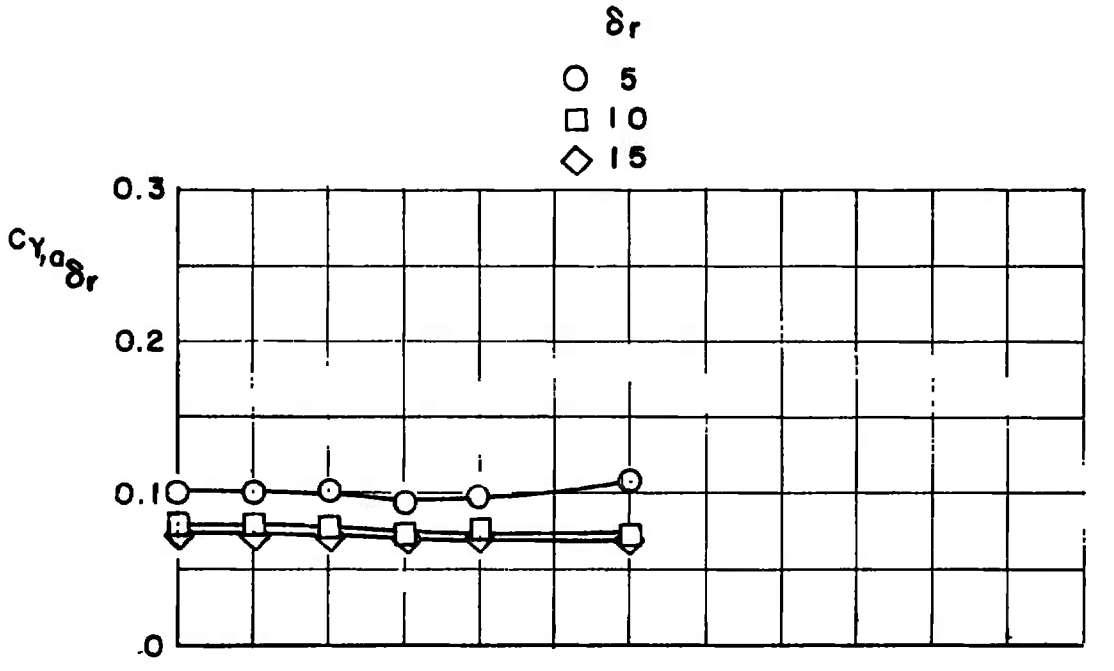
e. $M_\infty = 1.05$
Figure 10. Concluded.
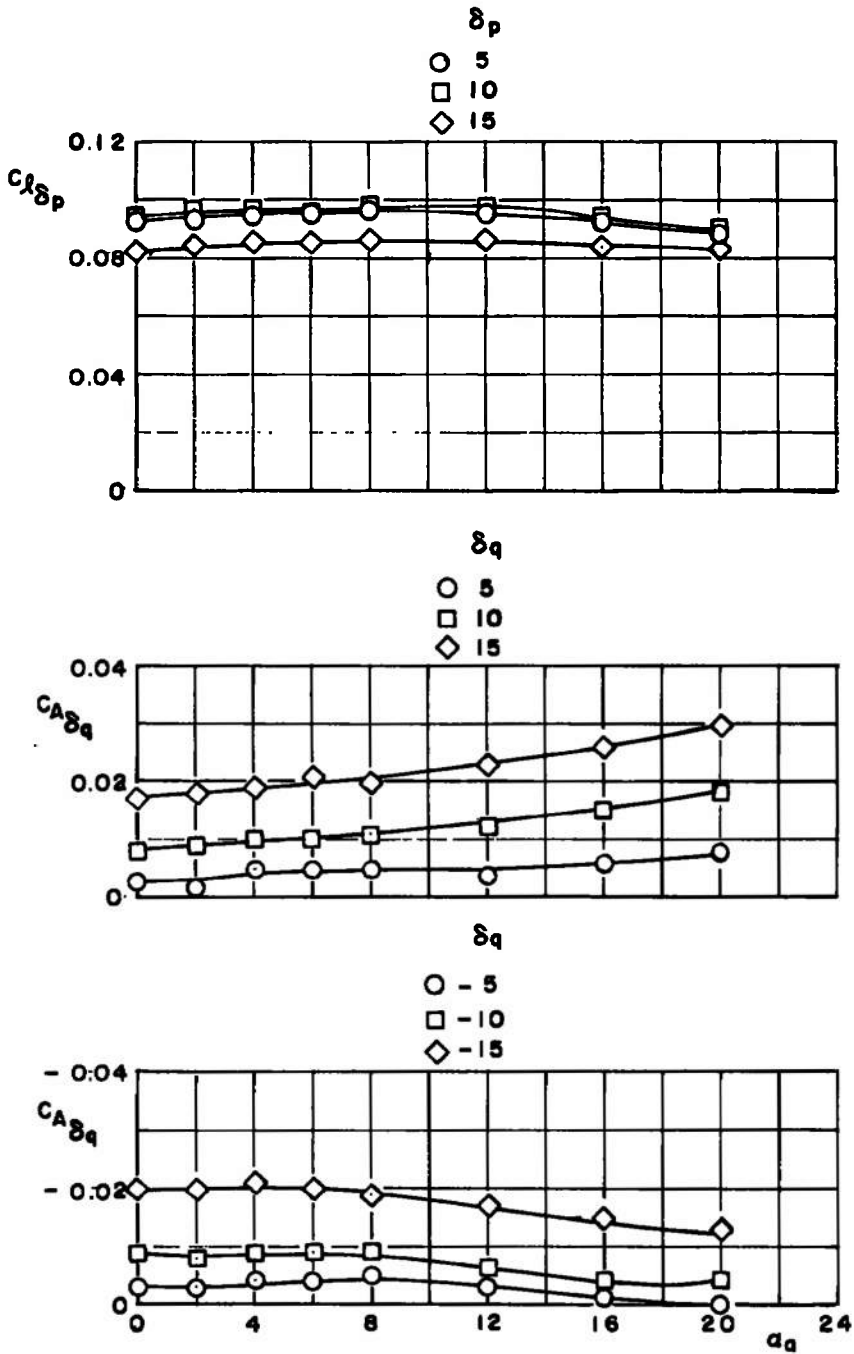
a. $M_\infty = 0.50$

Figure 11. Variation of the roll control effectiveness and axial-force increment with angle of attack.
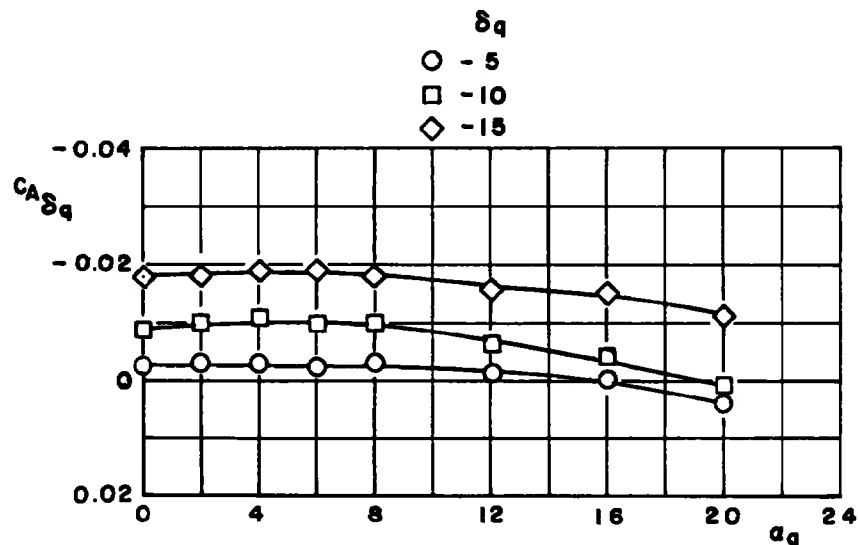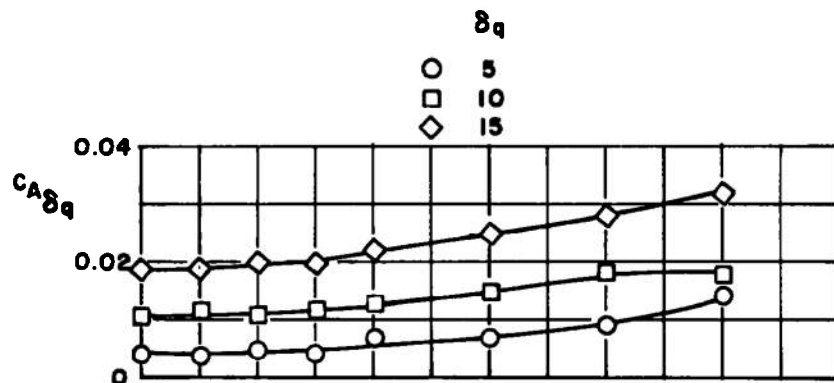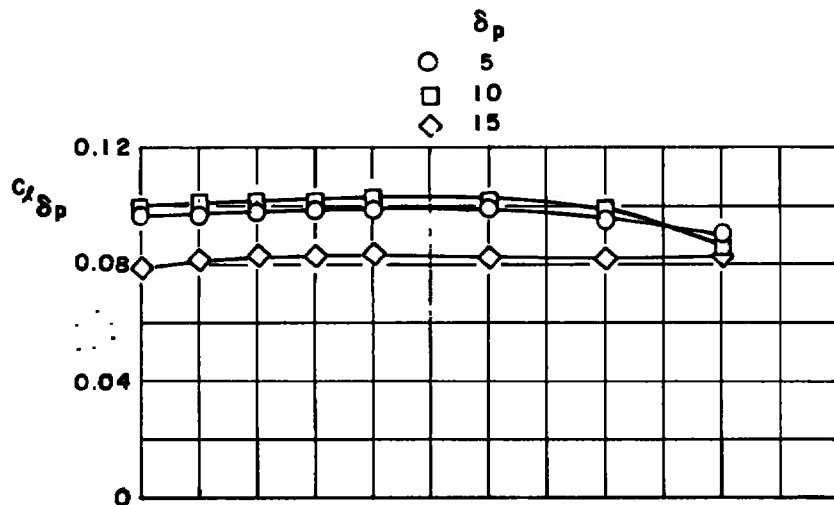
b. $M_\infty = 0.65$
Figure 11. Continued.

45
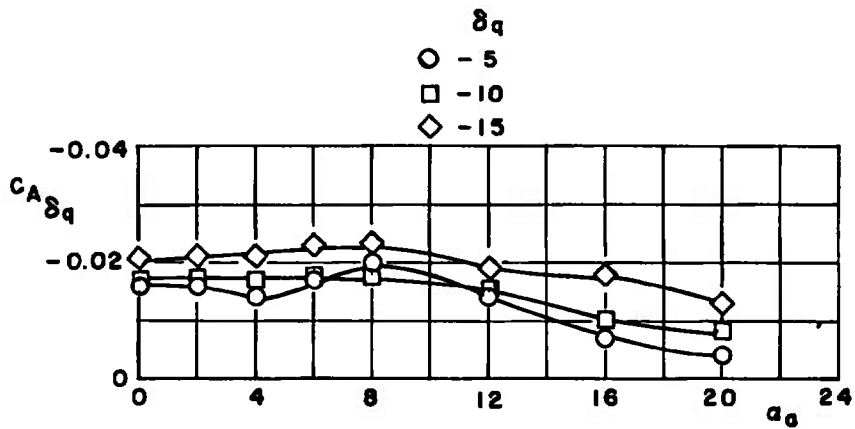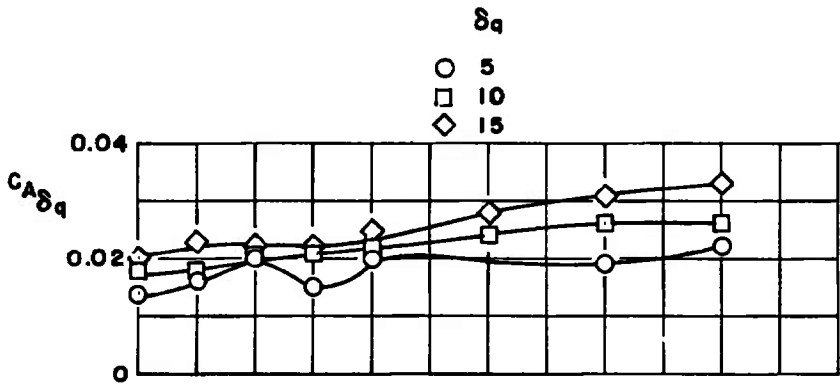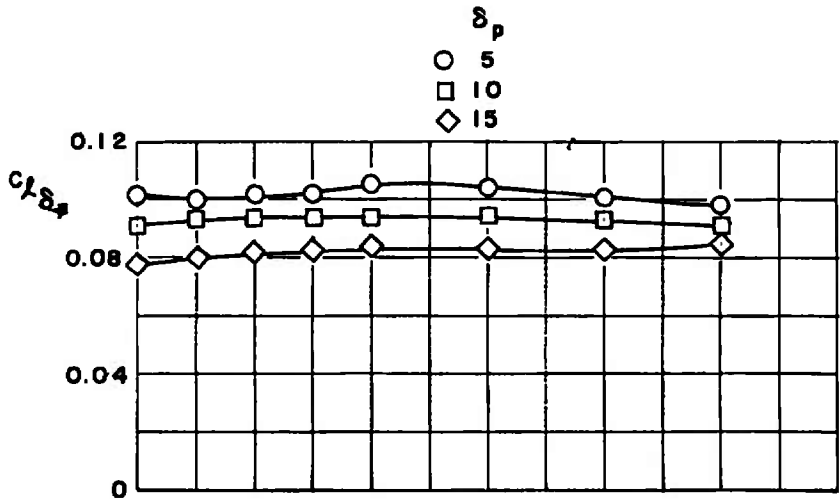
c. $M_\infty = 0.85$
Figure 11. Continued.
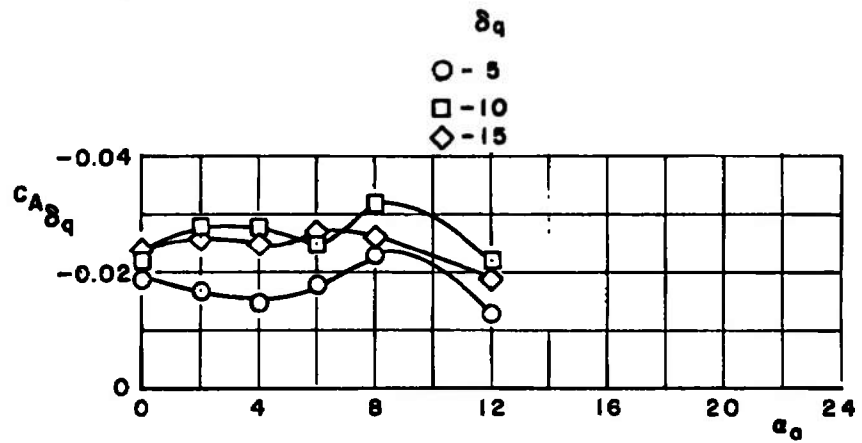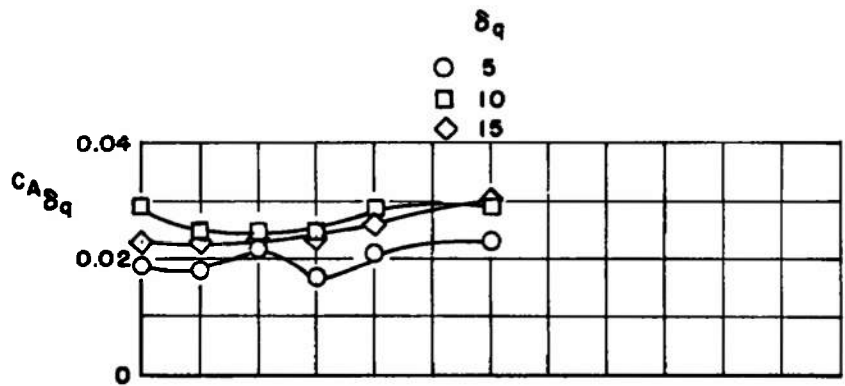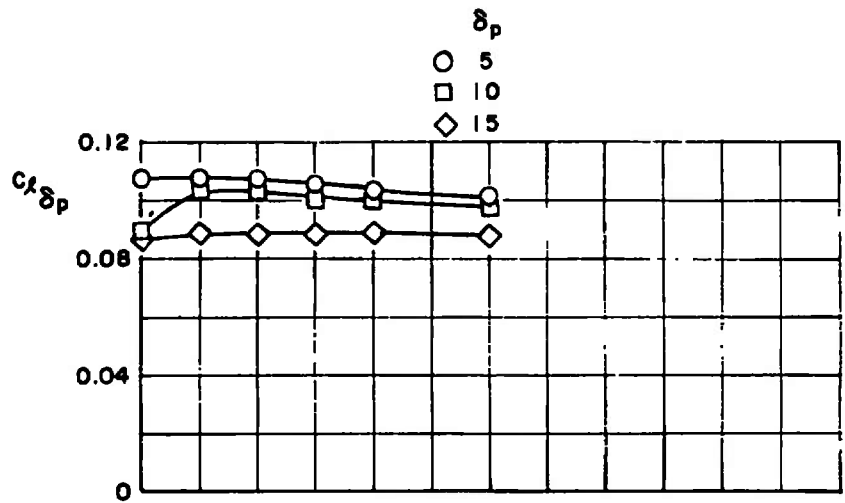
d. $M_\infty = 0.95$
Figure 11. Continued.
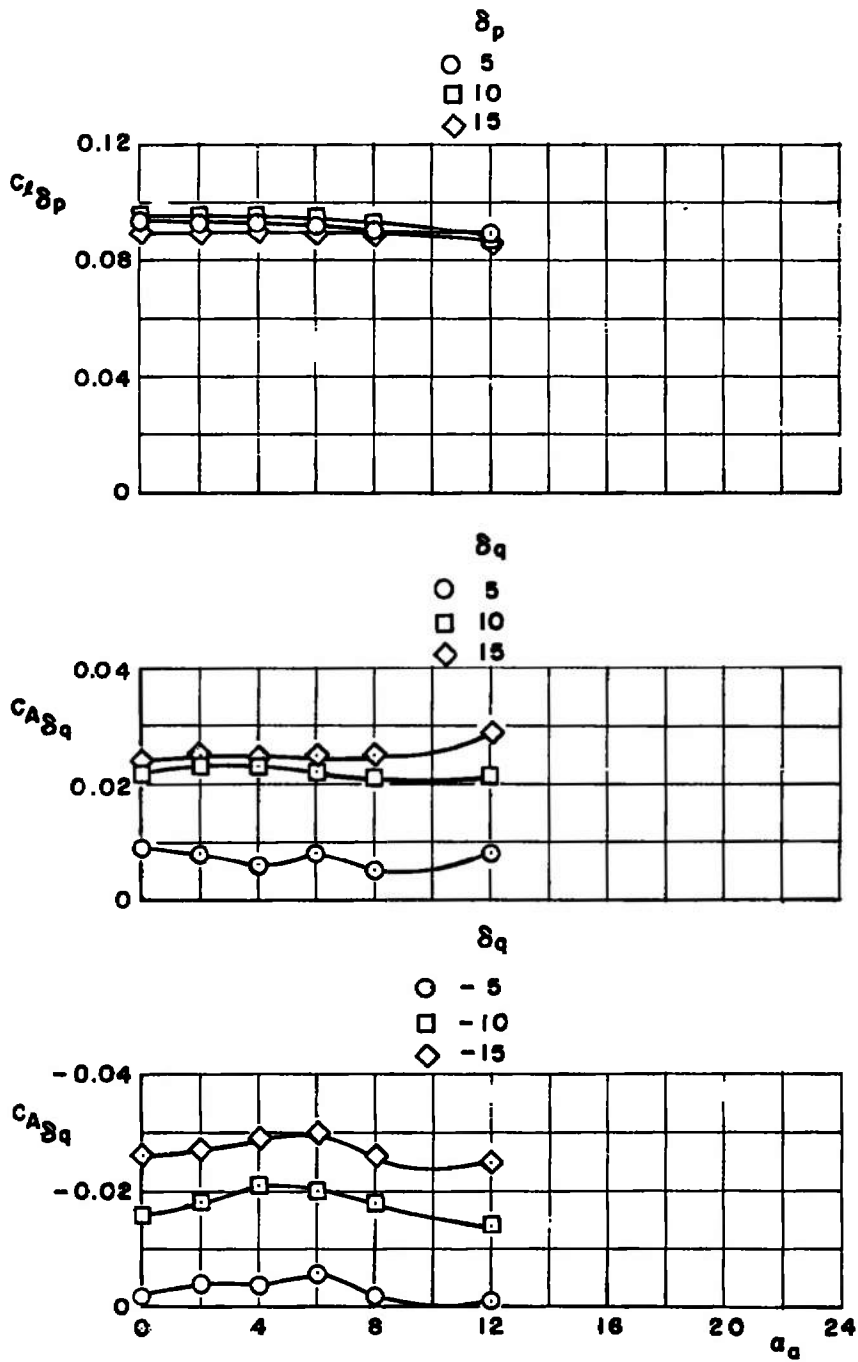
e. $M_\infty = 1.05$
Figure 11. Concluded.

48
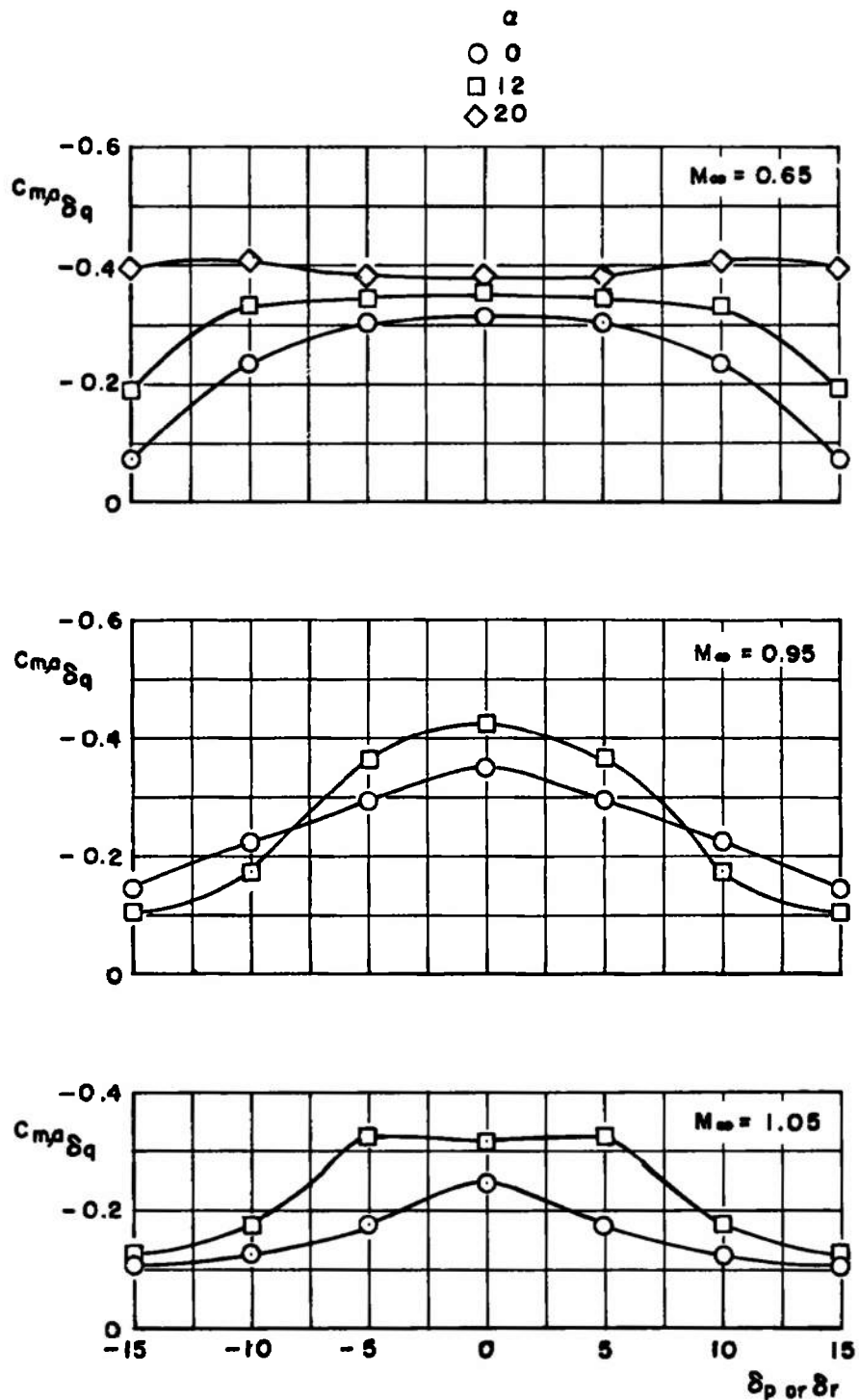
a. $\delta q = -5$

Figure 12. Effect of flap deflections in roll and yaw on the pitch control effectiveness.
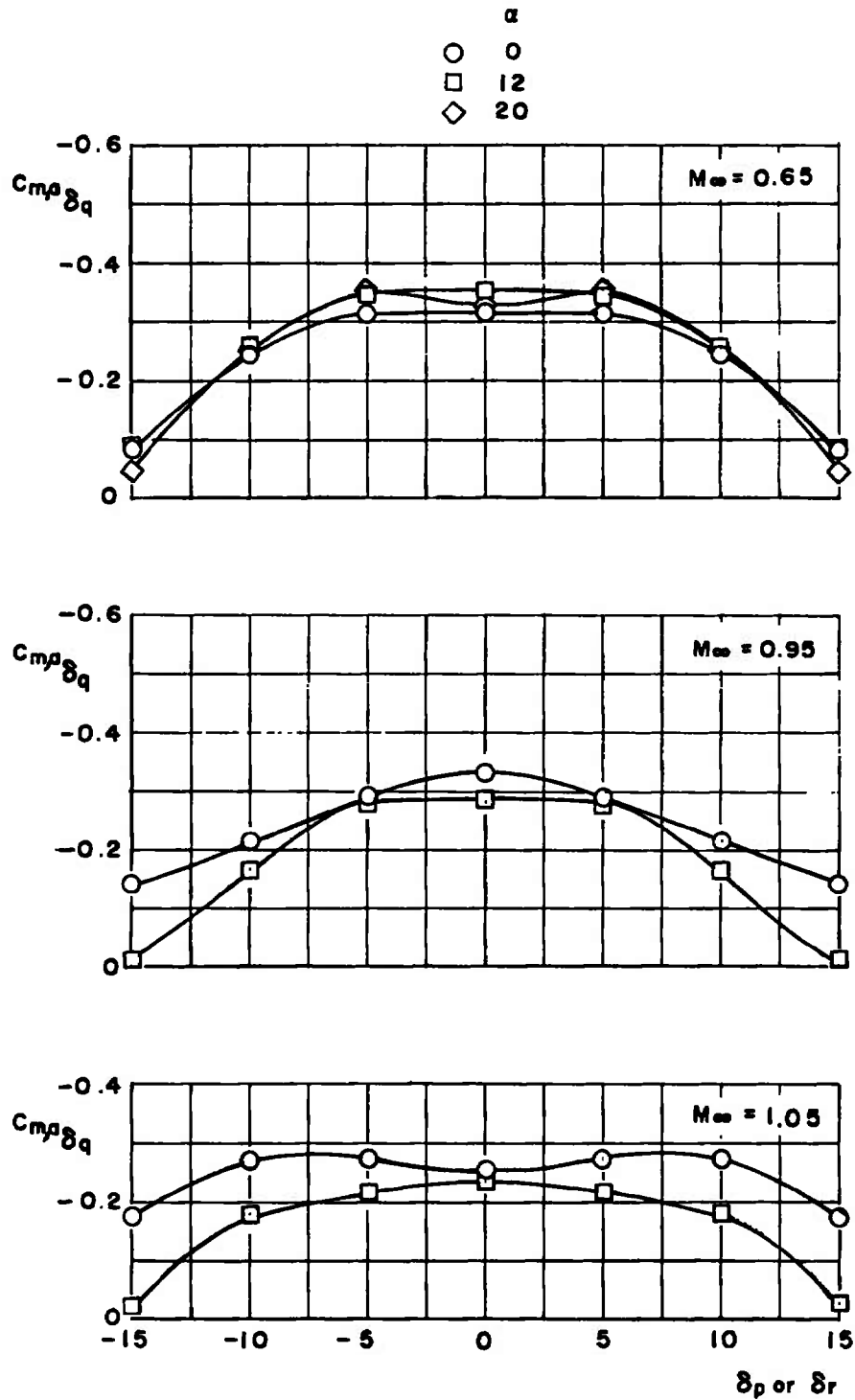
b. $\delta q = 5$
Figure 12. Continued.
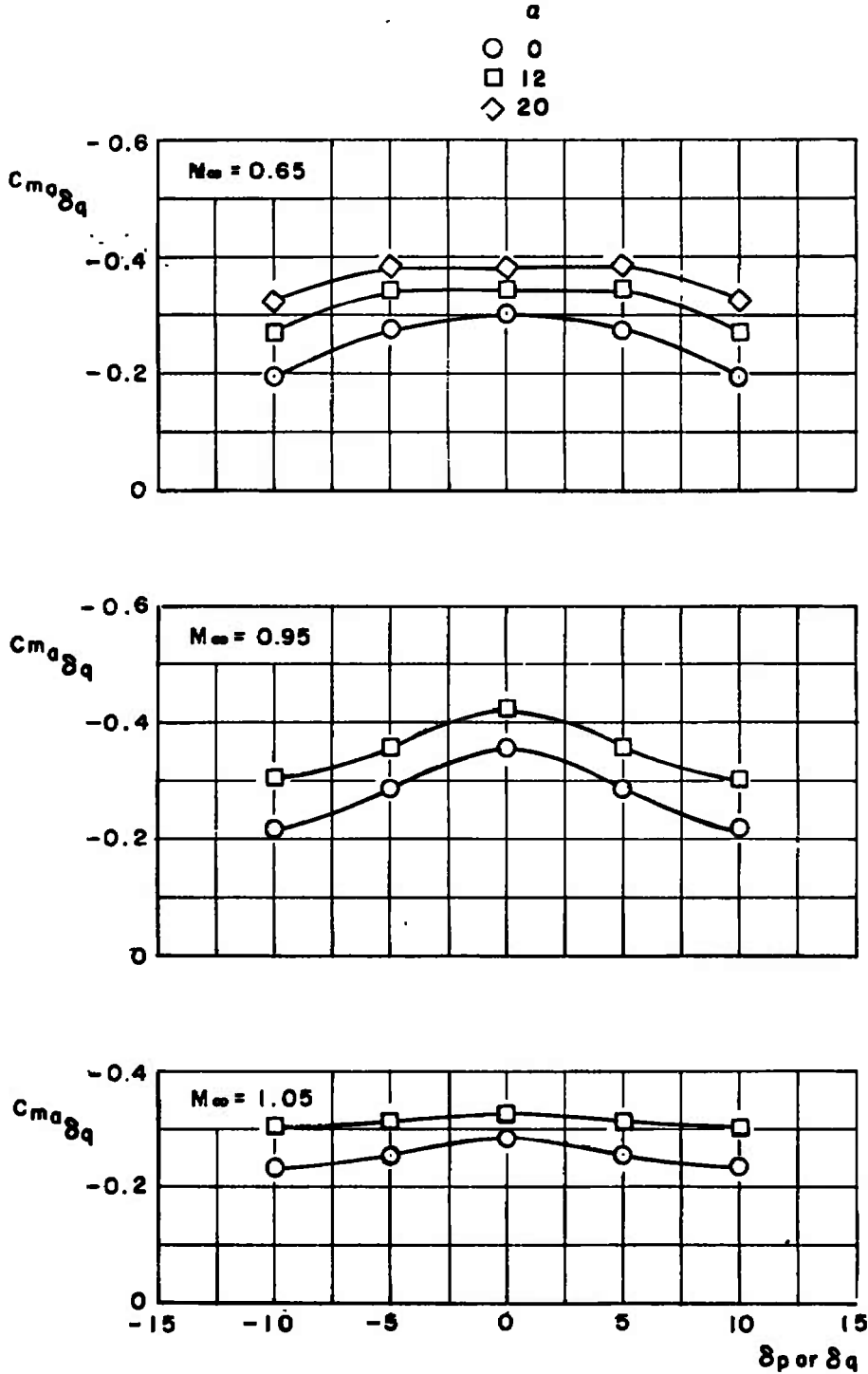
c. $\delta q = -10$
Figure 12. Continued.
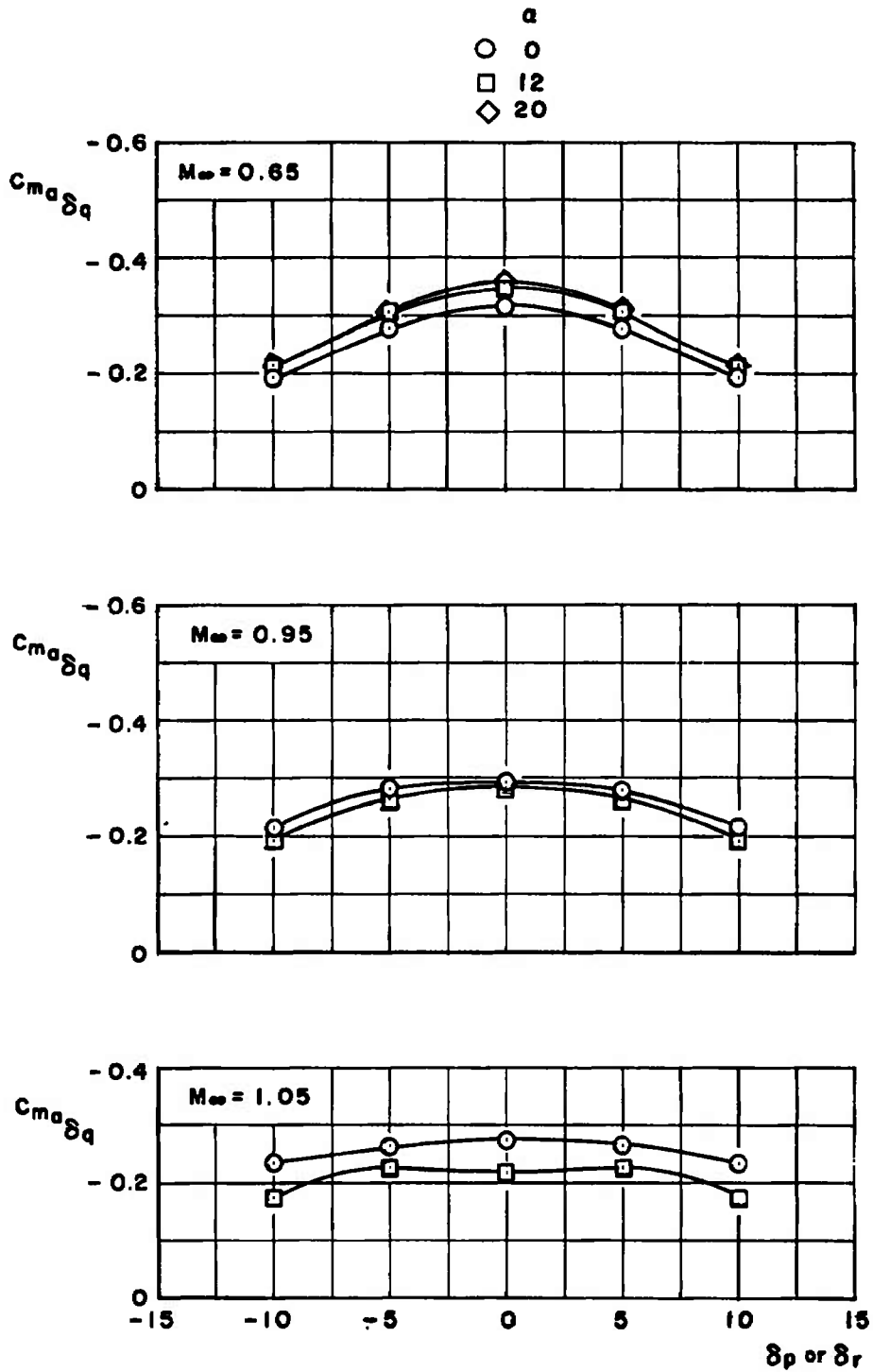
d. $\delta q = 10$
Figure 12. Concluded.
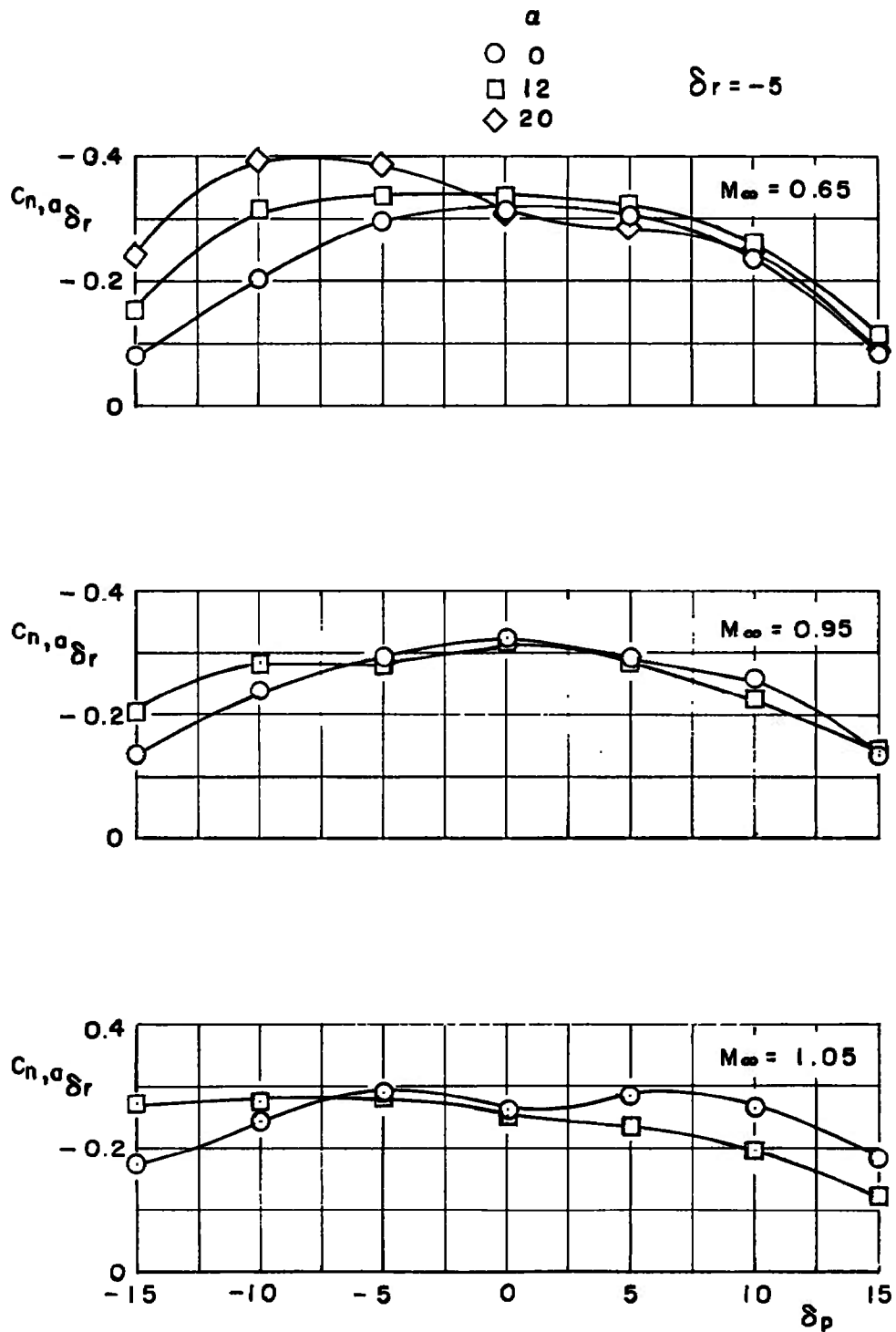
Figure 13. Effect of flap deflections in pitch on the yaw control effectiveness.
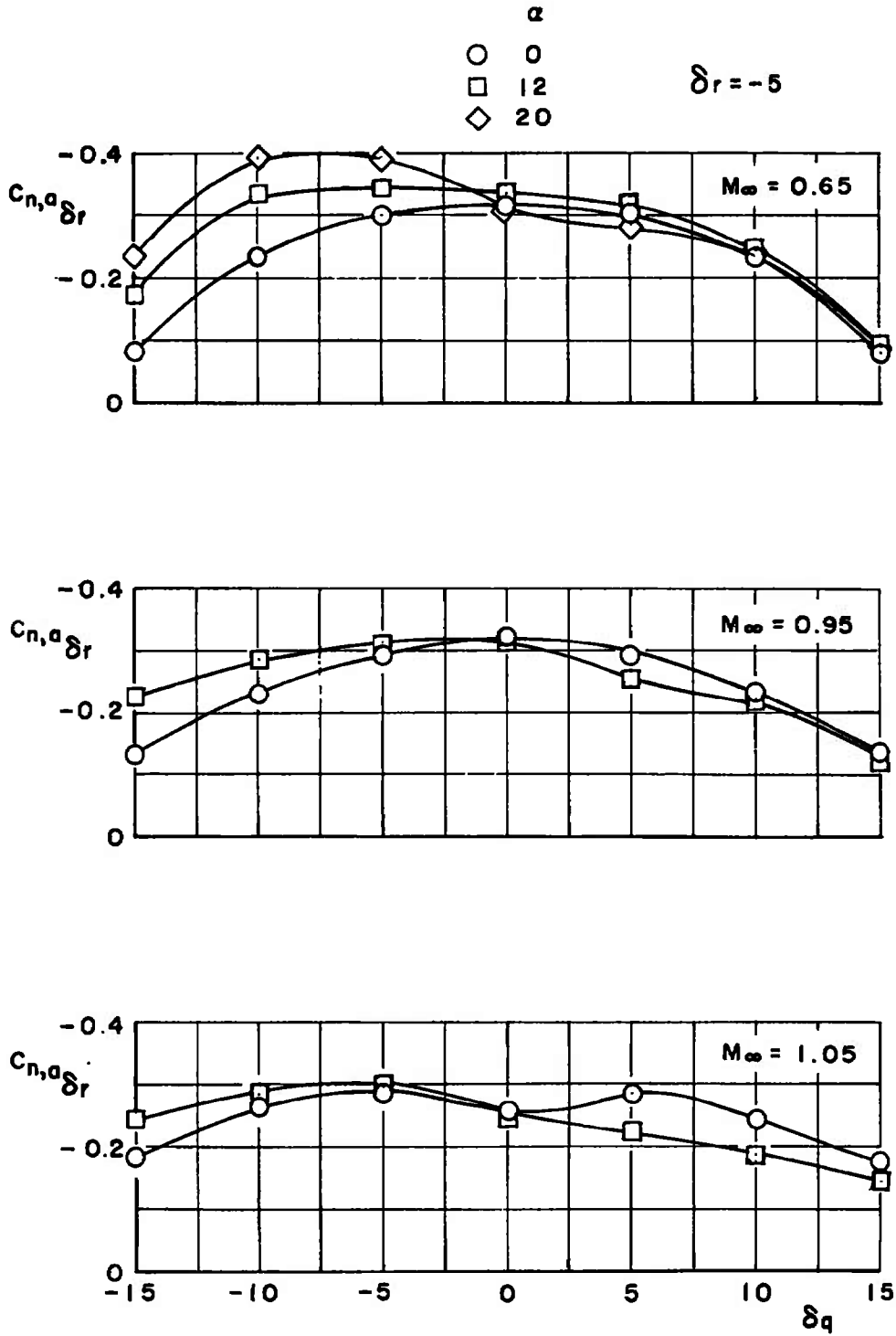
Figure 14. Effect of flap deflections in roll on the yaw control
effectiveness.

54
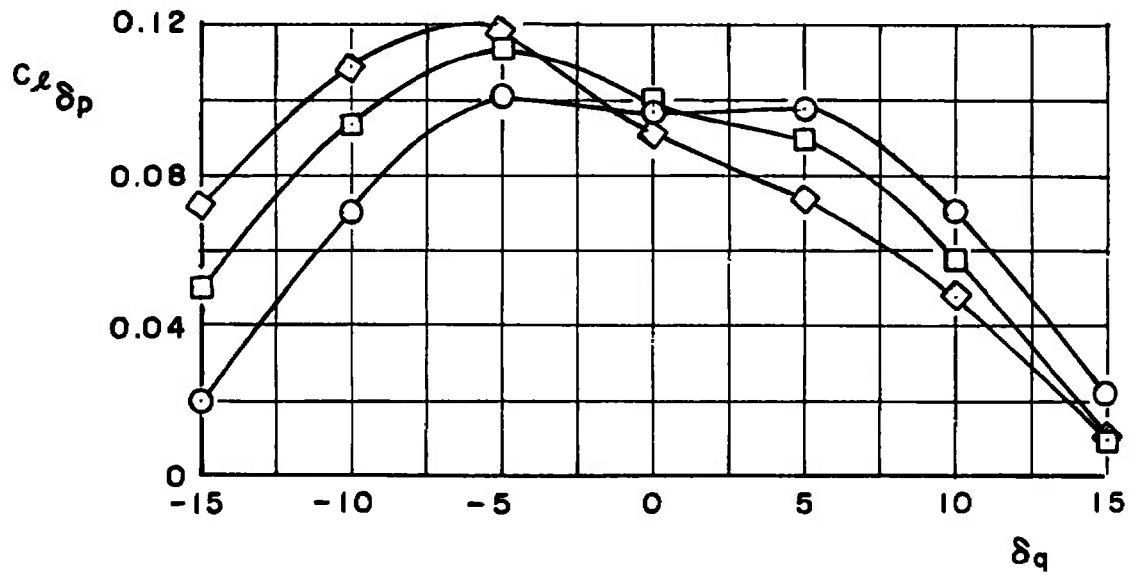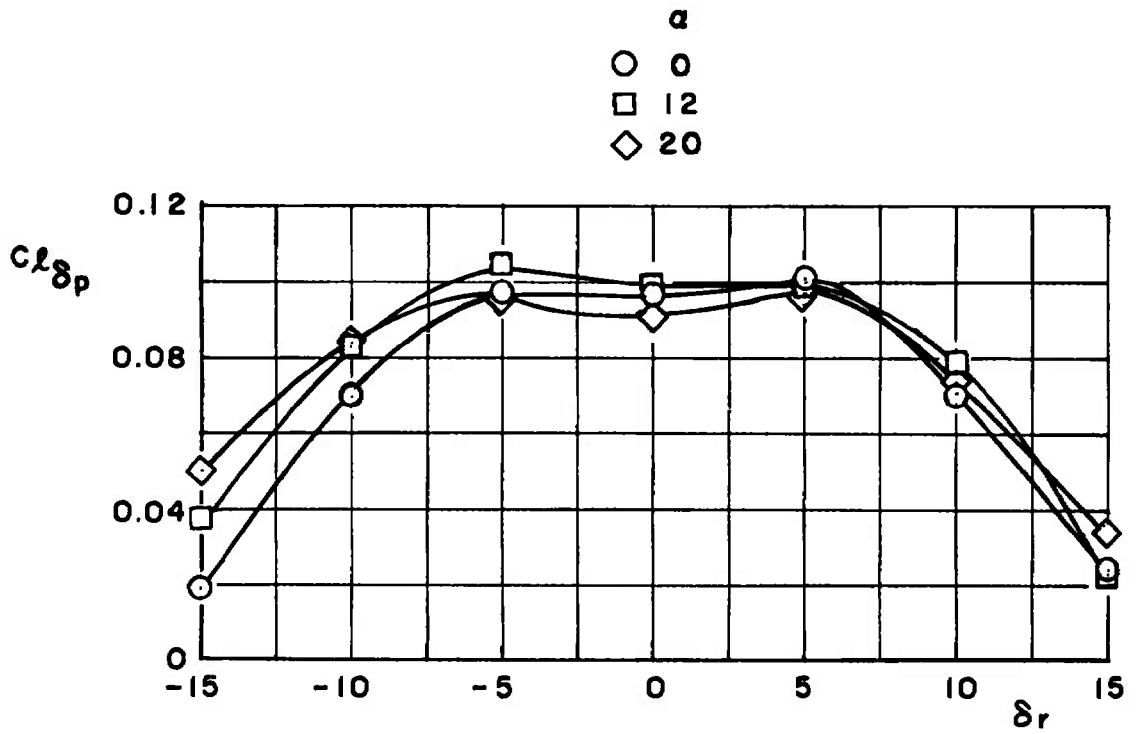
a. $M_\infty = 0.65$, $\delta p = 5$

Figure 15. Effect of flap deflections in pitch and yaw on the roll control effectiveness.
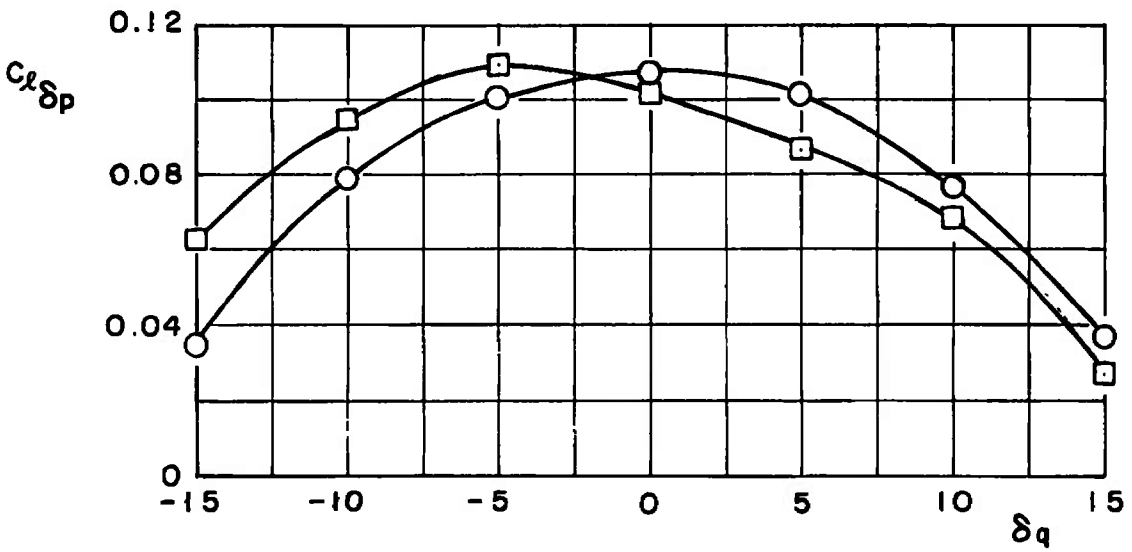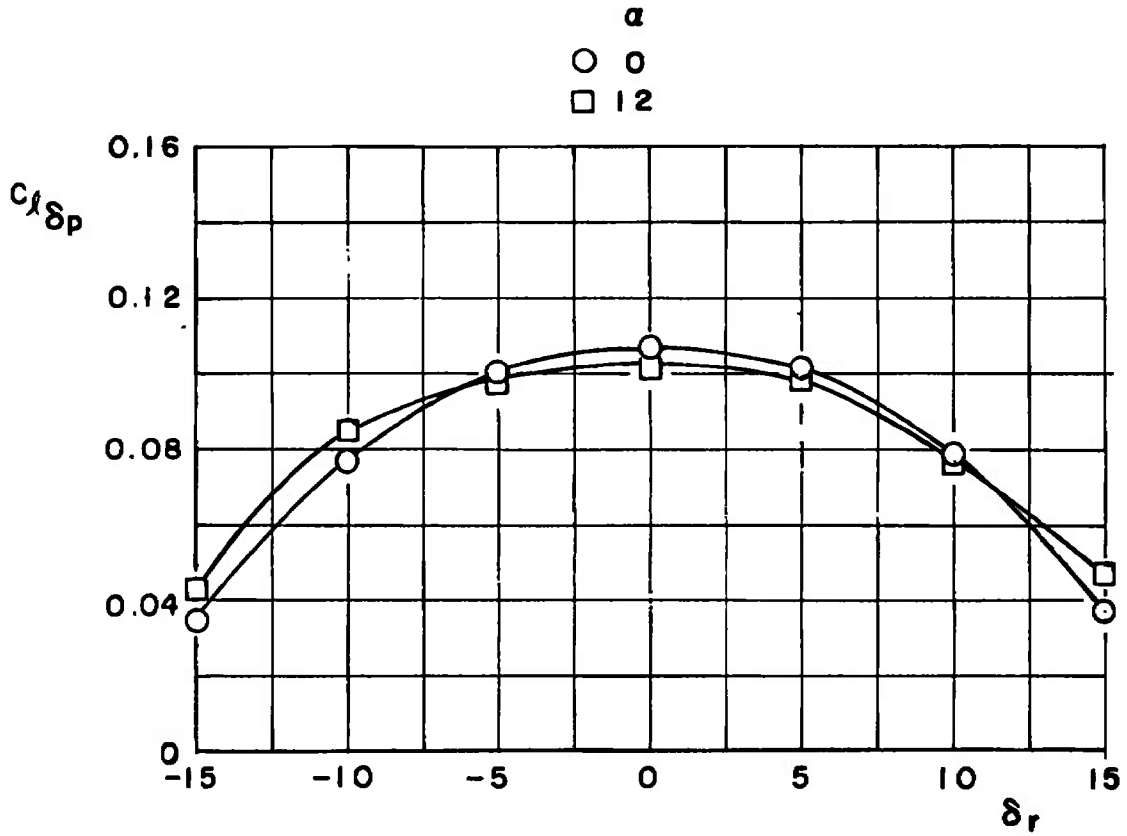
b. $M_\infty = 0.95$, $\delta p = 5$
Figure 15.   Continued.
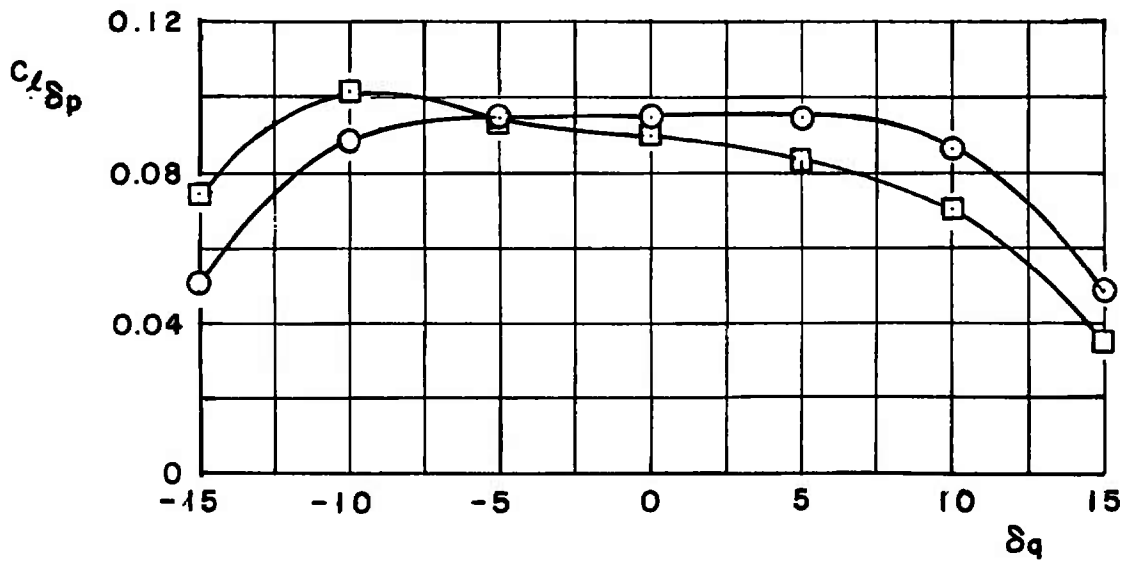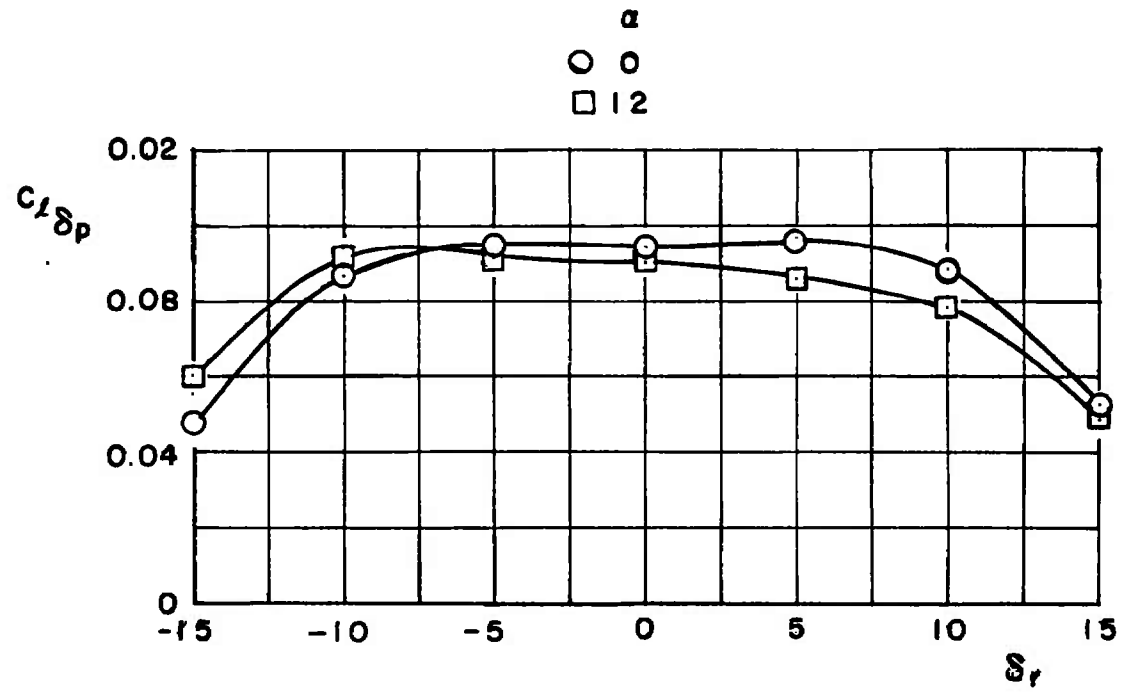
c. $M_\infty = 1.05$, $\delta p = 5$
Figure 15. Concluded.

$$\delta_p = 0, \quad \delta_q = 0, \quad \delta_r = 0$$
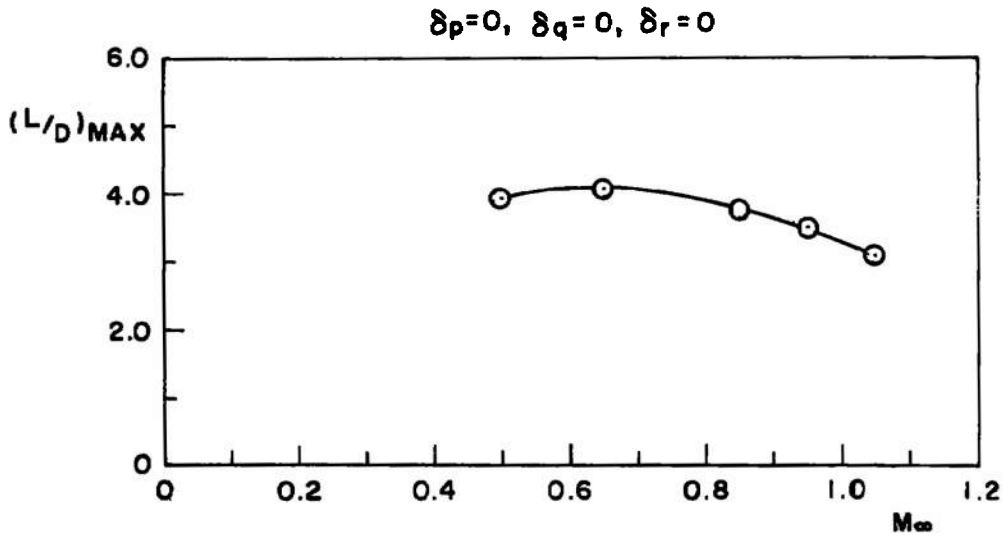
a. $(L/D)_{max}$ versus M_∞
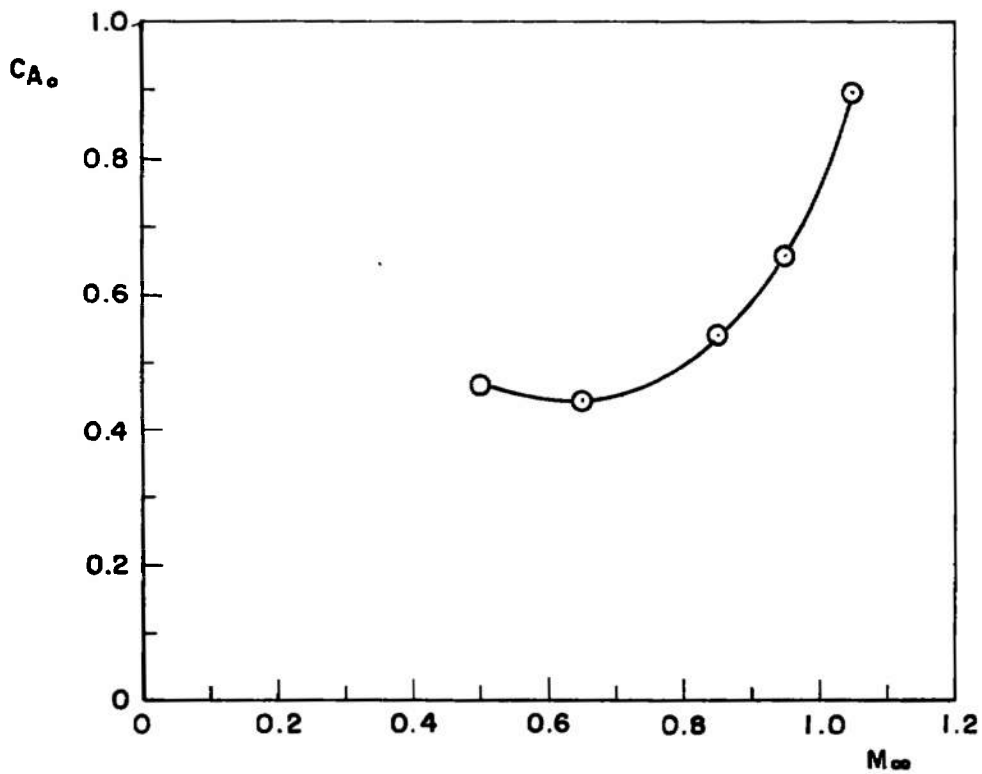
b. C_{A_o} versus M_∞

Figure 16. Variation of the maximum lift to drag ratio and axial-force coefficient with Mach number.
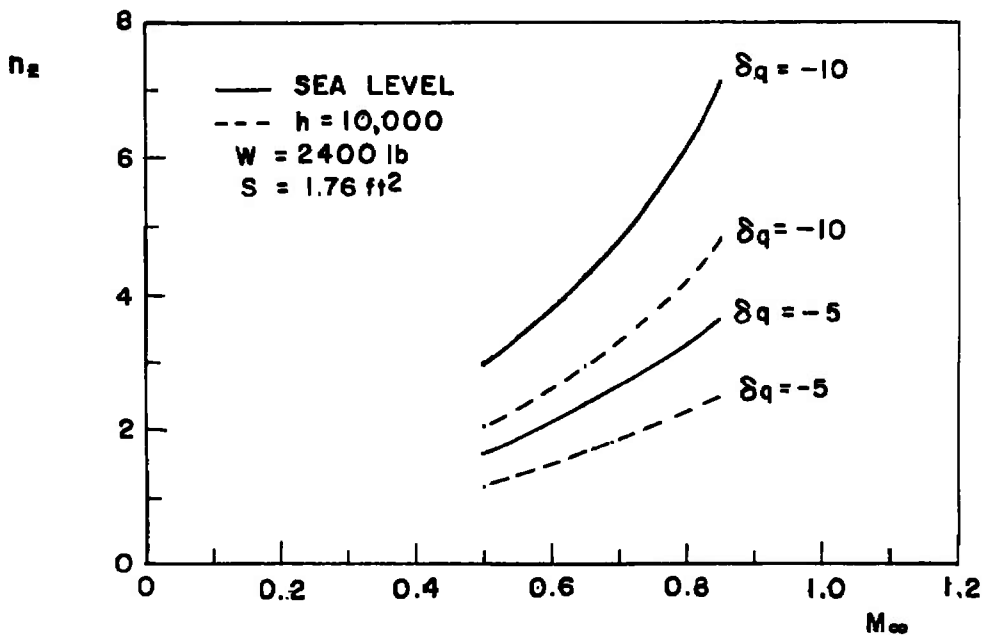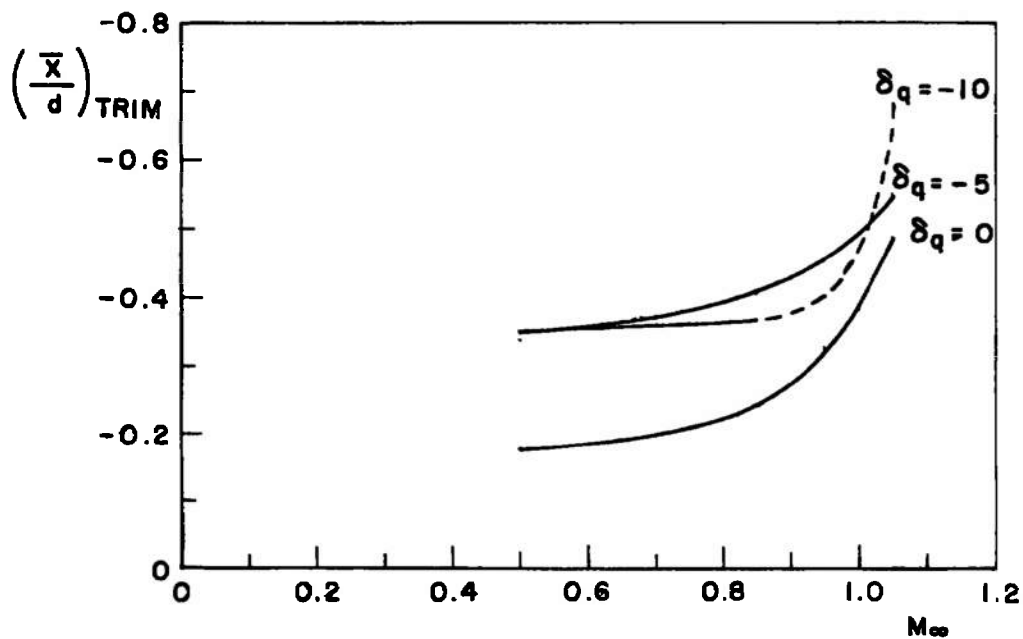
Figure 17. Variation of the trim static margin and the longitudinal
load factor with Mach number.
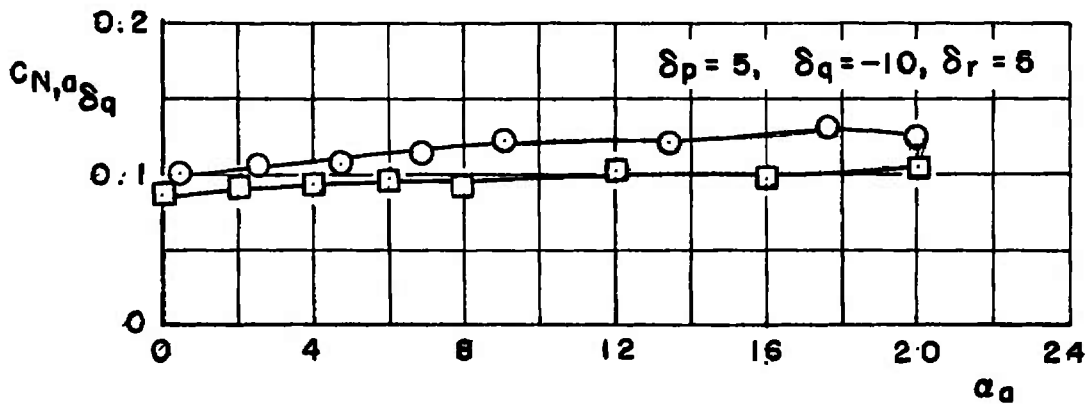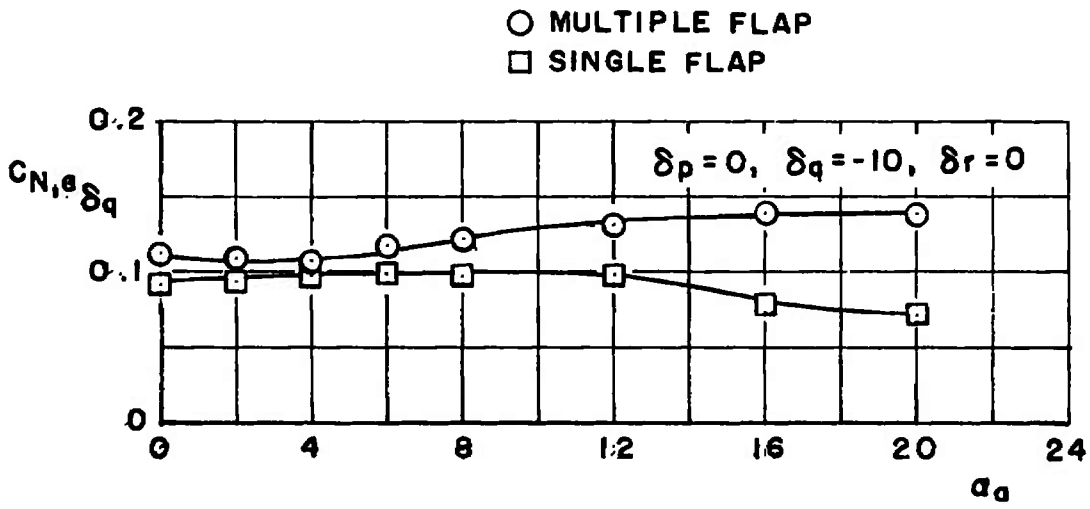
a. $M_\infty = 0.65$

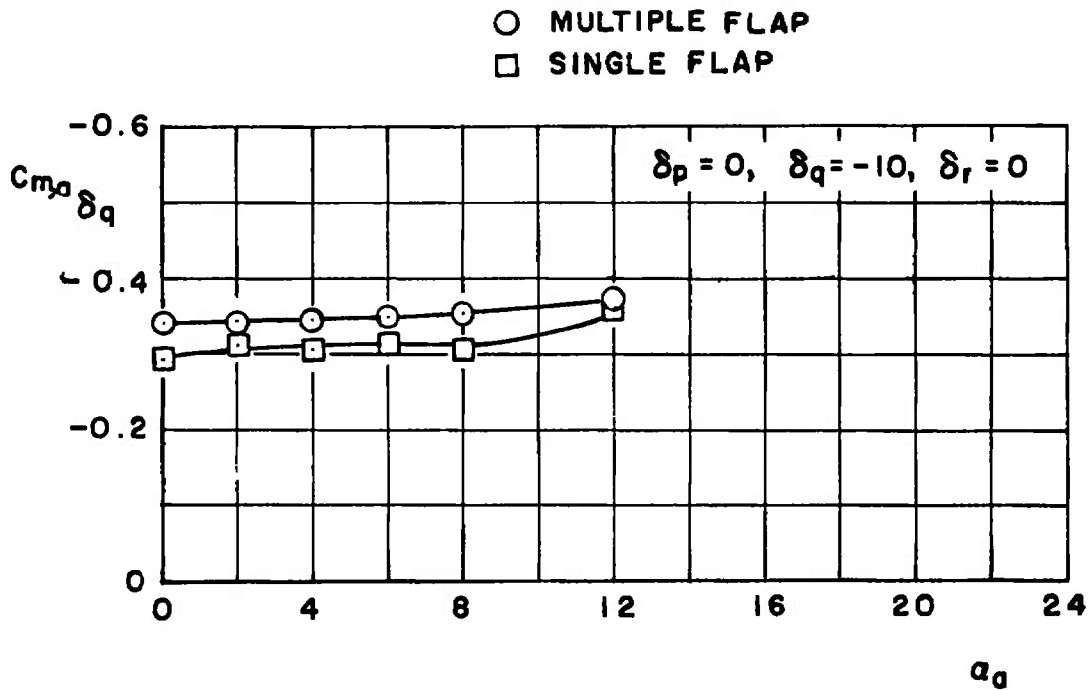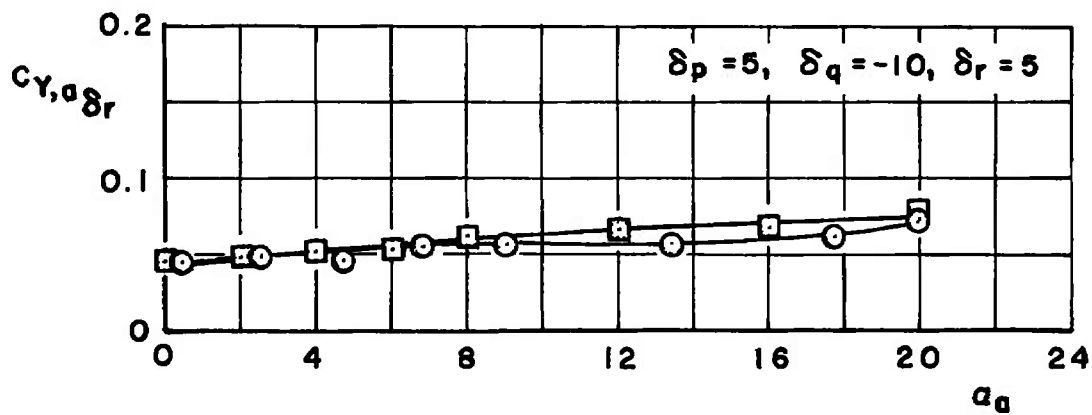Figure 18. Comparison of normal-force increment obtained using single flap and multiple flap test techniques.

○ MULTIPLE FLAP
□ SINGLE FLAP

$\delta_p = 0, \quad \delta_q = -10, \quad \delta_r = 0$

$\delta_p = 5, \quad \delta_q = -10, \quad \delta_r = 5$
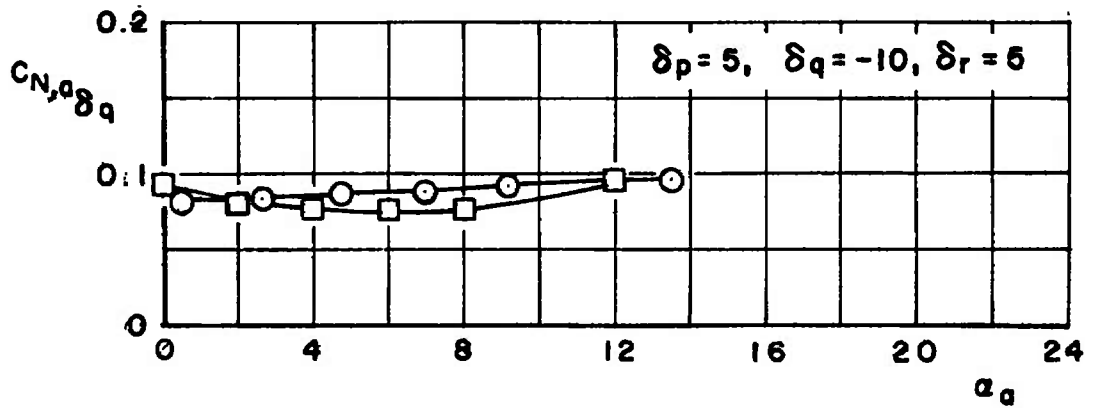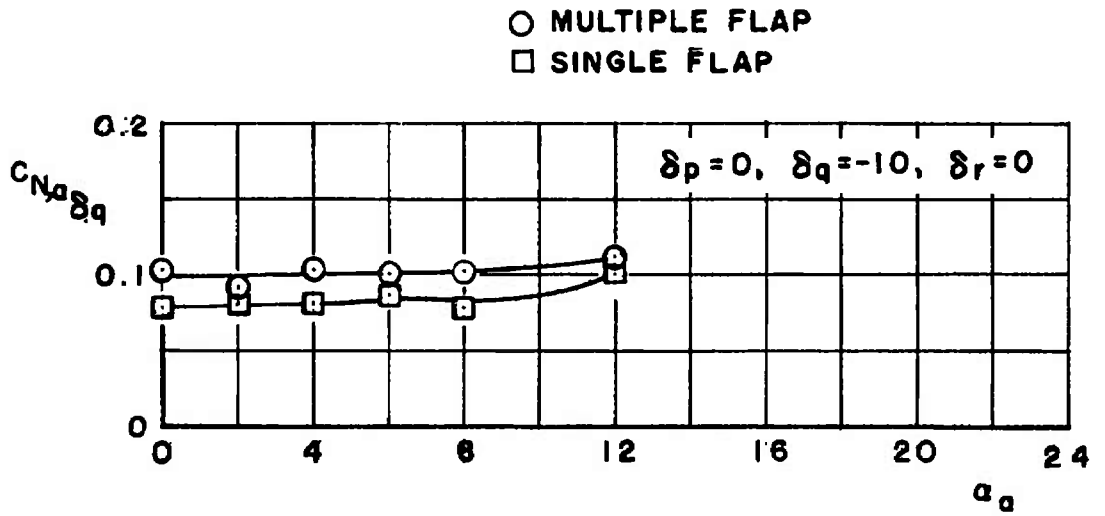
b. $M_\infty = 0.95$
Figure 18. Concluded.

61

○ MULTIPLE FLAP
□ SINGLE FLAP
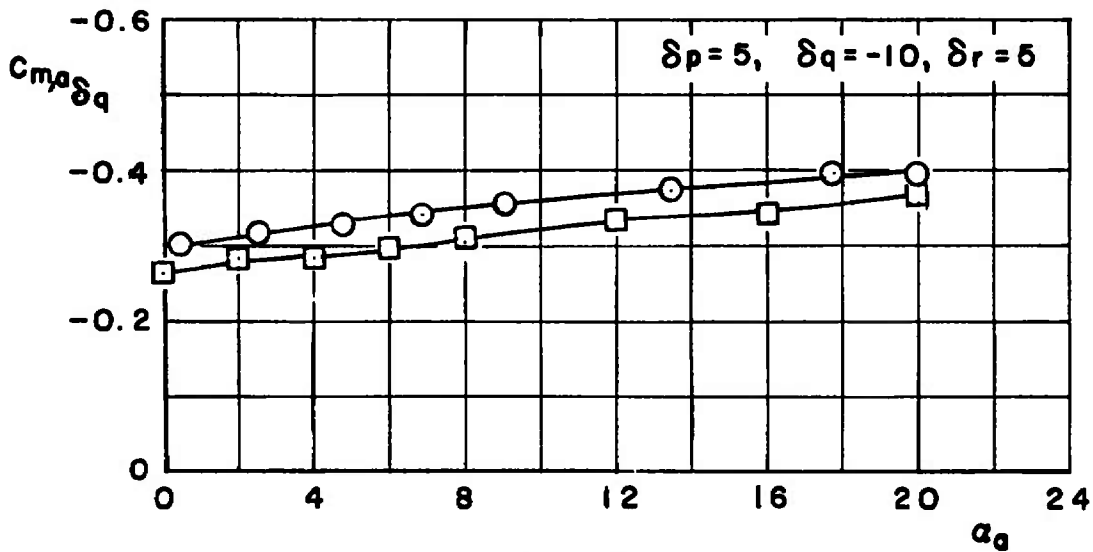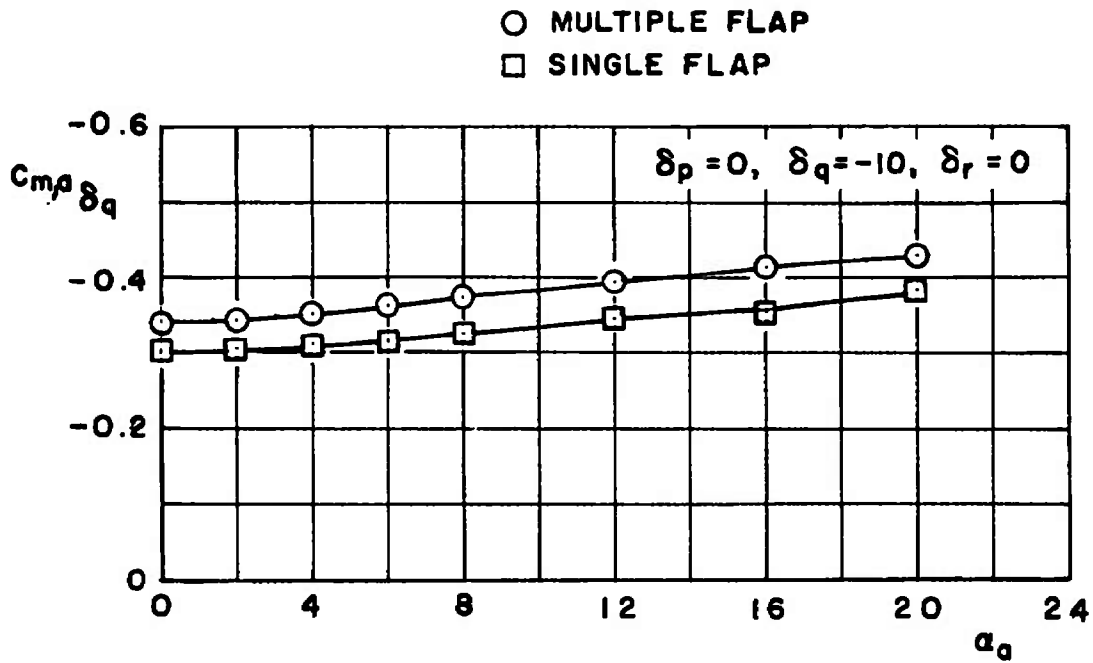
a. $M_\infty = 0.65$

Figure 19. Comparison of pitch control effectiveness obtained using single flap and multiple flap test techniques.
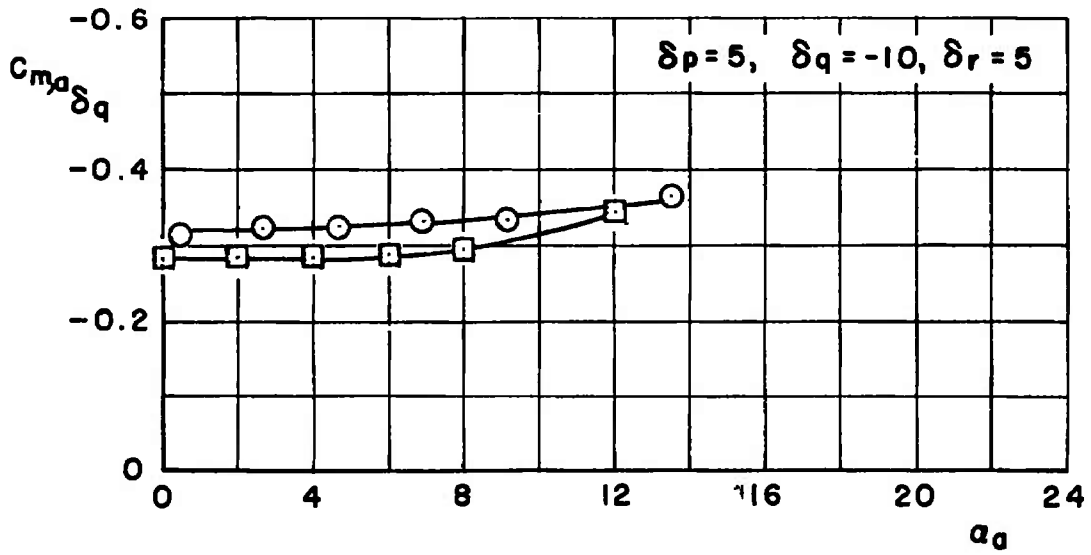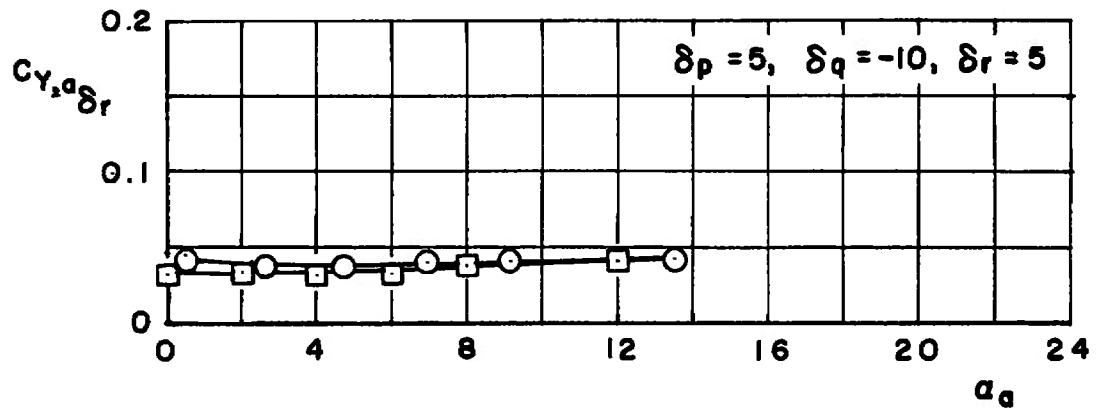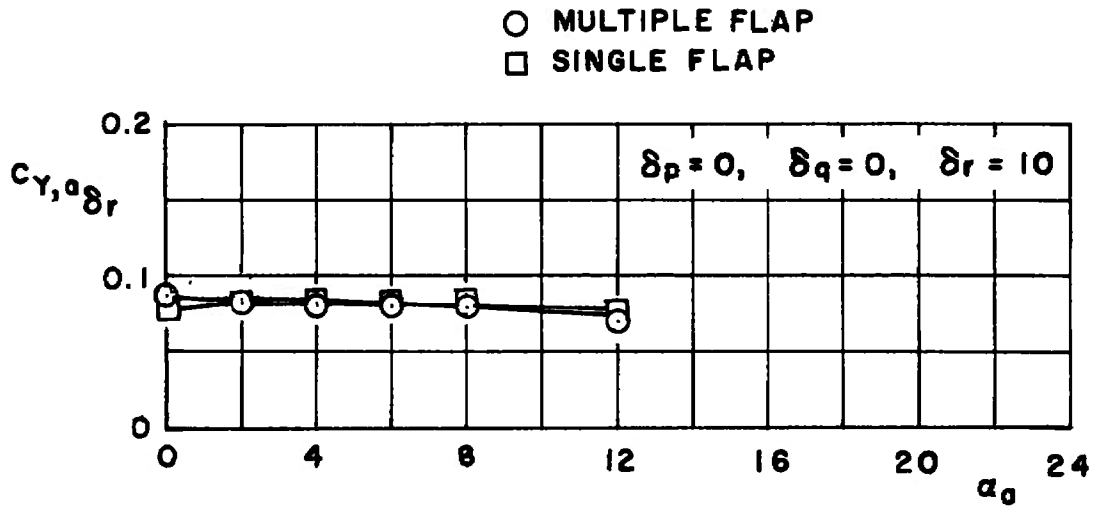
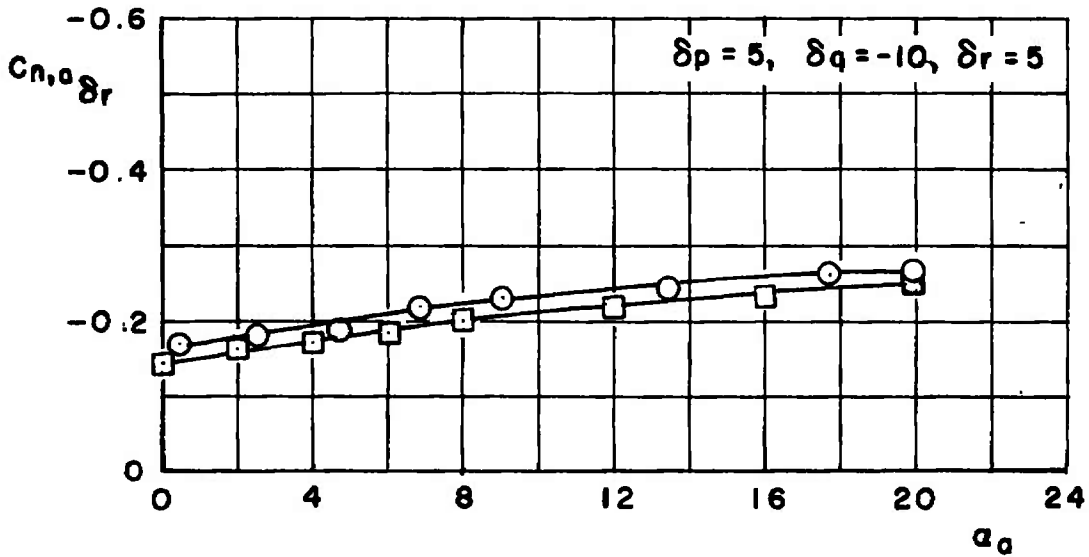b. $M_\infty = 0.95$
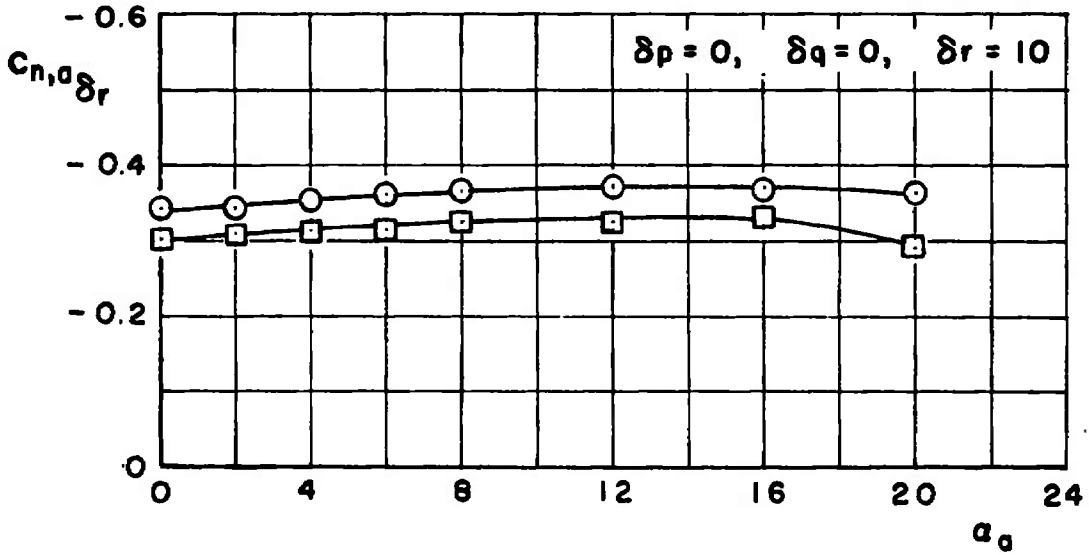Figure 19. Concluded.

63
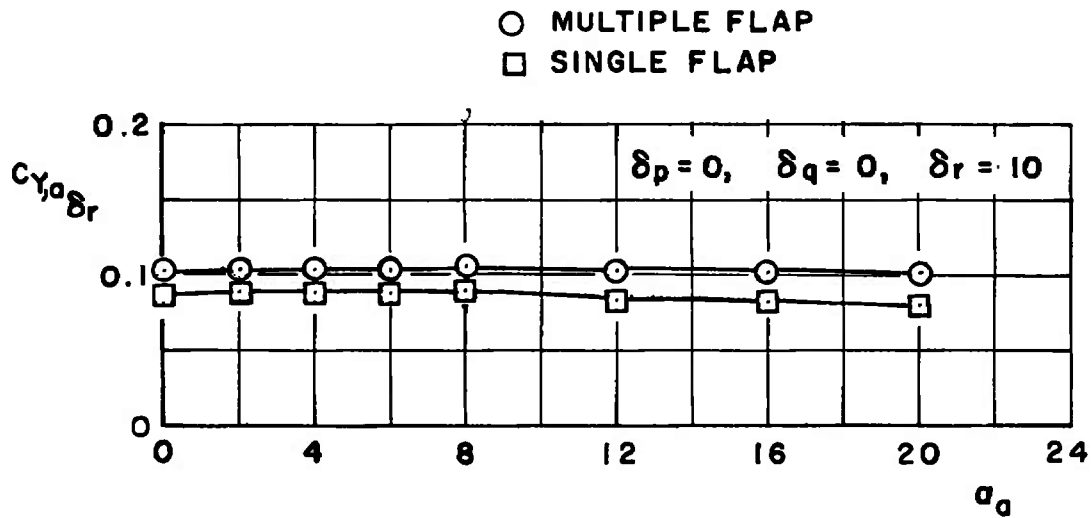
a. $M_\infty = 0.65$

Figure 20. Comparison of the side-force increment obtained using single flap and multiple flap test techniques.
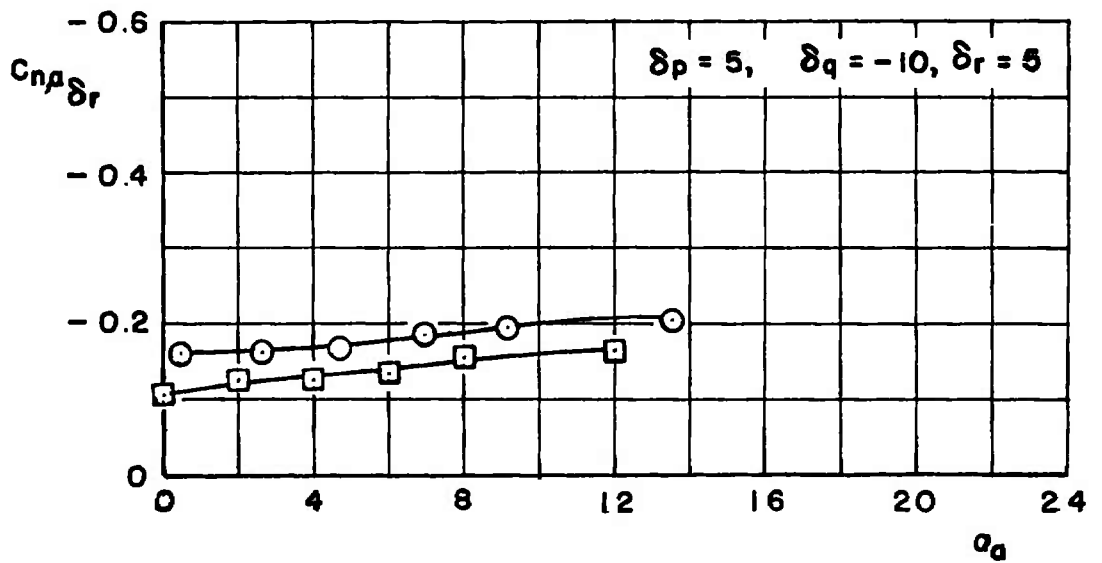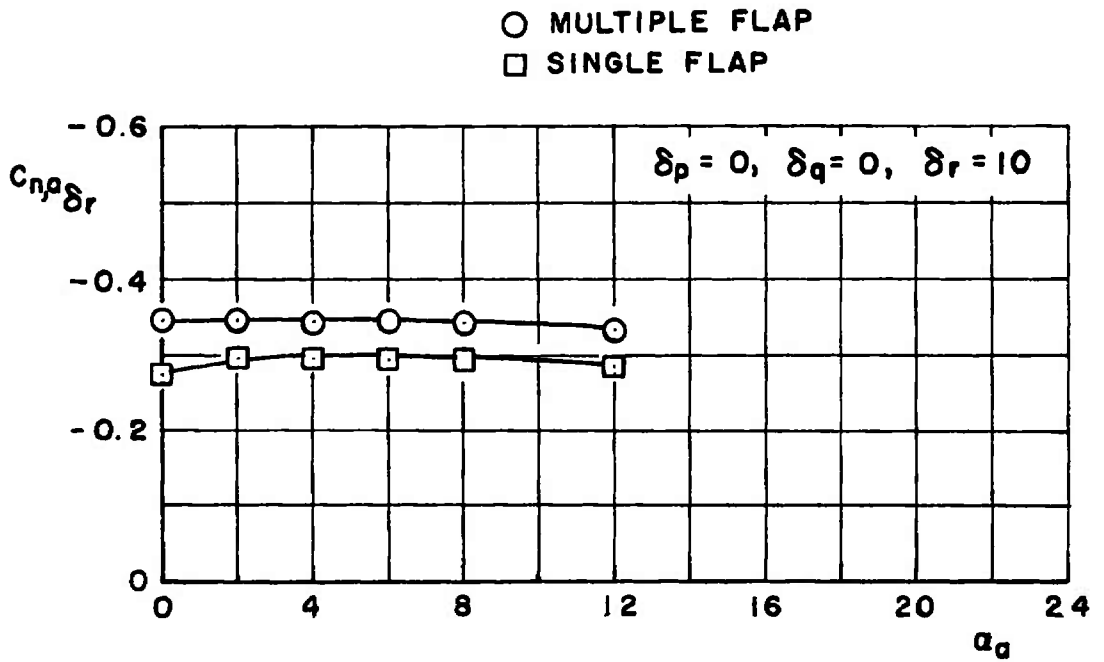
b. $M_\infty = 0.95$
Figure 20. Concluded.

a. $M_\infty = 0.65$

Figure 21. Comparison of the yaw control effectiveness obtained using
single flap and multiple flap test techniques.

○ MULTIPLE FLAP
□ SINGLE FLAP

$\delta_p = 0, \quad \delta_q = 0, \quad \delta_r = 10$

$\delta_p = 5, \quad \delta_q = -10, \quad \delta_r = 5$

b. $M_\infty = 0.95$
Figure 21. Concluded.
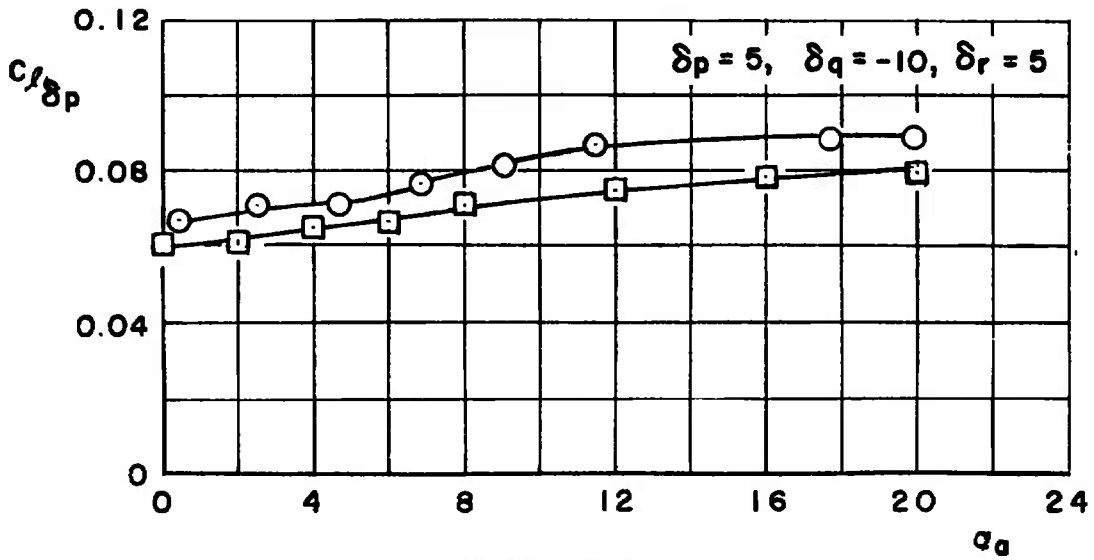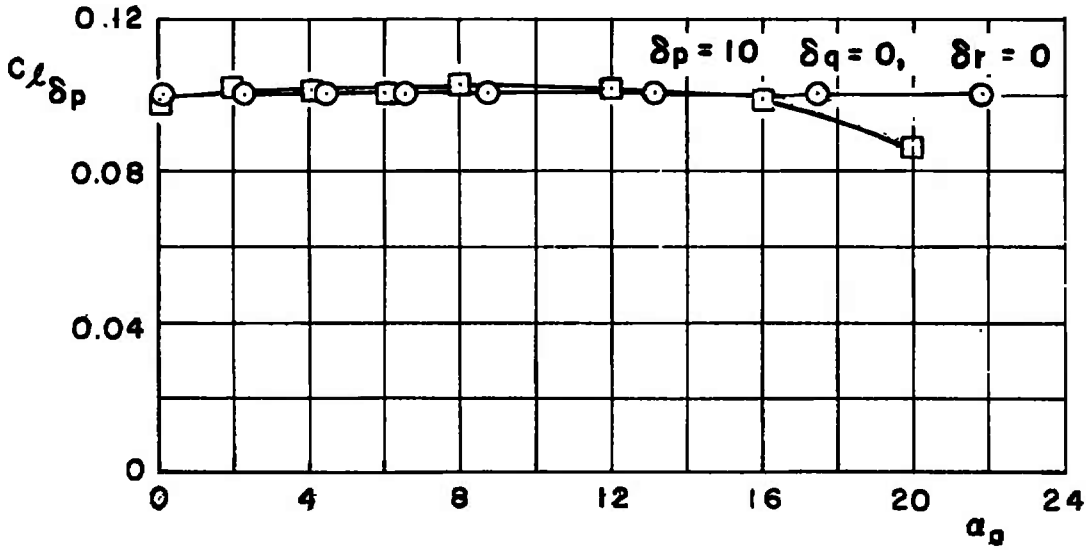
67

○ MULTIPLE FLAP
□ SINGLE FLAP

a. $M_\infty = 0.65$
Figure 22. Comparison of the roll control effectiveness obtained using
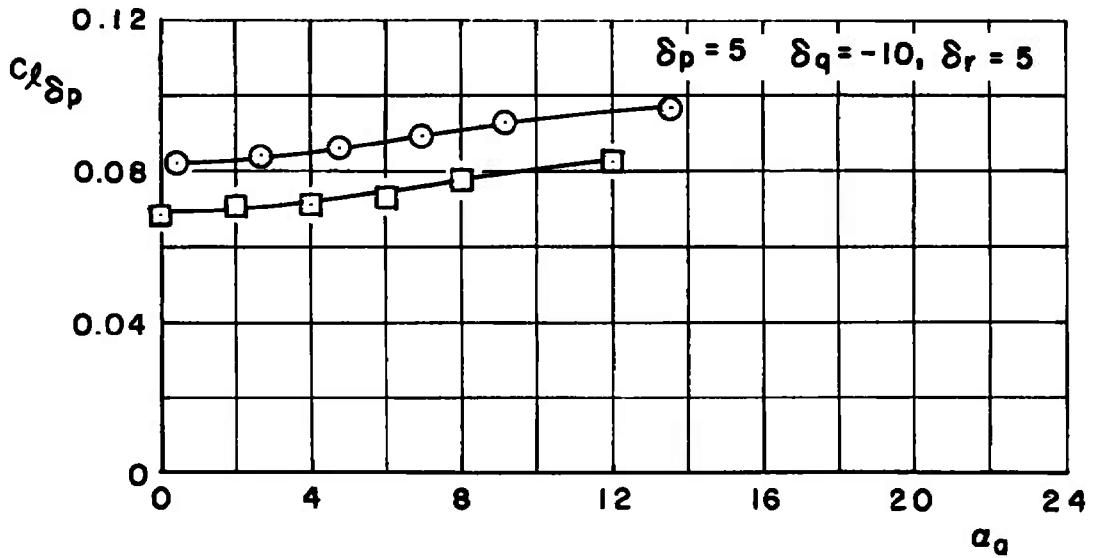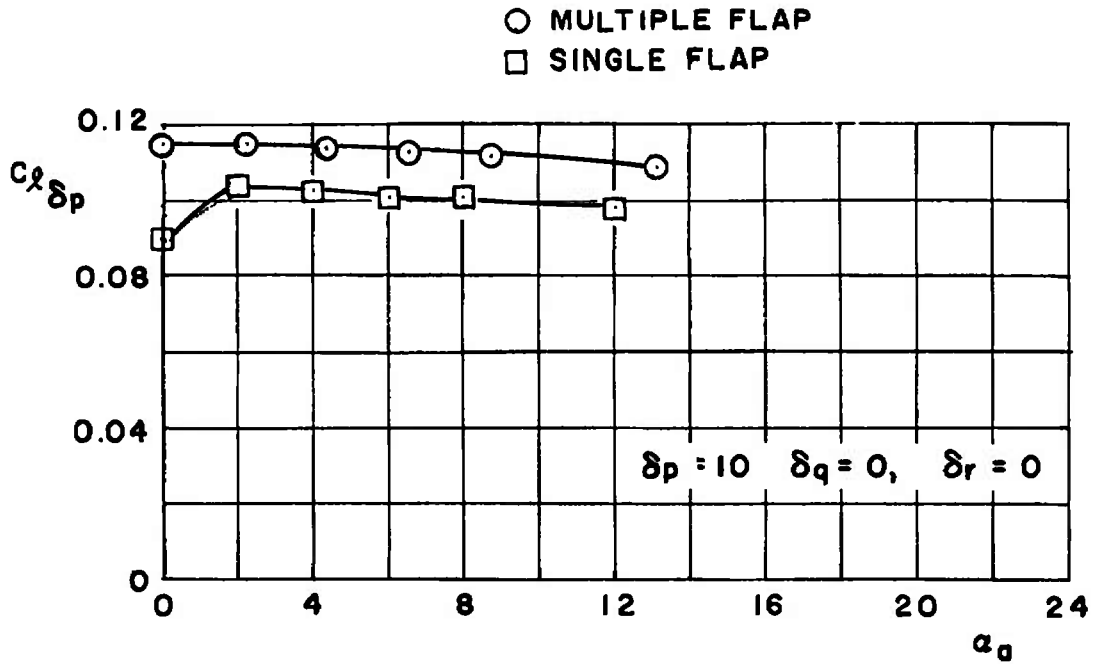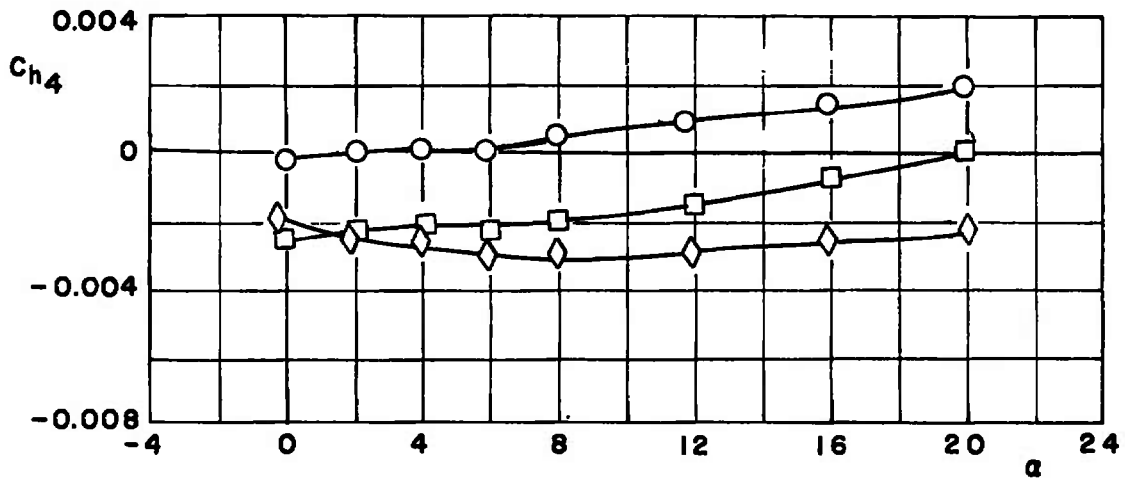single flap and multiple flap test techniques.

b. $M_\infty = 0.95$
Figure 22. Concluded.
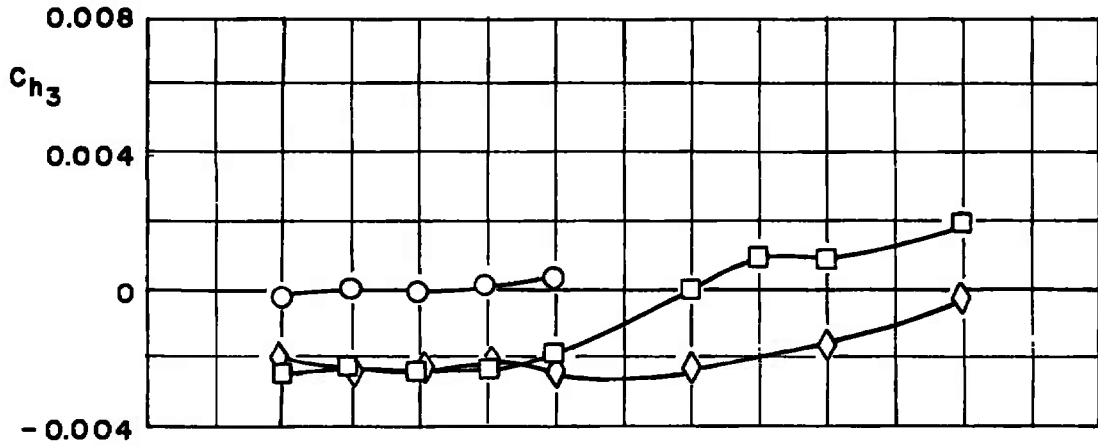
a. $M_\infty = 0.65$

Figure 23. Variation of flap hinge-moment coefficient with angle of attack.
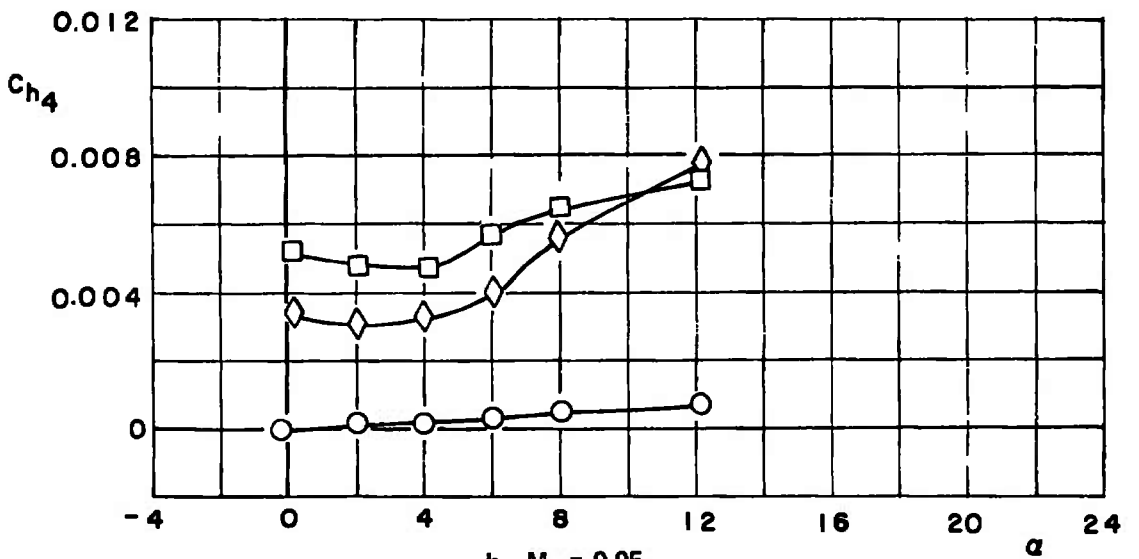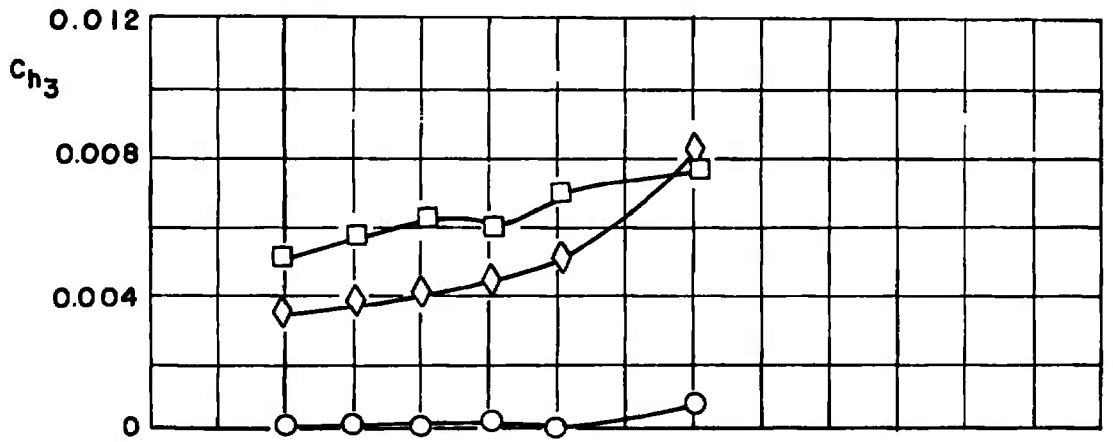
b. $M_\infty = 0.95$
Figure 23. Concluded.

SYMBOL	M_∞	α_M	H	δq
⊙	0.95	4.40	40000	0
⊡	0.95	4.40	40000	-15
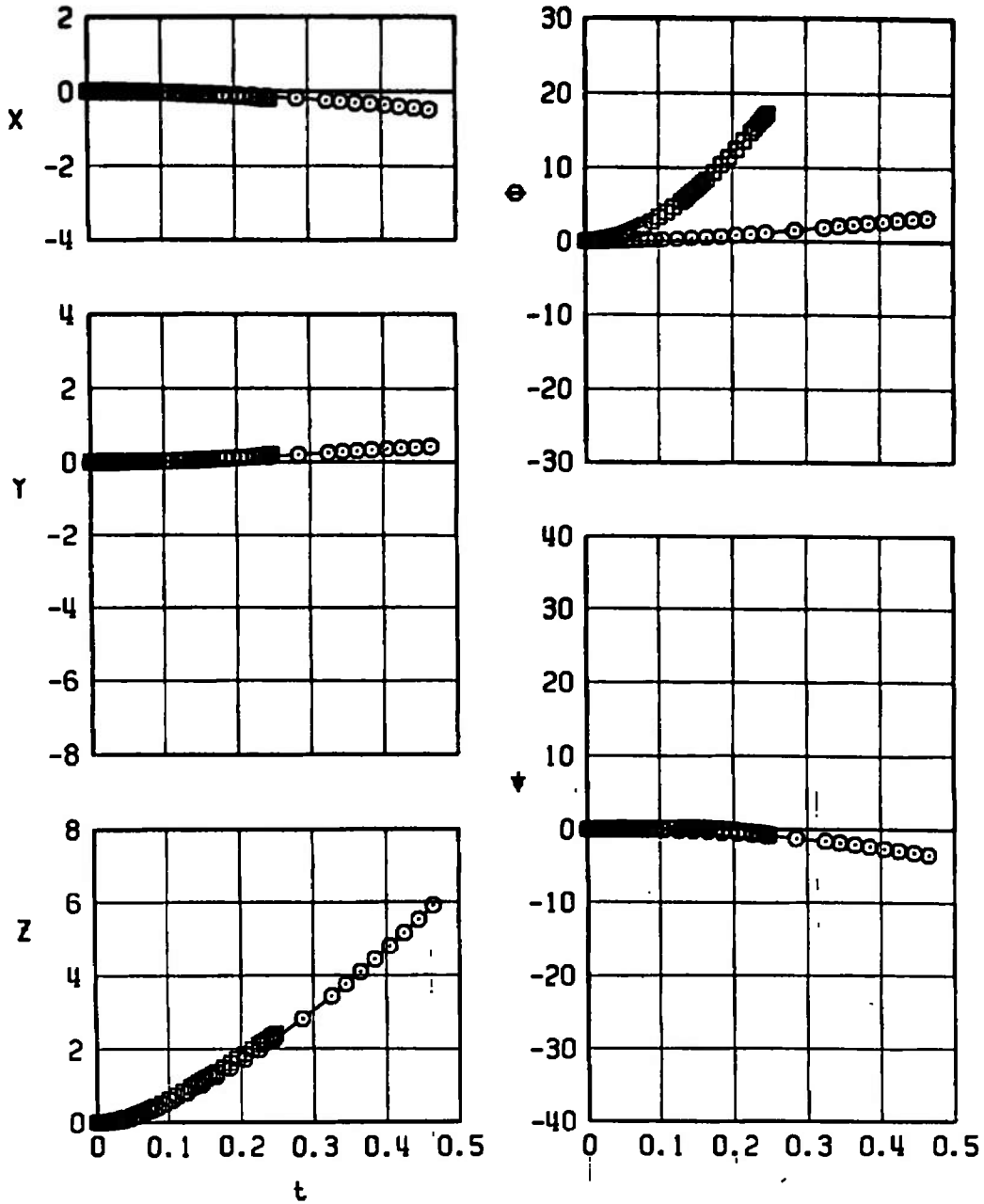
a. Trajectories for M_∞ = 0.95, δq = 0, and δq = -15

Figure 24. TCTV separation trajectories from the right inboard pylon
of the F-4 aircraft.
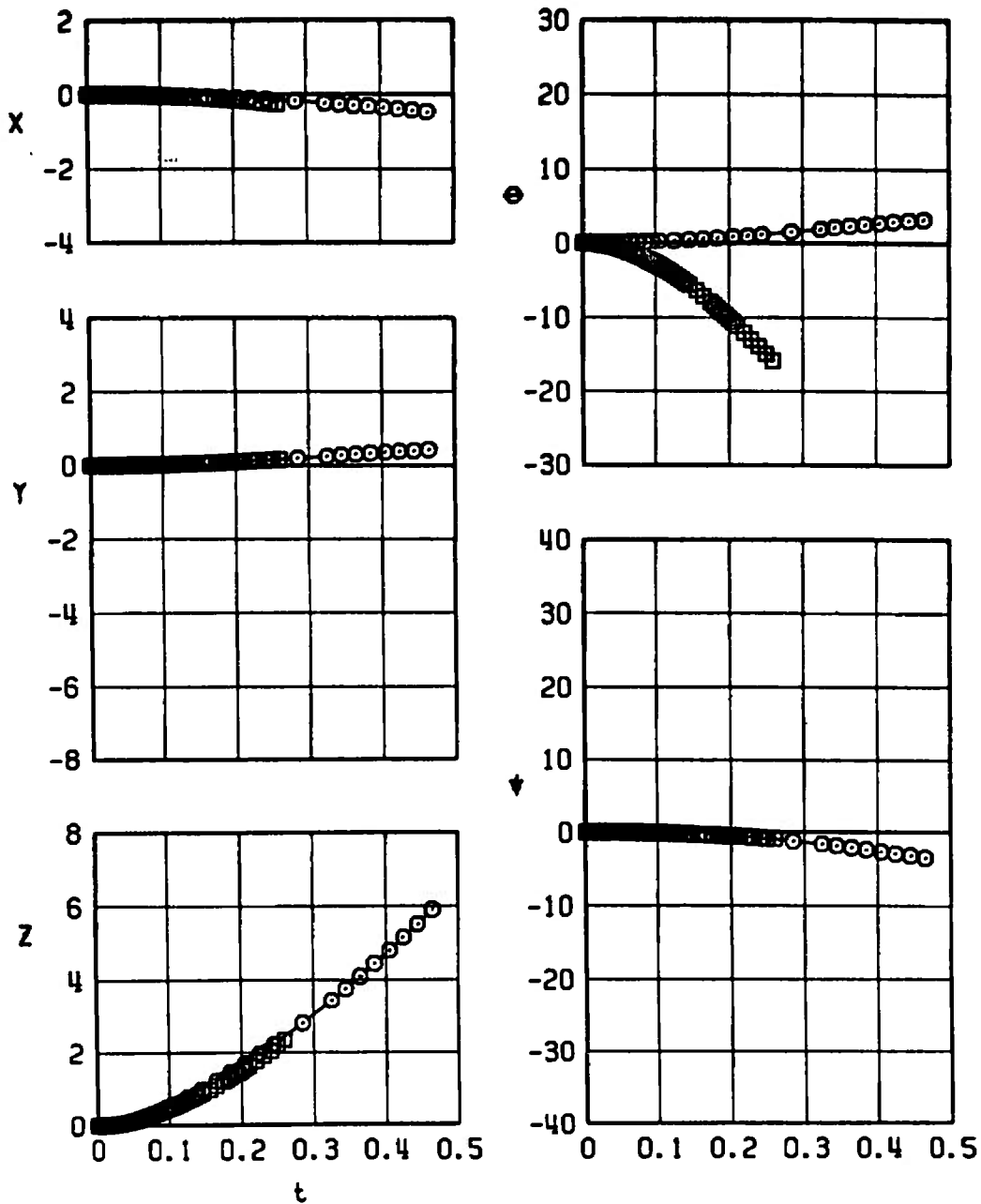
b. Trajectories for M_∞ = 0.95, δq = 0, and δq = +15
Figure 24. Concluded.

INITIAL MACH NO. = 0.95

INITIAL ANGLE OF ATTACK = 0 deg

SET DYNAMIC PRESSURE = 320
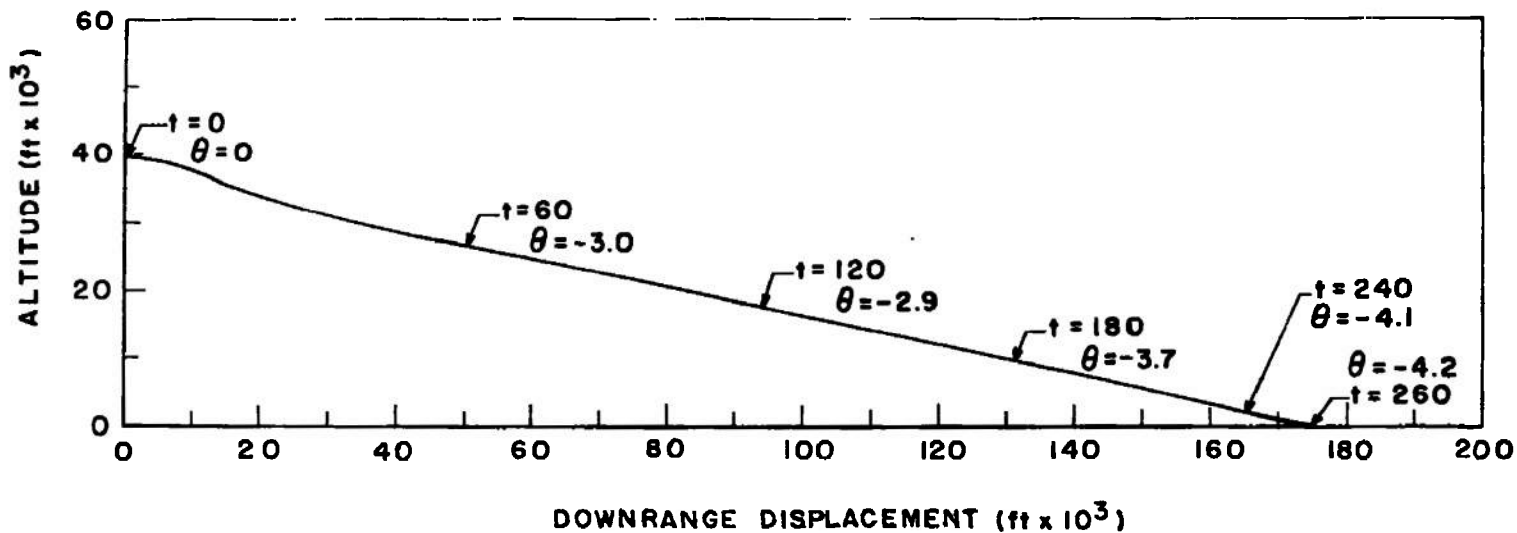
a. Trajectory

Figure 25. TCTV flight profile.
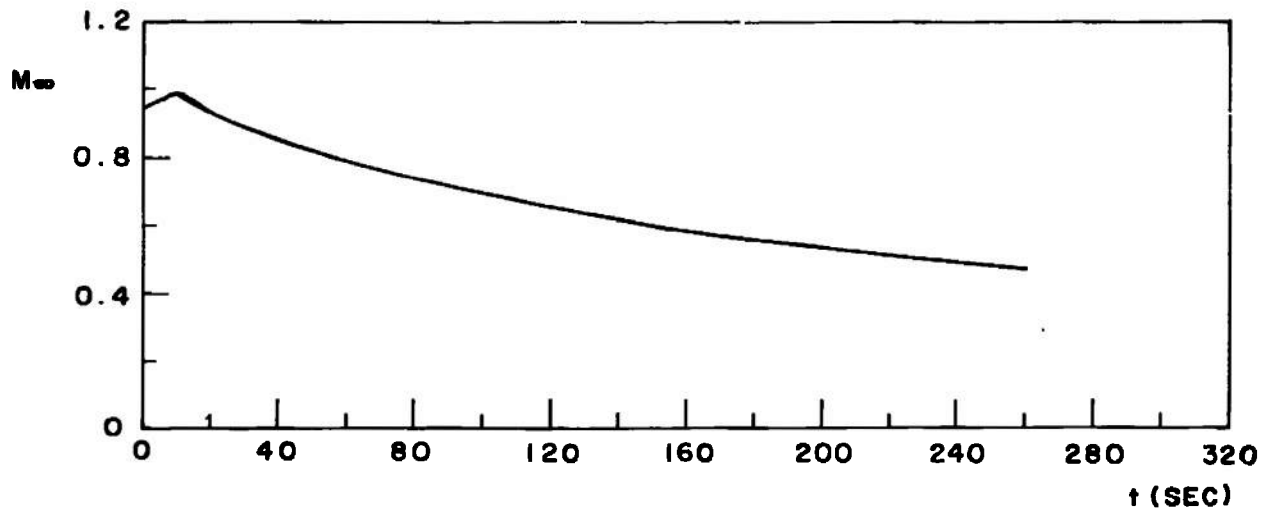
b. Mach number versus time
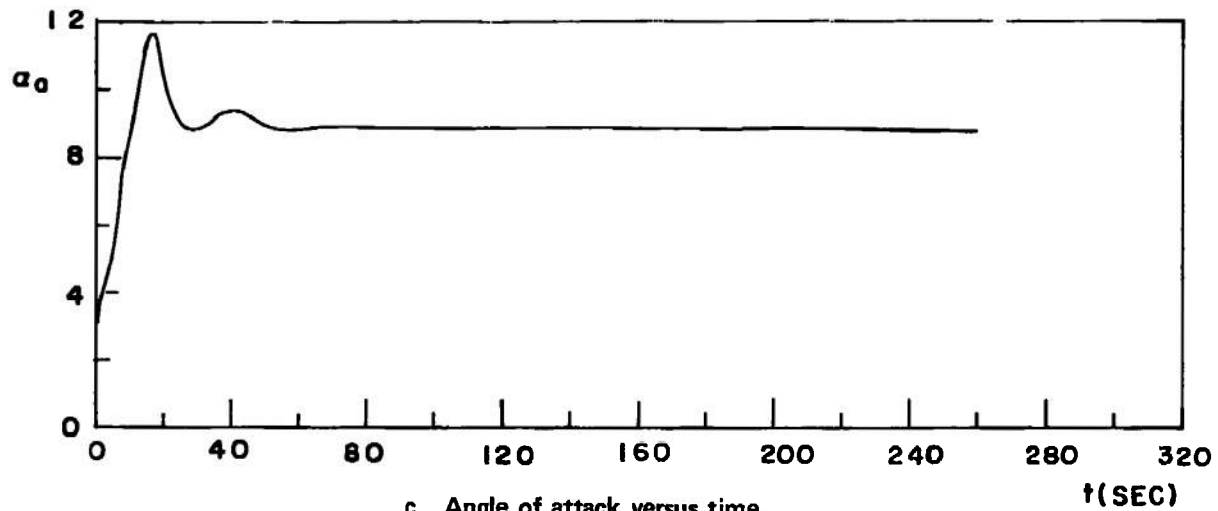
c. Angle of attack versus time

Figure 25. Continued.
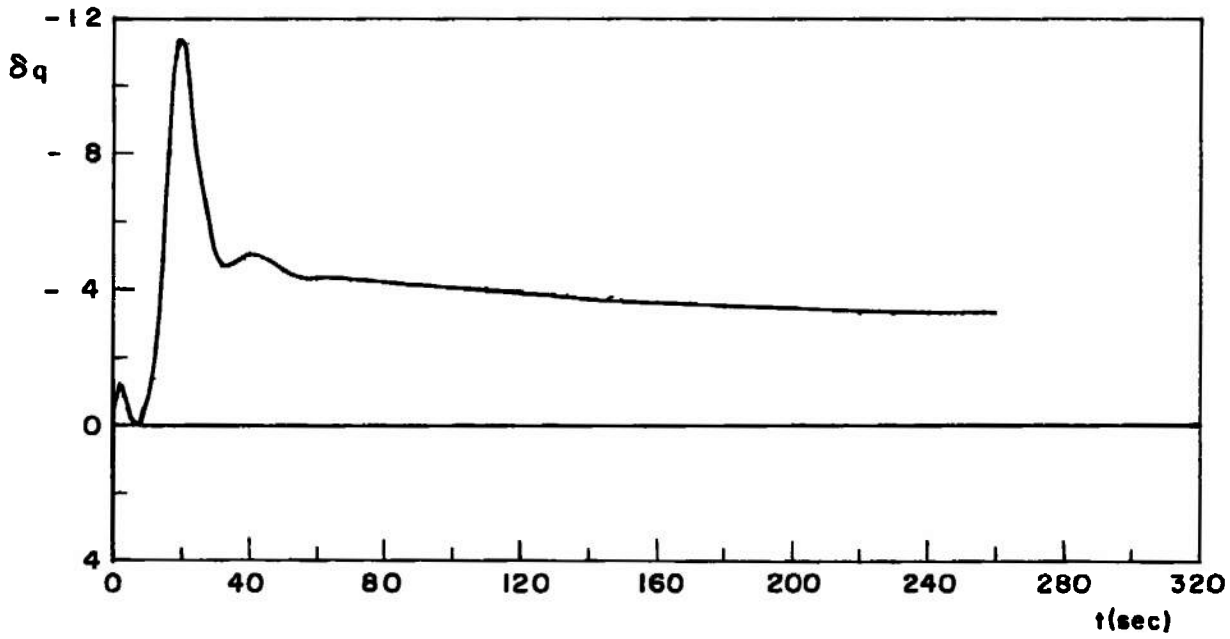
d. Pitch flap deflection versus time
Figure 25. Concluded.

INITIAL ALTITUDE = 10,000 ft
INITIAL MACH NO. = 0.574
INITIAL ANGLE OF ATTACK = 8.8 deg
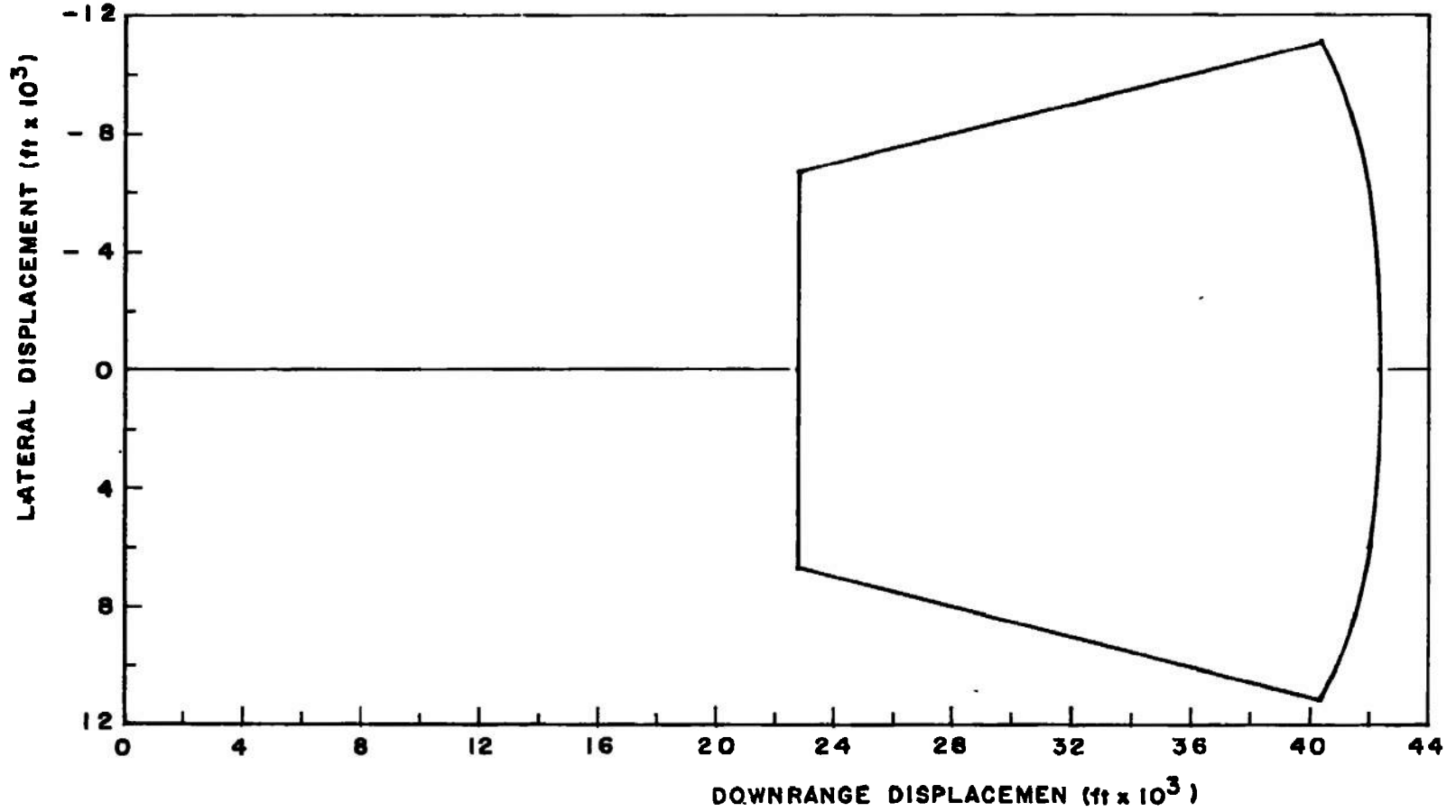
Figure 26. TCTV footprint.
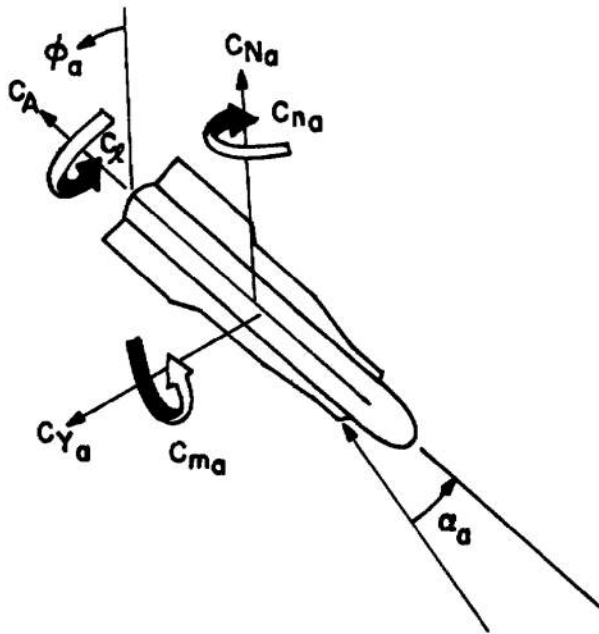
FLAP DEFLECTIONS

$$\phi_a = 0$$
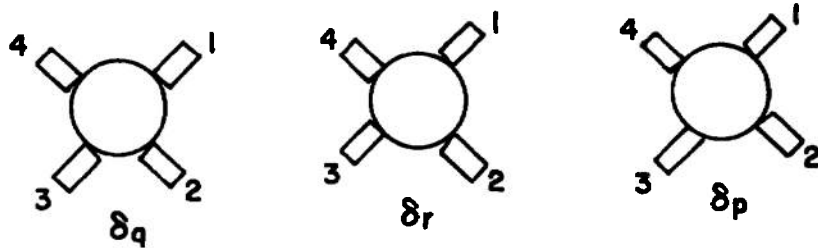
AFT VIEW

Figure 27. Axis system.

Table 1. Mass Properties and Dimensions Used in Wind
Tunnel and Simulator Work

Parameter	Phase 1 0.25 Scale	Phase 2 (CTS) and Full Scale
d, in.	4.5	18
S, in.	15.90	254.42
Mass, slugs	- - -	74.98
I_{xx}, slug-ft^2		33.93
I_{yy}, slug-ft^2		526.40
I_{zz}, slug-ft^2		526.64
Roll-Damping Derivative, $dC_{\ell_p}/d(pd/2V_\infty)$, rad^{-1}		-110.00
Pitch-Damping Derivative, $dC_M/d(qd/2V_\infty)$, rad^{-1}		-56.00
Yaw-Damping Derivative, $dC_{n_p}/d(rd/2V_\infty)$, rad^{-1}		-56.00

Table 2. Test Conditions and Data Precision

Phase 1

M_∞	q_∞	Re x 10^6	$\pm\Delta C_{m,a}$	$\pm\Delta C_{N,a}$	$\pm\Delta C_{n,a}$	$\pm\Delta C_{Y,a}$	$\pm\Delta C_{\ell,a}$	$\pm\Delta C_A$	$\pm\Delta C_{h_x}$
0.5	295	2.7	0.10	0.26	0.10	0.03	0.03	0.05	---
0.65	445	3.2	0.09	0.20	0.08	0.02	0.02	0.03	0.0002
0.85	410	2.5	0.10	0.20	0.07	0.02	0.02	0.03	---
0.95	460	2.6	0.10	0.10	0.05	0.02	0.02	0.03	0.0002
1.05	505	2.7	0.09	0.10	0.04	0.02	0.02	0.03	---

Phase 2

M_∞	q_∞	Re x 10^{-6}	$\pm\Delta X$	$\pm\Delta Y$	$\pm\Delta Z$	$\pm\delta\theta$	$\pm\delta\psi$
0.95	500	2.9	0.023	0.014	0.016	0.246	0.182

NOMENCLATURE

Coefficients are reduced to a nonrolling aeroballistic axis system (see Fig. 27).

C_{A_o} Measured axial-force coefficient at $a_a = 0$

$C_{A_{\delta q}}$ Axial-force increment due to a pitch control deflection,

$$\frac{[(C_A)_{\delta q = x} - (C_A)_{\delta q = 0}]}{\delta q = x}, \ 1/\text{deg}$$

C_{h_x} Flap hinge-moment coefficient, referenced to flap hinge line, hinge moment/$q_\infty Sd$, positive moment tends to force trailing edge down

C_ℓ Rolling-moment coefficient, rolling moment/$q_\infty Sd$

$C_{\ell_{\delta p}}$ Roll control effectiveness,

$$\frac{[(C_\ell)_{\delta p = x} - (C_\ell)_{\delta p = 0}]}{\delta p = x}, \ 1/\text{deg}$$

$C_{m,a}$ Pitching-moment coefficient, referenced to a point 19.879 in. aft of model nose, pitching moment/$q_\infty Sd$

$C_{m,a_{\delta q}}$ Pitch control effectiveness,

$$\frac{[(C_{m,a})_{\delta q = x} - (C_{m,a})_{\delta q = 0}]}{\delta q = x}, \ 1/\text{deg}$$

$C_{N,a}$ Normal-force coefficient, normal force/$q_\infty S$

$C_{N,a_{\delta q}}$ Normal-force increment due to a pitch control deflection,

$$\frac{[(C_{N,a})_{\delta q = x} - (C_{N,a})_{\delta q = 0}]}{\delta q = x}, \ 1/\text{deg}$$

$C_{n,a}$ Yawing-moment coefficient referenced to a point 19.879 in. aft of model nose, yawing moment/$q_\infty Sd$

$C_{n,a_{\delta r}}$ Yaw control effectiveness,

$$\frac{[(C_{n,a})_{\delta r = x} - (C_{n,a})_{\delta r = 0}]}{\delta r = x}, \ 1/\text{deg}$$

$C_{Y,a}$ Side-force coefficient, side force/$q_\infty S$

$C_{Y,a_{\delta r}}$ Side-force increment due to a yaw control deflection,

$$\frac{[(C_{Y,a})_{\delta r = x} - (C_{Y,a})_{\delta r = 0}]}{\delta r = x}, \ 1/\text{deg}$$

d	Reference length, model diameter, 0.375 ft
L/D	Lift/drag ratio
I_{xx}, I_{yy}, I_{zz}	Full-scale moment of inertia about the store body-axis system where the coordinate axes rotate with the store in roll, yaw, and pitch, slug-ft^2
M_∞	Free-stream Mach number
n_Z	Longitudinal load factor, $\dfrac{(C_{N,a})_{trim}\, q_\infty S}{w}$
p_∞	Free-stream static pressure, psfa
q_∞	Free-stream dynamic pressure, $0.7\, p_\infty M_\infty^2$, psf
S	Model reference area, $\pi d^2/4 = 0.110$ ft^2
t	Time, sec
w	Vehicle weight, lb
X	Separation distance of store cg parallel to the free-stream wind vector, ft, full scale measured from the prelaunch position, positive direction is forward as seen by the pilot
$\overline{X}$	Resultant center of pressure, ft
$\left(\dfrac{\overline{X}}{d}\right)_{trim}$	Vehicle static margin $\left(\dfrac{dC_{m,a}}{dC_{N,a}}\right)_{trim}$, reference diameters
Y	Separation distance of store cg perpendicular to the X and Z directions, ft, full scale measured from the prelaunch position, positive direction is to the right as seen by the pilot
Z	Separation distance of store cg perpendicular to the X and Y directions, ft, full scale measured from the prelaunch position, positive direction is downward
a_a	Model total angle of attack in aeroballistic axis system, deg
$(a_a)_{trim}$	Trim angle of attack, deg
δp	Roll control surface deflection for four flaps, $\delta p = (-\delta 1 - \delta 2 + \delta 3 + \delta 4)/4$, deg

δq — Pitch control surface deflection for four flaps,
$\delta q = (\delta 1 + \delta 2 + \delta 3 + \delta 4)/4$, deg

δr — Yaw control surface deflection for four flaps,
$\delta r = (-\delta 1 + \delta 2 - \delta 3 + \delta 4)/4$, deg

$\delta 1$-4 — Control deflection angles for the respective control surfaces 1-4 (see Fig. 27), positive when trailing edge is down. deg

ϕ_a — Model roll angle in aeroballistic axis system, deg

ϕ_m — Model roll angle in wind tunnel, deg

θ — Glide path angle, deg